

A Stain-Free Detection System for Electrophoresis.

by

Namik Kemal Yilmaz

B.S., Mechanical Engineering
Middle East Technical University, 1998

Submitted to the Department of Mechanical Engineering
in Partial Fulfillment of the Requirements for the Degree of

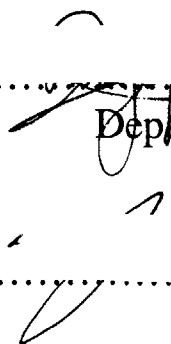
Master of Science
at the

Massachusetts Institute of Technology

February 2001

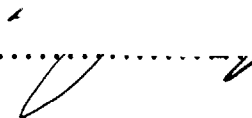
© 2001 Massachusetts Institute of Technology. All rights reserved.

Signature of Author



Department of Mechanical Engineering
January 19, 2001

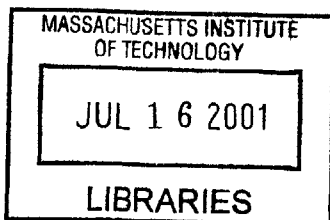
Certified by



Kamal Youcef-Toumi
Professor

Accepted by

Ain A. Sonin
Chairman, Department Committee on Graduate Students



BARKER

A Stain-Free Detection System for Electrophoresis

by

Namik Kemal Yilmaz

Submitted to the Department of Mechanical Engineering
on January 19, 2001, in Partial Fulfillment of the
Requirements for the Degree of
Master of Science

Abstract

In this thesis, a novel stain free detection system for slab gel electrophoresis is examined. Currently, stained techniques are used to identify electrophoretic bands in gels. The stains utilized in these methods involve health risks since they are mutagenic. Also stains like EtBr are intercalating agents meaning they wedge themselves into the grooves of DNA and stay there. Since this includes a physical contact the stains remain in the DNA at the end of the experiment. This makes further use DNA very difficult. The stains need to be removed by chemical techniques which are timewise very costly. Also these operations are very inefficient, retrieve rates are very low which leads to waste of most of the analyte.

The specific method we addressed aims to eliminate the use of any kind of stains and therefore inherently increase the end product efficiency. The method introduces the absorption method as the means of detection. The physical law governing the absorption technique is the Beer-Lambert Law. The Beer-Lambert Law defines the linear relation, which correlates absorption value to the analyte concentration, path length of the light and wavelength-dependent absorptivity coefficient. Although the proposed method is intended to apply to all kind of different analytes, to achieve primary goals and prove the feasibility of the method, as the first step detection of DNA molecules are targeted. Hence absorption pattern at a wavelength of 254 nm (which is characteristic absorption peak for DNA) is examined. After the method is proven to work robustly, it will be extended to all kind of different analytes. The unique approach used in the proposed detection system is the use of a scanning technique incorporated with absorption technique utilizing a high QE (Quantum efficiency) CCD camera as the detector. Experiments have been performed to determine the only unknown parameter -wavelength-dependent absorptivity coefficient $a(\lambda)$ - in the Beer-Lambert Law. The value of $a(\lambda)$ is dependent on the wavelength and also on the transmission media. In our case wavelength of interest is 254 nm and the specific transmission media is agarose gel with 0.8% concentration. Each lane in the agarose gel is scanned under UV light and transmittance values at 254 nm are recorded as a function of position. The recorded data are processed to see the absorption pattern along the lane. The drop in the signal indicates the existence of a DNA band.

Experiments have been performed on three different agarose gels, which are 4 mm thick, and with 0.8% concentration. The value of wavelength-dependent absorptivity coefficient $a(\lambda)$ was determined within an error margin. The resolution of the method was found to be 4 ng/ μ l.

Thesis Supervisor: Kamal Youcef-Toumi
Title: Professor

Acknowledgments

First of all, I am grateful to Professor Kamal Youcef-Toumi for his guidance as well as his allowing me to work on this challenging project. In particular I would like to thank all my colleagues in Mechatronics Research Laboratory for their valuable advices and excellent companionship. I am thankful to Mehmet Yunt, Aykut Firat, Cagri Savran, Osamah El-Rifai bin Mahmud bin Ali, Dantes Bernardo Aumond, Kashif Ahmed Khan and Jalal Mohammad Khan for their friendship. I am especially indebted to Bilge Demirkoz for being such a passionate, understanding and kind confidant. Also special thanks must go to Galatasaray soccer team for making some Wednesday&Thursday afternoons real fun and memorable.

Finally, I would like to express my sincerest gratitude to all of my family members without whose support and encouragement, this thesis would not be possible.

TABLE OF CONTENTS

1. INTRODUCTION	11
1.1 What is Electrophoresis?	11
1.1.1 General Principles of the Process	11
1.1.2 Materials and Matrices	13
1.1.3 Application of Slab Gel Electrophoresis:	17
1.1.4 Detection Techniques	19
1.2 Problems of Slab Gel Electrophoresis	22
1.3 Problem Statement	22
1.3.1 General Machine Idea.....	23
1.4 References	24
2. DIFFERENT SOLUTIONS FOR IMAGING PROBLEM	25
2.1 Laser Induced Fluorescence (LIF).....	25
2.2 UV Absorption Method.....	28
2.3 Method Comparison and Proposed Technique	31
2.4 References	33
3.1 Overview of the Hardware	34
3. GENERAL DESIGN OF THE SYSTEM	34
3.1.1 Light Source and Filter	34
3.1.2 CCD Camera and the Spectroscopy System.....	36
3.1.3 X-Y Table	38
3.1.4 Fiber Probe, the Transilluminator and Gel Tray Holder	40
3.2 Overview of the Software.....	42
3.2.1 Description of User Interface	43
3.2.1 Algorithm to control the X-Y stage Control.....	45
3.2.2 Spectra acquisition from the spectrometer using COM technology.....	46
3.3.3 Data processing.....	46
3.3 References	49

4.	EXPERIMENTS.....	50
4.1	Introduction	50
4.2	General Procedure	50
4.3	The Transmittance of the Gel Tray	52
4.4	Preliminary Results with DNA on the Gel Tray	54
4.5	Results with First Gel	59
4.6	Results with Second Gel.....	69
4.7	Results with Third Gel	75
4.8	Comparison of Results	82
5.	CONCLUSION	84
6.	APPENDIX A: C++ CODE	87

TABLE OF FIGURES

Figure 1.1, Chemical Structure of Agarose.....	14
Figure 1.2, Forming of Gel Structure.....	14
Figure 1.3, Loading of the Gel.....	17
Figure 1.4, Power Supply.....	18
Figure 1.5, Run Gel.....	18
Figure 1.6, Ran Gel Under UV Light.....	19
Figure 1.7, General Machine Design.....	23
Figure 2.1, Laser Induced Fluorescence Setup.....	26
Figure 2.2, Introduction to CE, Basics of Molecular Movement in the Capillary.....	27
Figure 2.3, Absorption of Light by a Sample.....	28
Figure 2.4, Example of a Working Curve.....	29
Figure 2.5, CCD Based DNA Detection in Systems for Electrophoretic Gels.....	30
Figure 2.6, Overall System Design.....	32
Figure 3.1, UV Transilluminator.....	34
Figure 3.2, Spectrum of the UV Transilluminator.....	35
Figure 3.3, Transmittance Graph of the Band-pass Filter.....	36
Figure 3.4, QE (Quantum Efficiency) of the CCD Array.....	36
Figure 3.5, Spectrometer System.....	37
Figure 3.6, 402 LN Series XY Table from Daedal.....	38
Figure 3.7, Specifications of the XY Table.....	39
Figure 3.8, Technical Drawing of the XY Table.....	40
Figure 3.9, Fiber Probe Attached to the Cable.....	41
Figure 3.10, Frame Holding the Transilluminator and Gel Tray.....	41
Figure 3.11, Variation of Power Level of the Transilluminator Along a Horizontal Line.....	42
Figure 3.12, Fixture Used to Carry The Gel Tray on the XY Table.....	42
Figure 3.13, First Page of the User Interface.....	43
Figure 3.14, Second Page of the User Interface.....	44
Figure 3.15, An SPE Format File Opened in WinSpec.....	47
Figure 3.16, Plot Showing Intensity as a Function of Location.....	48
Figure 4.1, Example of a Working Curve.....	50
Figure 4.2, Scanning Setup.....	51
Figure 4.3, Modification on the Transilluminator to Avoid Excessive UV Light Exposure to the Gel.....	52
Figure 4.4, Spectra of the Transilluminator.....	53

Figure 4.5, Spectra of the Gel Tray on the Transilluminator.	53
Figure 4.6, 1 ng/ μ l Solution.	54
Figure 4.7 10 ng/ μ l Solution.	55
Figure 4.8, 100 ng/ μ l Solution.	55
Figure 4.9, 1 μ g/ μ l Solution.	56
Figure 4.10, 10 μ g/ μ l Solution.	56
Figure 4.11, Water without DNA.	57
Figure 4.12, Principle of Refraction for Converging Lens	58
Figure 4.13, Picture of Duplicate Gel (Run with EtBr) Under UV Light.	60
Figure 4.14, Lane 1: 100 ng Plasmid (Ladder) DNA, First Run.	60
Figure 4.15, Lane 1: 100 ng Plasmid (Ladder) DNA, Second Run.	62
Figure 4.16, Lane 1: 100 ng Plasmid (Ladder) DNA, Third Run.	62
Figure 4.17, Lane 2: 100 ng Mouse DNA, First Run.	63
Figure 4.18, Lane 2: 100 ng Mouse DNA, Second Run.	63
Figure 4.19, Lane 2: 100 ng Mouse DNA, Third Run.	64
Figure 4.20, Lane 3: 1 μ g Mouse DNA, First Run.	65
Figure 4.21, Lane 3: 1 μ g Mouse DNA, Second Run.	65
Figure 4.22, Lane 3: 1 μ g Mouse DNA, Third Run.	66
Figure 4.23, Lane 4: 5 μ g Mouse DNA, First Run.	67
Figure 4.24, Lane 4: 5 μ g Mouse DNA, Second Run.	67
Figure 4.25, Lane 5: 10 μ g Mouse DNA, First Run.	68
Figure 4.26, Lane 5: 10 μ g Mouse DNA, Second Run.	68
Figure 4.27, Lane 5: 10 μ g Mouse DNA, Third Run.	69
Figure 4.28, Picture of Duplicate Gel Run With EtBr Under UV Light. Lane 1 is the Leftmost Lane.	70
Figure 4.29, Lane 8: 400 ng plasmid DNA, First Run.	73
Figure 4.30, Lane 8: 400 ng plasmid DNA, Second Run.	73
Figure 4.31, Lane 8: 400 ng plasmid DNA, Third Run.	74
Figure 4.32, Snapshot Image of Lane 8. The Band is at Located at an Absolute Position of 45 mm.	74
Figure 4.33, Picture of Duplicate Gel Run With EtBr Under UV Light. Lane 1 is the Leftmost Lane.	75
Figure 4.34, Lane 1: 100 ng Plasmid DNA. Two Different Runs With 1 mm Offsets.	76
Figure 4.35, Lane 2: 250 ng Plasmid DNA. Four Different Runs With 1 mm Offsets.	78
Figure 4.36, Lane 3: 400 ng Plasmid DNA. Three Different Runs With 1 mm Offsets.	79
Figure 4.37, Lane 4: 550 ng Plasmid DNA. Three Different Runs With 1 mm Offsets.	79

Figure 4.38, Lane 5: 700 ng Plasmid DNA. Three Different Runs With 1 mm Offsets..... 80
Figure 4.39, Lane 6: 850 ng Plasmid DNA. Four Different Runs With 1 mm Offsets. 81

LIST OF TABLES

Table 2.1 Method Comparison.....	31
Table 4.1, Calculation of $a(\lambda)$, Wavelength-dependent Absorptivity Coefficient($\mu\text{l}/\text{mm}\text{-ng}$).	61
Table 4.2, Contents of Gel 2.	69
Table 4.3, Calculation of $a(\lambda)$, Wavelength dependent Absorptivity Coefficient ($\mu\text{l}/\text{mm}\text{-ng}$).....	72
Table 4.4, Calculation of $a(\lambda)$, Wavelength-dependent Absorptivity Coefficient ($\mu\text{l}/\text{mm}\text{-ng}$) from the Snapshot Image.	72
Table 4.5, Contents of Gel 3.	75
Table 4.6, Calculation of $a(\lambda)$, Wavelength-dependent Absorptivity Coefficient($\mu\text{l}/\text{mm}\text{-ng}$).	77
Table 4.7, Calculation of $a(\lambda)$, Wavelength-dependent Absorptivity Coefficient ($\mu\text{l}/\text{mm}\text{-ng}$). ..	77
Table 4.8, Results of Experiments with First Gel.	82
Table 4.9, Results of Experiments with Second Gel.....	82
Table 4.10, Results of Experiments with Third Gel.....	82

1. INTRODUCTION

1.1 What is Electrophoresis?

Electrophoresis is a method that separates macromolecules (either nucleic acids, carbohydrates, lipids, proteins and etc.) on the basis of size, electric charge, and other physical properties.

A gel, which is the media for electrophoresis, is a colloid in a solid form. The term electrophoresis describes the migration of charged particle under the influence of an electric field. *Electro* refers to the energy of electricity. *Phoresis*, from the Greek verb *phoros*, means, "to carry across." Thus, gel electrophoresis refers to the technique in which molecules are forced across a span of gel, motivated by an electrical current. Activated electrodes at either end of the gel provide the driving force. A molecule's properties determine how rapidly an electric field can move the molecule through a gelatinous medium.

Many important biological molecules such as amino acids, peptides, proteins, nucleotides, and nucleic acids, possess ionisable groups and, therefore, at any given pH, exist in solution as electrically charged species either as cations (+) or anions (-). Depending on the nature of the net charge, the charged particles will migrate either to the cathode or to the anode. [1]

1.1.1 General Principles of the Process

Electrophoresis separates particles based on their movement due to an applied electric field. The electric field results in an applied force on the particles proportional to their charge or surface potential. The resulting force causes a distinct velocity for different substances or molecules. This allows for the separation of molecules based on their surface potential. In other words, if an electric field is applied for a fixed amount of time across a matrix that contains a mix of molecules with different surface potentials, the molecules will be at different locations on the matrix when the field is stopped. [1]

The study of electrophoretic motion focuses on electric potential on the surface of an object or molecule, and the relation of that potential to the velocity of the object in an electric field. The surface potential of the molecules is caused by an interaction between the surface of the molecule and the media around it. A charge separation between a thin layer on the surface of the particle and a thin layer of the media around the particle results from the interface of the two surfaces. This charge separation results in charge density in

each layer and thus an electric potential between the layers. The electric field applied to the matrix by an electrophoretic instrument acts on the charge density. In this sense molecules of the media and sample if free will move in opposite directions due to the different charges. Also molecules can be separated by their size. This is possible because the larger a molecule the more surface area and thus the larger the surface potential.

The thin layer at the surface of the dispersed particles and the thin layer of media around the particle that give a charge separation, together are called the electric double layer. Using this terminology, when the electric field is applied to the matrix the positive and negative portions of the double layer move away from each other. In other words either the particle or the matrix or both will move depending on whether they are immobile or free for motion. In electrophoresis the sample particles are free to migrate.

To make it possible to apply math to the electrophoretic phenomena it is necessary to treat the electric double layer surrounding the particle as a capacitor. With this in mind an equation for the potential difference across the two plates or layers can be stated as follows in equation (1.1):

$$(1.1) \quad \zeta = 4\pi e d / D$$

The potential difference between the layers is known as the zeta potential, thus the symbol ζ . In the equation d is the parallel distance between the plates in cm, e is the charge per cm^2 , D is the dielectric constant of the medium between the plates. An equation for the velocity of a particle in an electric field was established which takes into account the balance of forces applied to a particle by an electric field and forces of friction that work against the motion of the particle (equation 1.2):

$$(1.2) \quad V = \mu E$$

In this equation V represents velocity, E is equal to the electric field strength in volts/cm, and μ is given by equation 1.3.

$$(1.3) \quad \mu = [(\epsilon \epsilon_0) / \eta] f(\kappa a)$$

In equation (1.3) ϵ stands for the relative permittivity and ϵ_0 is the permittivity of free space which is equal to $8.854 \times 10^{-14} \text{ C}/(\text{V} \times \text{cm})$ and η is viscosity in $\text{g}/(\text{cm} \times \text{s})$. In the function $f(\kappa a)$, a is the particle diameter in cm and the inverse of k or $1/\kappa$ is the thickness of the double layer. With this in mind, $f(\kappa a)$ is 1 when the particle has a much larger diameter than the double layer and 1.5 when the particle diameter is much lower than the double layer. When the diameters are close to the same, the particle behavior is complex.

When one is concerned with capillary electrophoresis, another phenomenon needs to be considered. This is the phenomenon of electroosmotic flow. Electroosmosis is when the

bulk fluid migrates with respect to an immobilized charged surface where as electrophoresis is when a particle migrates in respect to the bulk fluid. Electroosmotic flow is generally minimized in a polymer matrix such as gels, but is significant in open channels such as capillaries. Electroosmotic flow is represented by equation (1.4):

$$(1.4) \quad F = [(\epsilon \epsilon_0) / \eta] \pi r^2 E$$

In equation (1.4) F is for flow rate in mL/s and r is the radius of the cylindrical flow channel in cm.

One of the most common problems with electrophoresis is the generation of heat due to electrical resistance in the medium. Heating effects have turned out to be the limiting factor for electrophoretic separations. In electrophoretic separations, greater the electric field strength better the resolution. In order to maintain a higher field strength, resistive media is typically used. The use of resistive media results in the generation of heat energy. A formula for the generation of heat energy is given by equation (1.5):

$$(1.5) \quad W = EI$$

Where W is power in watts and I is current in amps. The current and the electric field strength are related by the conductivity of the electrophoretic medium by Ohm's law:

$$(1.6) \quad E = I/C$$

In this equation C is the medium conductivity in $(W \times cm)^{-1}$. One can see from this equation that the lower the conductivity the larger the electric field strength. This would mean that it makes more sense to use highly resistive material as the matrix in order to get better resolution. [2,3,4]

1.1.2 Materials and Matrices

Electrophoresis typically is not carried out in free solution but in a support matrix such as agarose, polyacrylamide, paper, or capillaries. The movement of the charged molecules can be slowed down by these matrices based on the size of the molecules relative to the pore size of the matrix.

Slab Gel Agarose Electrophoresis:

Dilute agarose gels are fairly rigid and easy to handle at low concentrations and are therefore typically used to separate large macromolecules such as large proteins or DNA.

Polyacrylamide gels can be used to separate nucleic acids of 25 to 2000 bp (base-pair) whereas agarose gels are used for DNA fragments 10 times this size. Some DNA samples can range in size from less than 1 Kbp to 20 kbp.

Agar is isolated from the red algae *Rhodophyceae*, consisting of two components, agarose and agraropectin. Agarose is suitable to use as an electrophoresis matrix because it is nearly uncharged. Agarose is a chain made up of repeating units of alternating D-galactose and 3,6-anhydro-L-galactose as shown below, with side chains of 6-methyl-D-galactose.

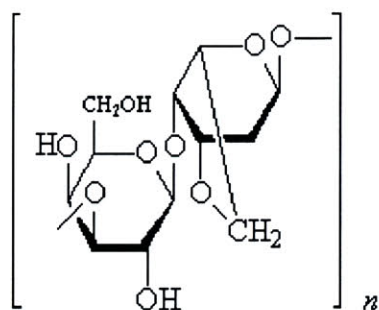


Figure 1.1, Chemical Structure of Agarose. [5]

Agarose adopts a 3D structure of a double helix with a threefold screw axis whose central cavity is large enough to hold water. (Agarose gels can hold up to 99.5% water.) Pairs of these chains can form double helices, which lead to the formation of a stable gel that is used as a matrix.

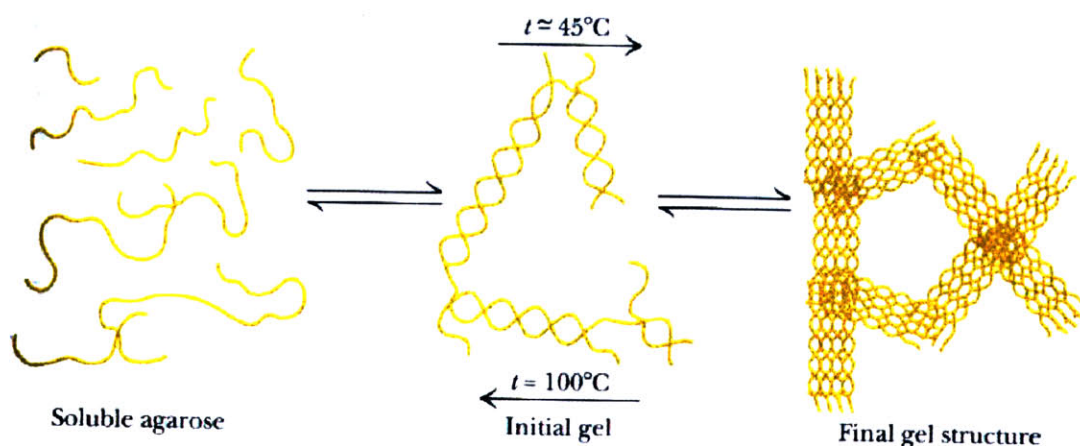


Figure 1.2, Forming of Gel Structure. [5]

In preparing the gel, agarose and buffer are heated until the agarose solid dissolves and boils. The cooled solution is then poured onto a warm gel casting apparatus. After the gel

sets, it can then be used for electrophoresis. Extra agarose solution can be stored and used later. Agarose mixtures are dilute, usually only 0.5% to 2% agarose weight-to-volume. Agarose is an easy matrix to work with because no cross-linkers are added for polymerization, it is non-hazardous, low concentrations are fairly rigid, and it is inexpensive. Agarose electrophoresis can be used in combination with Southern blotting, polymerase chain reaction (PCR), and fluorescence.

Slab Gel Polyacrylamide Electrophoresis:

Polyacrylamide gels separate most proteins and small oligonucleotides, samples which are smaller than those used for agarose gels. Polyacrylamide gels are formed by acrylamide ($\text{CH}_2=\text{CHCONH}_2$) monomers polymerized into long chains and covalently linked by a comonomer crosslinker. This crosslinker holds the structure together. The most common crosslinker is N,N'-methylenebisacrylamide $[(\text{CH}_2\text{CHCONH})_2\text{CH}_2]$. Other crosslinkers whose properties help in solubilizing polyacrylamide are ethylenediacrylate (EDA) and N,N'-diallyltartardiamide (DATD).

The crosslinking of the acrylamide monomer with the comonomer is what determines the pore size of the gel matrix. The pore size can be controlled by adjusting the percentage of these in the gel. The gel composition can be expressed in two ways: %T and %T,%C. %T is the weight percentage of the total monomer, the acrylamide plus its crosslinker. A 15% gel would have 15% w/v (weight/ volume) of acrylamide plus bisacrylamide. As the percent composition increases, the pore size decreases. %T,%C is a way to express the percentage of the crosslinker in relation to the %T. 15%T, 5% C_{bis} means that there is 15% w/v acrylamide plus bisacrylamide, and bisacrylamide is 5% of the total weight of the acrylamide present. This is another way to control the pore size. For any %T, 5% crosslinking makes the smallest pore size. Increasing or decreasing the %C value increases the pore size of the gel.

Unlike the agarose gel, polyacrylamide gels require additives to make the gel polymerize. Ammonium persulfate is the initiator, and tetramethylenediamine (TEMED) is the catalyst for the reaction. TEMED causes ammonium persulfate to produce free radicals. The mixture should be degassed by purging with an inert gas. The free radical production causes the polymerization, and the mixture should be quickly put into the gel casting apparatus. The gel will form a meniscus when poured. This can be eliminated by layering a thin layer of water on top before the gel has set. The water can then be poured off after polymerization, leaving a flat surface on the gel.

Polyacrylamide gel is a commonly used electrophoretic matrix because it is useful for characterizing proteins and nucleic acids and because many samples can be analyzed on the same gel. For more on polyacrylamide gels, see SDS-PAGE and Western Blotting.

Paper Electrophoresis:

Paper was used in some of the very first electrophoresis separations. Unlike gels, paper (Whatman 3MM (0.3mm) and Whatman No. 1 (0.17 mm) requires no preparation. Paper also does not have charges that can interfere with the separation of the samples. A sample is placed directly onto the paper. At each end, there is a buffer solution where the electric field is applied. Standards and charged dyes can be combined with the samples to monitor the migration of the samples on the paper. Sample movement is best when the current flow is parallel to the fiber axis of the paper. The voltage applied to a paper matrix is higher than the voltage used in agarose or polyacrylamide because the paper's resistance is higher.

Disadvantages of paper electrophoresis are the pore size of the paper cannot be controlled as in the gels, and the technique is relatively insensitive and difficult to reproduce.

Capillary Electrophoresis:

The glass capillaries used as support media range from 20 to 200 μm in diameter and can be filled with buffer or gel. Capillaries are a suitable medium because of their high surface to volume ratio, which allows the use of high voltages without the heating effects that can be seen in gel matrices. However because of the size of the capillaries, problems with sample clearance and limits of detection exist.

Because of the size of the capillaries, sample size is correspondingly small. In a 20 μm capillary, there is 0.03 $\mu\text{L/cm}$ capillary length, 1/100 to 1/1000 of the sample volume loaded onto a gel. On-line detectors have been developed to detect these small sample amounts. These detectors use conductivity, laser Doppler effects, or lasers to detect absorbance or fluorescence.

Sample clearance in capillaries is a problem that has not been easily solved. Most capillaries are coated on their inner surface and others are filled with gel. Because of the expense of the capillaries, the capillaries cannot be discarded after use. Therefore, all of the sample has to be cleared from the capillary tube before its next use. This becomes a problem because some capillaries are 100 cm long and because some of the sample can absorb to the inner surface of the capillaries. Coating the capillaries has helped to solve some of this problem because electroosmosis along the capillary walls adds velocity to the sample and helps it to clear the capillary.

Electroosmosis is the preferred way to generate flow in a capillary because changes in the flow profile happen within a fraction of κr from the wall. Cations and anions can be analyzed in the same sample because of electroosmotic flow. For this to occur, the electroosmotic flow in one direction has to be greater than the electrophoresis of the oppositely charged ion in the opposite direction.

Capillary electrophoresis is becoming a widely used analytical technique. These separations are fast, use high voltage sources, and require a small amount of automation.

This matrix is advantageous because it avoids the heating effects that can occur in gels and because data is in the form of a chart recording instead of a stained gel. [5]

1.1.3 Application of Slab Gel Electrophoresis:

Among the different electrophoresis methods discussed above slab gel electrophoresis is the most suitable technique for separation in large quantities. To give better insight about how the technique works detailed information about it will be given.

After the gel has been prepared, wells are formed by use of a comb at one side of the gel. Figure 1.3 shows a view from the top (and at an angle) of the running tank as the gel (this case agarose) is loaded with the DNA samples. The instrument being used to load the samples is called a Micropipettor and can pipette very small volumes. In fact, 5-10 μl is all that is typically loaded into each well. In the photo, all of the wells are being used, and loading of the last well is almost complete.

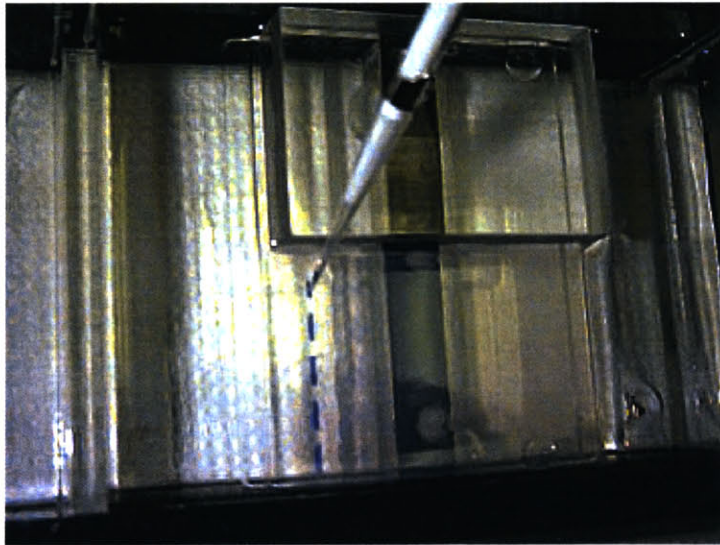


Figure 1.3, Loading of the Gel. [6]

Once the gel has been prepared and loaded, the electrical leads on the running tank are connected to a power supply like the one shown in the Figure 1.4. The power supply has 3 needle gauges on it, showing what the voltage, current, and power levels are. Power

supplies like this can be run in constant mode for any of the 3 variables, and the dials below the gages are used to set the constant level.



Figure 1.4, Power Supply. [6]

Figure 1.5 shows a run gel. A gel this size probably ran about 30 minutes at roughly 100 V in TBE buffer to advance to this point. The blue arrow shows the location of the "leading dye," the one that advanced the farthest. Always orient yourself by looking for the wells at one end of the gel. The red arrow marks the location of the "trailing dye," the dye that ran more slowly. DNA lies somewhere in between those markers. [6]

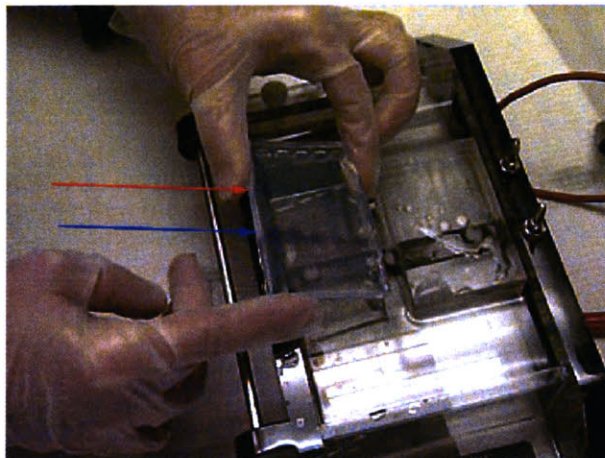


Figure 1.5, Run Gel. [6]

1.1.4 Detection Techniques

After analyzing samples by electrophoresis, the sample components are usually invisible to the naked eye. Methods have been developed to quantify the sample components. Staining techniques or autoradiography, followed by densitometry, or blotting to a membrane are frequently used.

Staining

Most popular stain used for *DNA staining* is EtBr. EtBr is an **Intercalating Agent**, meaning it wedges itself into the grooves of DNA and stays there. More base pairs mean more grooves, which in turn means more EtBr can insert itself. This is an important concept. EtBr also has the property of fluorescing under UV light. If the gel is soaked in a solution of EtBr, it will intercalate into the DNA, and then if gel is placed on or under a UV source, the DNA can be seen by actually detecting the fluorescence of the EtBr. Wherever there is DNA, a bright band at that point in the gel will be observed. More DNA exists in a lane, brighter the lane will be. EtBr can be added to a solution in which the gel soaks following electrophoresis, or it can be added to the agarose solution at the very beginning. The latter has the advantages of not requiring a soaking period after running the gel, and being able to check the gel as it is running with a hand-held UV source. The obvious disadvantage is that the gel and buffer have a carcinogen in them.

Figure 1.6 shows a stained gel under UV light.

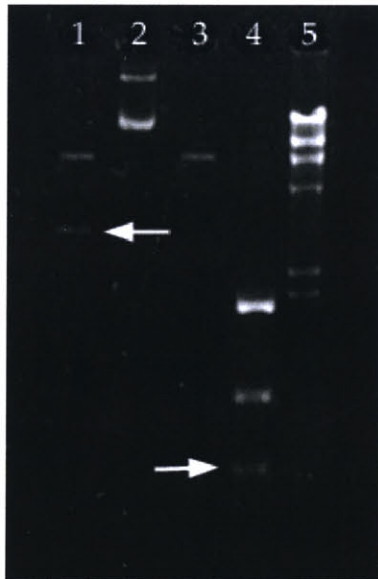


Figure 1.6, Ran Gel Under UV Light. [6]

The white bands in Figure 1.6 represent DNA of a particular size. The arrows are included to point out bands that are legitimate, yet might be overlooked as background

noise until enough gels are examined to recognize them. There exist two reasons one band is brighter than another;

- The DNA exists in equal amounts, but one fragment is larger than the other
- On a molar level, much more DNA of one size is present in that band than in a different band, although the lesser amount may be a larger fragment

Photos like Figure 1.6 are typically oriented with the wells at the top. In this particular photograph, the lane numbers are written over the wells. Smaller fragments are at the top of the photo, because they move faster.

Lanes 1-3 contain the DNA samples, perhaps from the same stock of DNA digested with 3 different Restriction Enzymes, or maybe from different pieces of DNA altogether. When one is interested in determining the success of a particular digest, often the size of these bands must be calculated. The information in lanes 4 and 5 could be used.

Lanes 4 and 5 are called “Standard Lanes” or sometimes “Molecular Weight Markers” or “Ladders”. They are similar to the “Control” in an experiment, how they are going to turn out every time is known exactly. These lanes contain DNA of a specific, predetermined size from a known source, digested with a “Restriction Enzyme” that cuts that piece of DNA a known number of times, yielding a predicted number of bands whose size known exactly. For example, Lane 5 is DNA from the *E. coli* bacteriophage Lambda, digested with *Hin* dIII. How long each of the visible fragments are exactly known.

There is a logarithmic relationship between the size of a DNA fragment and the distance it migrates on a gel, so by measuring how far the bands in various standard lanes (4 and 5 in this case) migrate, one can construct a standard curve since the fragment sizes are known. Then the distance our experimental bands migrated are measured (lanes 1-3), and plotted it on a standard curve. This will give the approximate size of the experimental fragment. The more points on the standard curve, and the more separation gotten on the gel, the more accurate approximation will be.

One important sample every experiment should include is uncut DNA. Uncut DNA exists in as many as three different forms: supercoiled, relaxed circular, and linear. Just because any RE was not added to the sample does not mean it hasn't gotten nicked or even cut at some point in its preparation. Nicking causes supercoiling to be relaxed, while cutting causes linearization. Nothing has been removed from this piece of DNA, so all 3 forms are the same size. This does not mean they will migrate the same. In Figure 1.6, lane 2 is most likely to be the uncut sample. That observation is based solely on experience in looking at gels--you would need to know exactly which sample went into each lane to be certain.

Protein staining can be done using three different stain reagents: Amido Black, Coomassie Brilliant Blue, and silver stains. Amido black is not very sensitive and less used than Coomassie Blue or the silver stains. Amido black interacts with proteins that are easily accessible, proteins that have been transferred from the gel to nitrocellulose paper. Coomassie Blue and the silver stains interact differently with more proteins and

are therefore more sensitive. Coomassie Blue, used for agarose and polyacrylamide gels, is five times more sensitive (to about 1 μ g of protein) than Amido black. Silver stains are one hundred times more sensitive than Coomassie Blue and are used with polyacrylamide gels. Silver staining is used when the protein concentration is very small or when as many bands as possible need to be analyzed. Because of its sensitivity, silver staining is more difficult to use and optimize.

After the gel has been stained, the proteins can be quantified using densitometry. The gel can be scanned or photographed, and the protein quantity can be determined by a densitometer coupled with computer software that allows comparison between bands or against a standard curve.

Autoradiography is another technique that uses densitometry to quantify the protein content. Radioactive samples are separated on a slab gel and then the gel is dried onto a sheet of paper and placed in contact with x-ray film. The film is exposed on the areas with the radioactive bands. This film can then be analyzed with densitometry.

Blotting

In blotting, the proteins on a gel are transferred to another matrix like nitrocellulose paper because the gel will not allow large molecules like antibodies or other ligands to diffuse into the gel matrix. After transfer, the nitrocellulose paper is treated with a ligand for a particular component in the sample. In Southern blots, the paper is incubated with radioactive RNA or DNA complementary to the DNA of interest. Northern blotting uses similar techniques except the strand of interest is RNA. Immunoblotting is used in western blotting where the nitrocellulose paper is treated with an antibody specific to the protein of interest. The antibody attached to the protein can then be treated with a secondary antibody, a substrate that can be detected by chemiluminescence, fluorescence, or densitometry.

SDS-Polyacrylamide Gel Electrophoresis (SDS-PAGE)

SDS, sodium dodecylsulfate, is also known as sodium lauryl sulfate. The hydrophobic tail of SDS interacts strongly with polypeptide chains.

The number of SDS molecules that bind to a protein is proportional to the length of the polypeptide. Nonreduced proteins bind 0.9-1.0 grams of SDS per gram of protein. Each SDS contributes two negative charges, overwhelming the charge already on the protein. This allows the sample to be separated only on molecular weight and not charge because the overall charge is largely negative after associating with the SDS. SDS also disrupts the tertiary structure of the proteins. β -mercaptoethanol disrupts disulfide bonds in a protein. Samples run with β -mercaptoethanol are reduced proteins and bind about 1.4 grams of SDS per gram of protein.

The electrophoretic mobility of proteins run using SDS-PAGE is inversely proportional to the log of the protein's molecular weight. Proteins with higher molecular weights travel slowest on the gel, having a lower relative electrophoretic mobility than those proteins with smaller molecular weights.[6]

1.2 Problems of Slab Gel Electrophoresis

The problems related with electrophoresis are generally in the detection process. The most crucial problem of electrophoresis process lies in the stains, which are used for visualization part. Most commonly used stains for DNA electrophoresis are intercalating and mutagenic. Being an intercalating agent means that the stain penetrates into the DNA ladder and gets physically bonded to the DNA. If the separated DNA is required to be used for further analysis, it cannot be used with the mutagenic agents it contains. It must be destained before further analysis. Destaining of DNA from intercalating agents is a costly process. Because most of the analyte cannot be recovered and gets lost during destaining. Also as the health of the operator is concerned, staining processes carries a high risk. Severe attention must be paid by the operator in order not to be exposed to EtBr. Another source of risk is the gel itself. The gel may also be dangerous. It may include hazardous chemicals in it. Another problem is the handling of the gel and excising of the band of interest from the gel. This requires manual operation and thus the accuracy may suffer. Low accuracy means waste of end product and decreased efficiency.

Therefore the problems to be addressed with electrophoresis may be listed as:

- The intercalation of stains makes it difficult to recover the biomolecules under investigation.
- This is a very low efficiency process.
- Health concerns.
- Handling problems.
- Low efficiency.

1.3 Problem Statement

The method to be presented in this thesis emerged as a part of the computer aided, robot assisted, high precision purifying machine for biologically active macromolecules. This machine is intended to blend the efficiency of gel electrophoresis system with the precision of a mini-robot and automate the whole electrophoresis process.

1.3.1 General Machine Idea

From the functional standpoint, this machine will have four-fold applications;

First, it will automate the manual electrophoretic procedures, which are routinely used all over the world by hundreds of thousands of scientific personnel. Specifically, the mini-robot system will speed up the purification of BAMs (Biologically Active Macromolecules) by:

- a) reducing the number of steps and automating repetitive steps.
- b) increasing the amount of end product by reducing the waste of the BAM.
- c) eliminating contact contamination.

Second, it should have the capability to:

- a) determine molecular weights of BAMs.
- b) quantify concentrations of BAMs.
- d) record/store data for photo-imaging.

Third, the built-in artificial intelligence of the machine should enable it to adjust to various situations and should allow a scientist to operate an experiment from a remote position, to access data in real time and to change experimental parameters at his/her will.

Fourth, it should have the capability to provide 24-hours real time on-line access to repository of molecular data (protein/DNA sequences, structural homologues, physico-chemical properties etc.) once an experimental run is complete.

A general view of the machine is given in Figure 1.7:

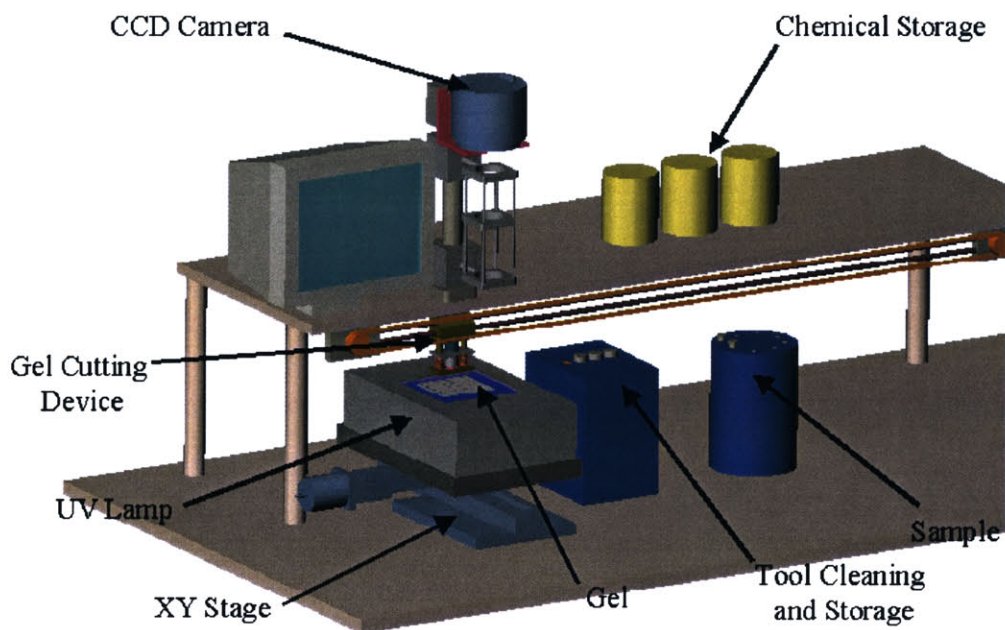


Figure 1.7, General Machine Design.

The unit including UV lamp, XY stage and the CCD camera is the visualization unit. After the gel is run this unit makes it possible to detect the BAMs bands in the lanes. After the bands are detected a map of band locations are displayed on the monitor. Through the computer interface the user can select the bands of interest. The selected bands are excised by gel cutting device and stored in sample storage for further use. The gel cutting device is then cleaned in the compartment named as tool cleaning and storage.

1.3.2 The Detection Problem in Electrophoresis:

As stated earlier one of the important problems associated with electrophoresis is the detection of bands after the gel is run. If the DNA is being separated then EtBr must be used as stain which has some health risks. With the robotic purification system explained above the health risk associated with staining is to be eliminated. First of all the handling of the gel is to be performed automatically by the help of robotic arms, preventing the contact of operator with gel. Second, no staining will be used making the further study and use of BAMs possible once they are excised out of the gel.

The focus of this thesis is to devise a detection system that will be stain free and generic (to be used for all different kind of BAMs). Since the whole BAMs spectra include a wide variety of different molecules it is a rather tough task to come up with a generic method. Thus priority will be given to DNA, which is the most common BAMs used in labs, and a solution will be sought initially for DNA detection. While doing this, the applicability of the proposed method to other BAMs will be born in mind as a prerequisite.

1.4 References

- 1) <http://www.bergen.org/AAST/Projects/Gel/intro.htm>
- 2) Jacqueline Kroschwitz, ed., *Encyclopedia of Chemical Technology*, 4th ed., John Wiley & Sons, 1994, p. 356.
- 3) Alan Townshend, ed., *Encyclopedia of Analytical Science*, vol. 2, Harcourt Brace and Company, 1995, p. 1041.
- 4) Jorgenson, J. W. *Analytical Chem*, **1986**, 58, 7, 743A.
- 5) <http://hendrix.pharm.uky.edu/che626/electrophoresis/matrix.html>
- 6) <http://www.life.uiuc.edu/molbio/geldigest/electro.html>

2. DIFFERENT SOLUTIONS FOR IMAGING PROBLEM

In this chapter different detection methods that can be used will be discussed. The candidates will be required to have some specifications, which can be listed as;

- Stain free operation, so that a clean end product may be obtained.
- To be generic, so that any BAMs may be detected.
- To be fast enough to be able to map all the band locations before the gel shrinks. Gel shrinkage is an important problem. When the gel is exposed to air it shrinks by time leading a distortion in shape. A shape distortion means the corruption of acquired band location information.
- Enough resolution to be able to detect small enough amounts.(below 500 nanogram)

2.1 Laser Induced Fluorescence (LIF)

Laser induced fluorescence (LIF) is a spectroscopy technique that is generally used in capillary electrophoresis. A molecule of interest is excited by a laser. When excited by a laser, it emits fluorescence at a wavelength. By detection and analysis of this emitted fluorescence, the sample may be characterized. A simple LIF system is shown in Figure 2.1.

A simple LIF detector requires only a laser beam passing through the capillary to excite the analyte, a microscope objective at 90 degrees to the laser to collect the fluorescence emission, and an optical filter and PMT to measure the emitted light.

Figure 2.1 shows an LIF system as a part of capillary electrophoresis (CE) system. Capillary electrophoresis (CE) is a technique in which an electrophoretic separation takes place in a narrow-bore fused silica capillary. The capillaries typically used in CE are commercially available at reasonable cost.

In a CE separation, the capillary is filled with buffer and each end is immersed in a vial of the same buffer. A sample of analyte is injected at one end, either by electrokinesis or by pressure, and an electric field of 100 to 700 volts/centimeter is applied across the capillary. As the analyte mixture migrates through the capillary due to the applied electric field (electrophoresis), differing electrophoretic mobilities drive each of the components

into discrete bands. At the other end of the capillary each of the separated analytes is detected and quantified.

Electrophoretic mobility is proportional to the charge of the molecule divided by its frictional coefficient. This is approximately equal to the charge to mass ratio of the molecule. So in general any molecules with differing charge to mass ratios can be separated by CE. Figure 2.2 is an attempt to help demonstrate this.

Focusing back on LIF method again, the analyte entering the sheath flow cuvette is delivered by the capillary, which is a component of CE. Rather than directing the laser beam through the capillary, the analytes are detected as they leave the capillary using a sheath flow cuvette. [1]

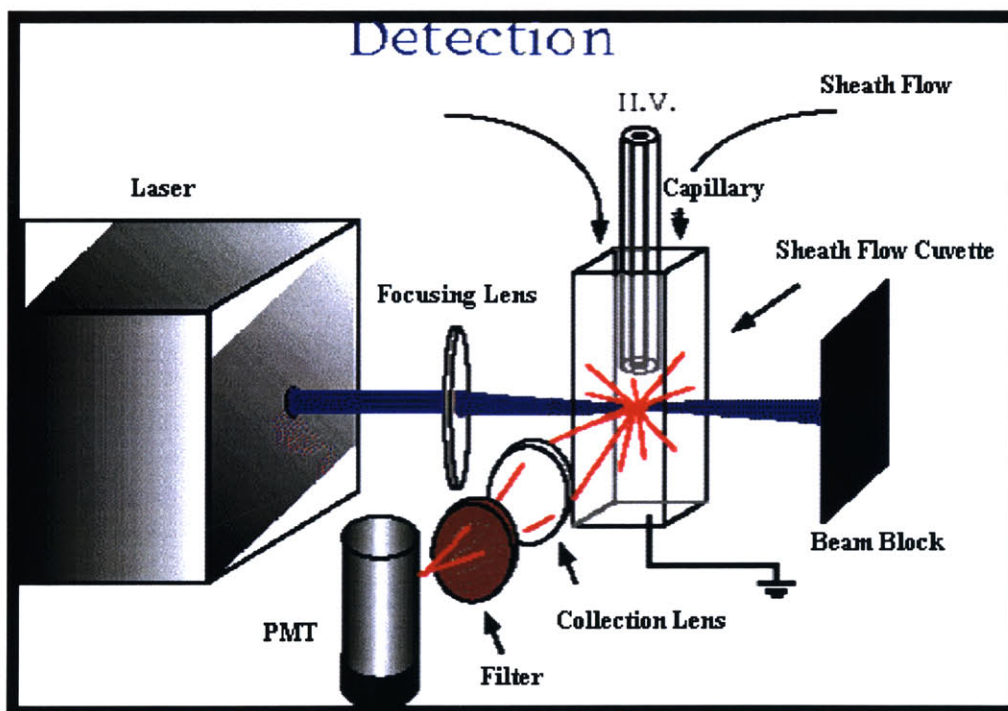


Figure 2.1, Laser Induced Fluorescence Setup. [1]

A sheath flow cuvette is simply a rectangular piece of optical quartz that has a square channel slightly larger than the outer diameter of the capillary running through it. The exit end of capillary fits snugly in this channel and the laser is focused to a point just below the tip of the capillary. A stream of buffer (the sheath flow) is constantly flowing around the capillary and acts to hydrodynamically focus the analyte stream in front of the detection optic. (The flow stream also carries the analyte to a waste reservoir following detection.)

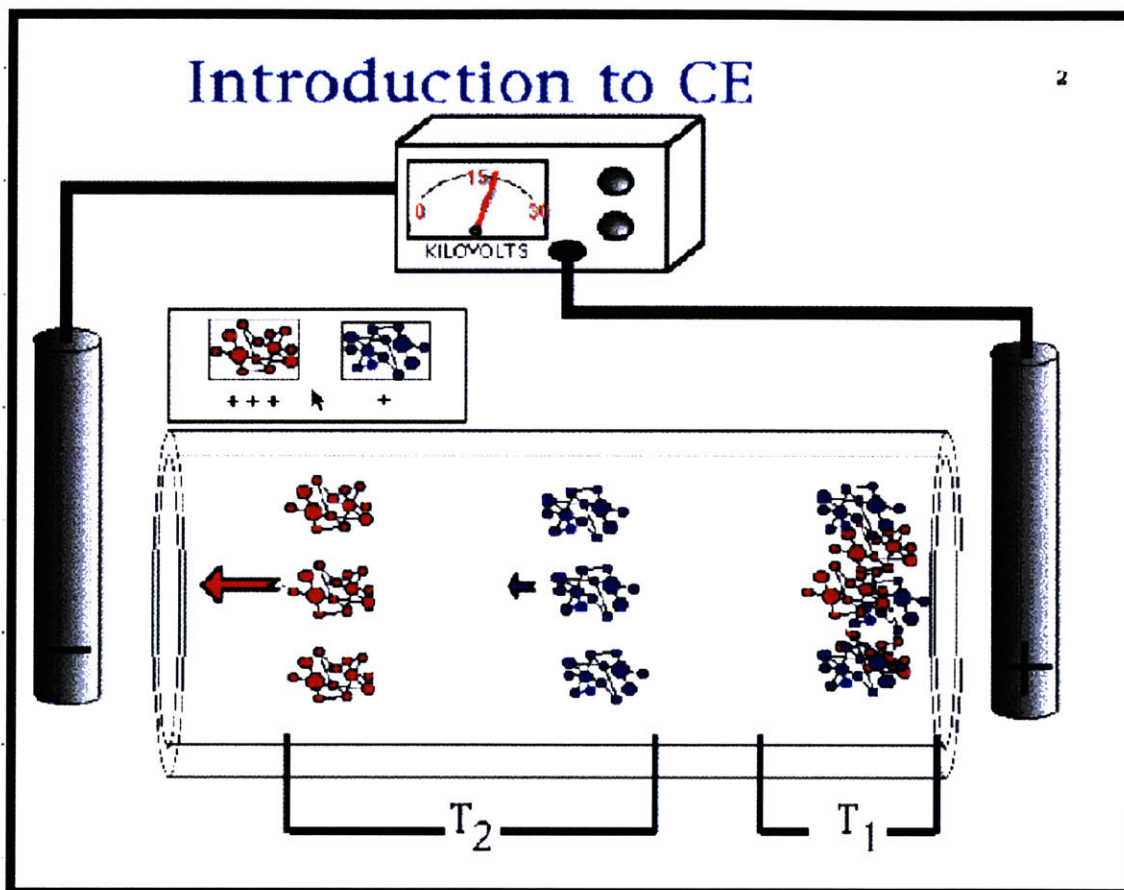


Figure 2.2, Introduction to CE, Basics of Molecular Movement in the Capillary. [1]

LIF technique has a high resolution has been generally used with CE. Because it is most effective when the analyte has direct contact with the laser having no obstacle on between. The nature of CE makes is possible to prepare such setup by use of a sheath flow cuvette. But while a slab gel can analyze several samples at once, CE instrument only one sample at a time. To keep pace with slab gel electrophoresis from an output rate standpoint, CE instruments needs to use tens and even hundreds of capillaries simultaneously. LIF uses stains to detect different kinds of analytes. Most common stains used for LIF include EtBr, thiazole orange TO-PRO-3 dye. [2]

But all of these stains are intercalating stains and conflict with our target of stain-free system. An LIF system needs different lasers to excite different analytes. This requires use of multiple lasers to accomplish a generic system. Or a variable laser may be used, but that will make the system cost very high.

2.2 UV Absorption Method

UV absorption method is another candidate method. Most analytes absorb at different wavelengths in UV region and this fact makes it possible to use UV absorption technique to detect the band locations in the gel. Beer-Lambert Law can explain the theory that lies behind UV absorption method.

The Beer-Lambert law:

The Beer-Lambert law (or Beer's law) is the linear relationship between absorbance and concentration of an absorbing species. The general Beer-Lambert law is usually written as:

$$(2.1) \quad A = a(\lambda) * b * c$$

where A is the measured absorbance, $a(\lambda)$ is a wavelength-dependent absorptivity coefficient, b is the path length, and c is the analyte concentration. When working in concentration units of molarity, the Beer-Lambert law can be written as:

$$(2.2) \quad A = \varepsilon * b * c$$

where ε is the wavelength-dependent molar absorptivity coefficient with units of $M^{-1} \text{ cm}^{-1}$. Experimental measurements are usually made in terms of transmittance (T), which is defined as:

$$(2.3) \quad T = I / I_0$$

where I is the light intensity after it passes through the sample and I_0 is the initial light intensity. The relation between A and T is:

$$(2.4) \quad A = -\log T = -\log (I / I_0).$$

Figure 2.3 depicts light absorption by a sample. [4]

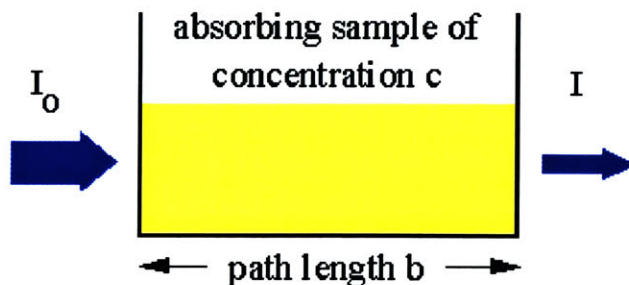


Figure 2.3, Absorption of Light by a Sample. [4]

Modern absorption instruments can usually display the data as either transmittance, %transmittance, or absorbance. An unknown concentration of an analyte can be determined

by measuring the amount of light that a sample absorbs and applying Beer's law. If the absorptivity coefficient is not known, the unknown concentration can be determined using a working curve of absorbance versus concentration derived from standards.[4]

A working curve as shown in Figure 2.4 is the plot of analytical signal as a function of analyte concentration. These working curves are obtained by measuring the signal from a series of standards of known concentration. The working curves are then used to determine the concentration of an unknown sample or to calibrate the linearity of an analytic instrument.

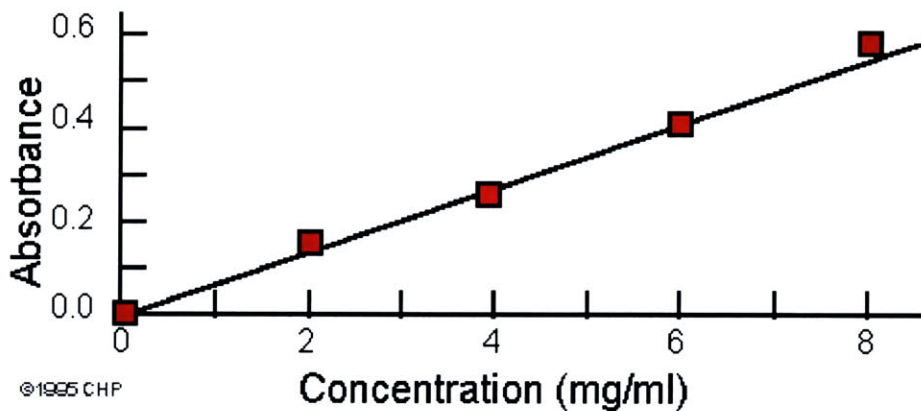


Figure 2.4, Example of a Working Curve. [4]

UV absorption method relies on the Beer-Lambert Law and the theory underneath it is quite simple. When the gel is illuminated, the regions which contain analytes of any kind absorb at a specific wavelength. When the intensity of light passed through the gel is detected at specific absorption wavelengths, behind the regions where analytes are located the intensity of transmitted light should be lower. Using this fact the analyte bands in the gel can be visualized. Looking at the literature, one of the earliest hybrid approaches utilizes UV absorption in conjunction with shadowing technique [2]. The gel is illuminated with UV light from bottom and is covered with a glass plate. Glass plate acts as an overlying fluorescent material. When excited by UV light the glass plate emits in visible range. At band locations some fraction of the UV light is absorbed. At his location less UV light impinges on the glass plate, resulting in less fluorescence emission. When the glass plate is visualized the darker regions will be DNA (or analyte) bands. The sensitivity of the method was around 0.5 μ gram.

A more recent approach employing UV absorption technique employs a CCD camera as a detection unit. [3]

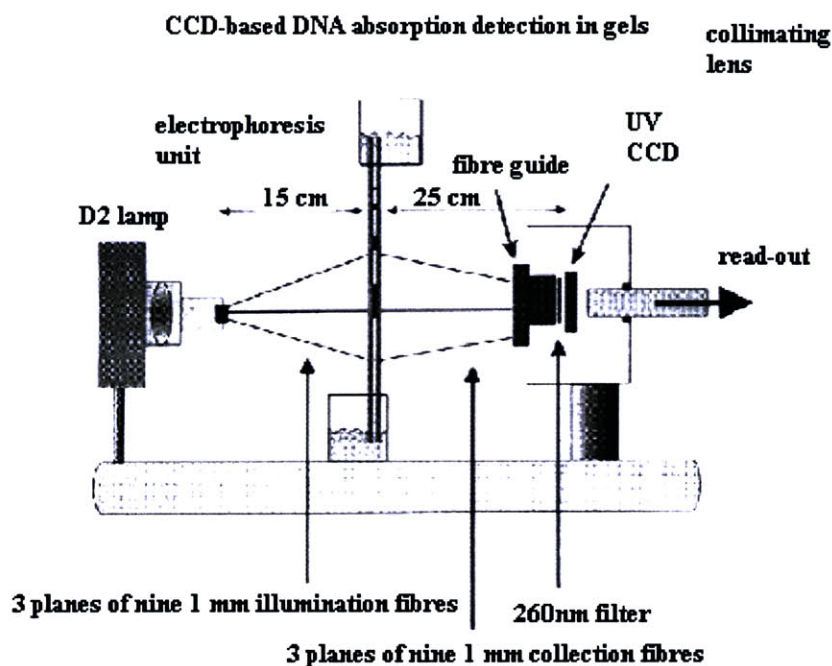


Figure 2.5, CCD Based DNA Detection in Systems for Electrophoretic Gels. [3]

Figure 2.5 shows the system setup. Gel is run in horizontal direction and is located in the middle. It is illuminated by a deuterium lamp, which is located at the left side. A collimating lens system is used to collimate the light before it falls on the gel. At the right side of the gel there is the CCD camera with a bundle of optical fibers attached on top of it. When the gel is run as time progresses the DNA moves upward. As DNA bands pass across the center line of UV light, an attenuation is detected in the transmitted signal through the gel. So time vs. intensity plot helps to correlate the band locations as long as the speed of analyte motion is known.

UV absorption technique can be used as a stain free detection method. But so far the biggest problem was the resolution of the sensors used for detection. Due to limited detection capacity direct detection UV absorption method without any stains was not very suitable. But the recent developments made it possible to use CCD cameras with high Quantum Efficiency (QE) as detectors. As mentioned above 2-10 ng resolutions have been achieved. Compared to the 0.1 ng resolutions, which are quite common with the stained detection techniques, the result is promising considering the fact that there is still room for improvement of QE of CCD detectors.

2.3 Method Comparison and Proposed Technique

The features of two methods discussed above can be tabulated in a table as follows;

<i>Method Name</i>	<i>Stain Free</i>	<i>Resolution</i>	<i>Ease of Application</i>	<i>Cost</i>	<i>Overall</i>
LIF	1	5	2	4	12
UV	4	4	4	3	15

Table 2.1 Method Comparison.

As it can be seen from above comparison UV absorption method is a better choice for our purpose and targets. Using UV absorption method a new approach will be taken. The UV absorption will be incorporated with a scanning approach. The proposed technique may be explained as follows:

- UV absorption technique will be used as detection method
- A high QE CCD camera will be used as the detector.
- An X-Y stage will be used to scan the entire gel area.
- The change in intensity of the recorded signal will be analyzed to locate the bands in the gel.

Figure 2.6 shows a plot of the overall system design.

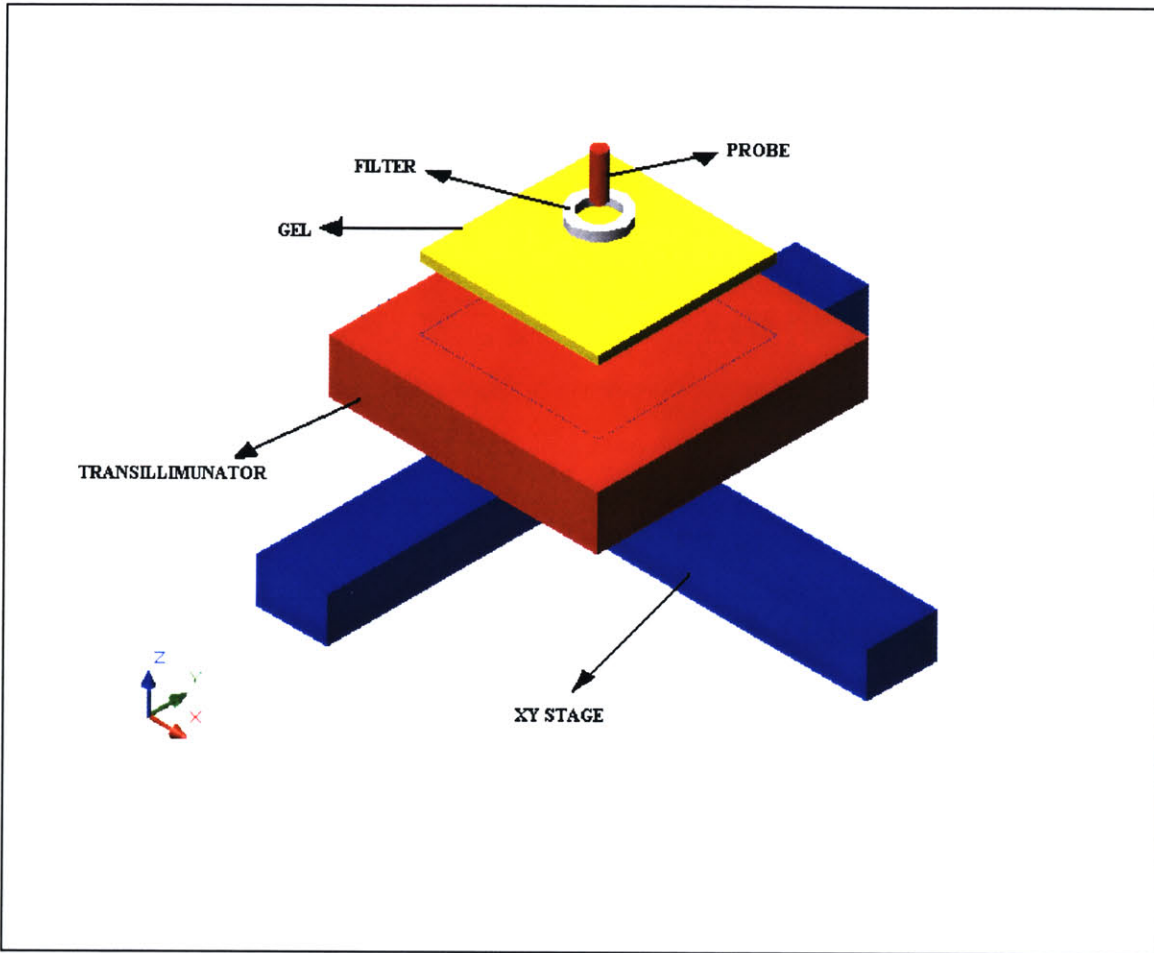


Figure 2.6, Overall System Design.

The method relies on UV absorption technique on the detection side. The basics of the method have been explained in the previous section. DNA absorbs at 254 nm, proteins absorb at 230 nm and RNA absorbs at 280 nm. A system that can analyze the gel in these different wavelengths will make it possible to identify a big variety of analytes. As the detector a CCD camera with a high QE will be used. The CCD camera will not be used as it is used for imaging. Since the change in intensity of the light transmitting through is of interest, the CCD surface will simply be used as a detector. To increase the resolution the pixels of the CCD array will be binned. So basically, the function of the CCD will be accumulating light falling on its surface and generating a signal proportional to its intensity. A fiber optic probe will be used to pick up the light and it will be transmitted by a fiber cable and be reflected on the CCD array. An XY stage will make it possible to scan the lanes in 2D and construct an absorption plot. And from the absorption plot the band locations can be determined. The details of each system component will be explained in next chapter.

2.4 References

- 1) <http://hobbes.chem.ualberta.ca/~chris/ceover/cesheath.html>
- 2) A. Guttman et al., *Journal of Chromatography A*, 828 (1998), 481-487
- 3) A. R. Mahon et al, *Med. Biol.*, 44 (1999) 1529-1541
- 4) <http://elchem.kaist.ac.kr/vt/chem-ed/specs/beerslaw.htm>

3. GENERAL DESIGN OF THE SYSTEM

3.1 Overview of the Hardware

As mentioned in Chapter 2, the whole purification system will include many units, which are used for different functions. What will be focused in this thesis is the detection unit of the whole machine. The method for detection has been discussed in previous chapter also and it will allow stain-free detection of analyte bands in an attempt to maximize the amount of end product from the electrophoresis process. In this chapter individual components of proposed detection system will be introduced.

3.1.1 Light Source and Filter

The primary target of the detection system will be detecting DNA in the gel. So a UV source centered around 254 nm is required since DNA has an absorption band around 254 nm. The UV source chosen for this purpose is a single UV wavelength transilluminator from Ultra-Lum Company. A transilluminator is a box that contains UV bulbs and controlling electronic circuitry with a screen at the top surface through which a constant UV light flux goes out. Figure 3.1 shows the UV transilluminator used.



Figure 3.1, UV Transilluminator. [1]

The size of the transilluminator is 400x240x100 mm. The light screen is 150x150 mm. It contains 4 UV bulbs of 8 W/cm power. It has 4 levels of power settings and the power can be set to 33%, 66% or to 100%. The spectrum is presented in Figure 3.2.

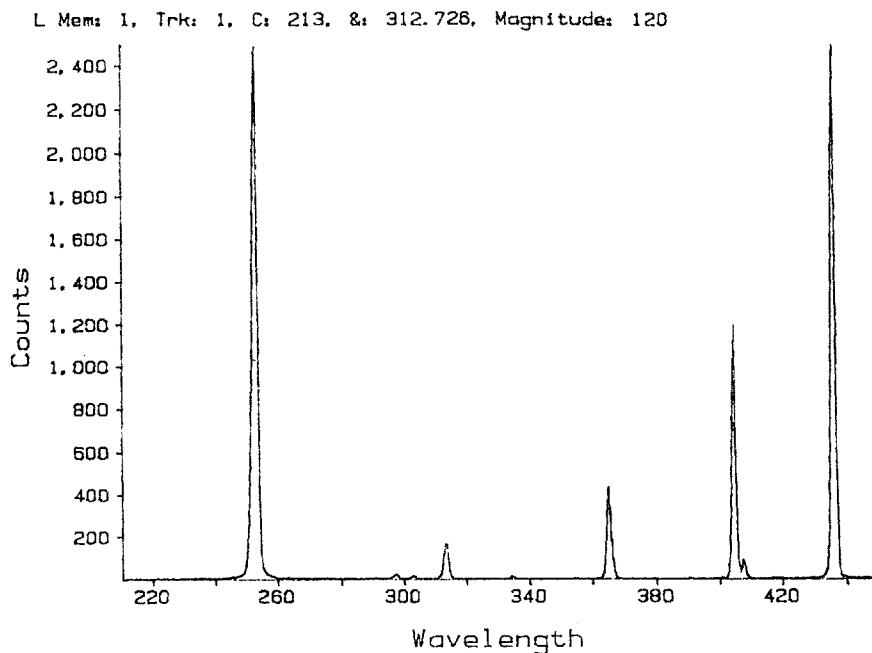


Figure 3.2, Spectrum of the UV Transilluminator. [1]

This illuminator can supply only one wavelength at 254 nm. It is only for our primary goals and later it will be replaced with a novel UV light source design that make it possible to work at different wavelengths for different analytes.

Although the transilluminator has an emission peak around 254, for the robustness of the experiment and ease of data acquisition it is beneficial to use a band-pass filter centered around 254. By using a filter everything except a range centered around 254 nm is cut off. As a result whatever falls on the CCD array are the wavelengths of interest and contribution to the signal generated is only from these wavelengths. If there are still some contributions from different wavelengths as a result of scattering or reflection from the ambient objects, this unwanted contributions could be eliminated by software filtering. Transmittance plot of the filter is presented in Figure 3.3.

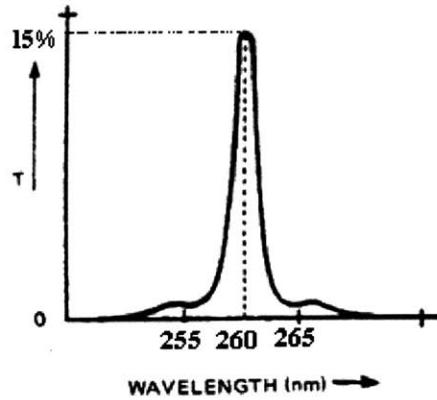


Figure 3.3, Transmittance Graph of the Band-pass Filter. [5]

3.1.2 CCD Camera and the Spectroscopy System

A spectroscopy system from Acton Research utilizing a CCD camera is used for detection. System used is a complete spectroscopy acquisition system that features a choice of back-illuminated and UV-coated Hamamatsu CCD in 1024 x 256 pixel format. The system comes standard with a 100-kHz, 16-bit analog-to-digital (ADC) converter and a 12-bit, 1-MHz ADC for rapid kinetics and fast system alignment. Acton Research SpectraSense™ software provides integrated acquisition versatility. As part of the packaged system, Acton Research SpectraPro150 spectrometer is also included. The QE (Quantum Efficiency) plot of Hamamatsu CCD is given in Figure 3.4. The CCD used in the spectroscopy setup is a back-thinned CCD and as it can be seen from Figure 3.4 has a considerably higher (50%-80%) QE in the UV range (200-400 nm) than front-sided CCD. This makes the spectrograph work in the UV range as well as visible range.

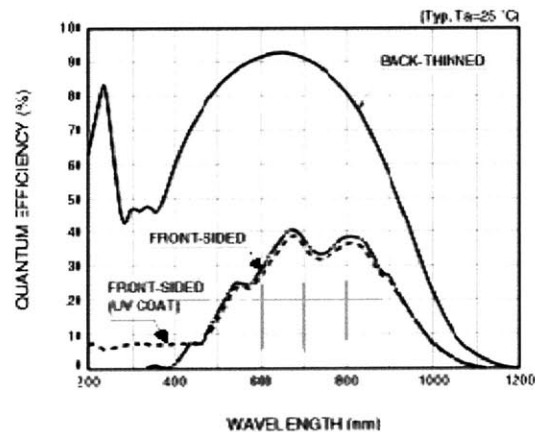


Figure 3.4, QE (Quantum Efficiency) of the CCD Array. [2]

A block diagram describing the working principle of CCD Spectrograph is given in Figure 3.5. Light emerges from light source and goes through the sample chamber. After it passes through the sample chamber it is collected by the fiber probe. Fiber probe consists of 8 fibers arranged in 2 rows. The light is transmitted into the spectrograph, which consists of reflector mirrors and gratings. The CCD detector is placed at the exit of the spectrograph. The light separated into wavelengths falls on the CCD surface and is converted into spectral information by the help of electronics and sent to the computer. At the computer the intensity vs. wavelength plot is generated. There are two A/D cards, one is 12 bits and another 16 bits. The 12 bits A/D card is suitable for applications requiring high-speed data acquisition. In applications favoring resolution over speed 16 bits card is preferred. Since in our case resolution is more important and the spectrograph operates at moderate data acquisition speeds, 16 bits A/D card is to be used. Choice of 16 bits A/D card creates intensity levels from 0-65535 units. The use of spectrograph system with a CCD camera detector in the system gives the spectral plot in the whole UV region. What is needed for DNA is the absorption characteristics around 254 nm. So it may be argued that a spectrograph is not really needed for this purpose, which is true. For the further phases of the projects light sources and lens systems which makes it possible to analyze certain wavelength regions of interest are to be designed to circumvent the complexity and cost of a spectroscopy system in the final product. In phase it is merely preferred due to its construction simplicity as an on-the-shelf product to gain time.

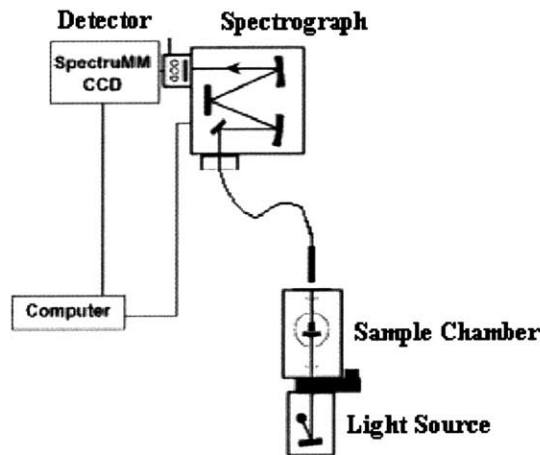


Figure 3.5, Spectrometer System. [3]

3.1.3 X-Y Table

For scanning process 2 dimensional motion is needed. For this purpose a 402LN Series table from Daedal is used. The 402LN Series tables are the smallest motorized linear positioners offered by Daedal. They are “all metric” tables with a linear square rail bearing system and either a leadscrew drive or a ballscrew drive for higher efficiency and duty cycle. They are designed for repeatable positioning of light payloads over short travels, and can be utilized in applications requiring horizontal, inverted, or vertical translation. They have a profile is only 32 mm X 60 mm *or* 1.3 inches X 2.4 inches. Figure 3.6 shows a picture of a 402 LN Series XY table.

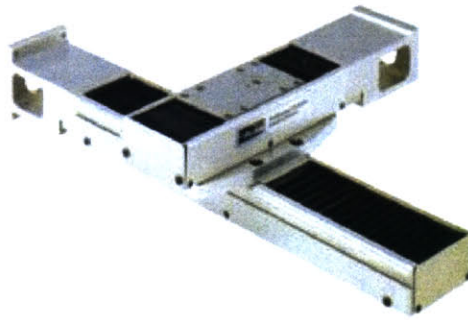


Figure 3.6, 402 LN Series XY Table from Daedal. [4]

The specifications of the table used are given in Figure 3.7.

Specifications		402006	
Travel		6	(150)
Life @rated specification X1 million inches (mm)		10	(250)
Positional Accuracy x0.001 in (mm)	Std Grd	2.9	(75)
Over Total Table Travel	Prec. Grd.	0.46	(12)
Positional Repeatability x 0.001 in (mm)	Std Grd.	± 0.46	(± 12)
	Prec. Grd.	± 0.078	(± 2)
Straight Line Accuracy x0.001 in (mm)	Std Grd	0.93	(24)
	Over Total Table Travel	Prec. Grd.	0.31
Flatness Accuracy \varnothing 0.001 in (mm)	Std Grd.	0.93	(24)
	Over Total Table Travel	Prec. Grd.	0.31
Max Screw Speed \varnothing rps	Std Grd	15	
	Prec. Grd	25	
Max Acceleration \varnothing in/sec (mm/sec)	Std Grd	386	(9800)
	Prec. Grd	386	(9800)
Duty Cycle \varnothing % of motion to dwell per cycle	Std Grd	50	
	Prec. Grd	75	
Direct Loading*** \varnothing lbs (kgf)	Normal	160	(72.7)
	Inverted	40	(18.2)
Load per Bearing \varnothing lbs (kgf)	Both grades, Normal	40	(18.2)
	Inverted	10	(4.5)
Axial Loading \varnothing lbs (kgf)	Std Grd	10	(4.5)
	Prec. Grd	28	(12.7)
Input Inertia** $\varnothing 10^3$ oz-in-sec ²		0.812	(0.585)
Maximum Running Torque \varnothing oz-in (N-m)		12	(0.0847)
Maximum Breakaway Torque \varnothing oz-in (N-m)		13	(0.0932)
Drive Screw Efficiency \varnothing Std & Prec Leadscrew \varnothing %		30	
Coefficient of Linear Bearing Friction		0.01	
Carriage Weight \varnothing lbs (kgf)		0.14	(0.06)
Longitudinal Span between Bearing Truck Center		1.485	(37.7)
Lateral Span between Bearing Rail Centers		1.456	(37.0)
Bearing Rail Center to Carriage Mounting Surface		0.541	(13.7)
Table Weight - lbs (kgf)		3.12	(1.42)

Figure 3.7, Specifications of the XY Table. [4]

The table used is a 4020006 series table which has 150 mm travel in X and Y directions. It has a positional accuracy of 75 μ m and a positional repeatability of 12 μ m. The width of possible smallest lane is around 1 mm, so the desired step size is 0.1 mm and this table with a positional accuracy of 75 μ m is capable of achieving the desired motion. The stages are driven by stepper motors from Compumotor. A digital I/O card is used to generate and send pulses to the power amplifier, which is connected to the stepper motors.

Technical drawings of the XY table are given in Figure 3.8.

Miniature Linear Positioning Systems

40200LN Series Dimensions

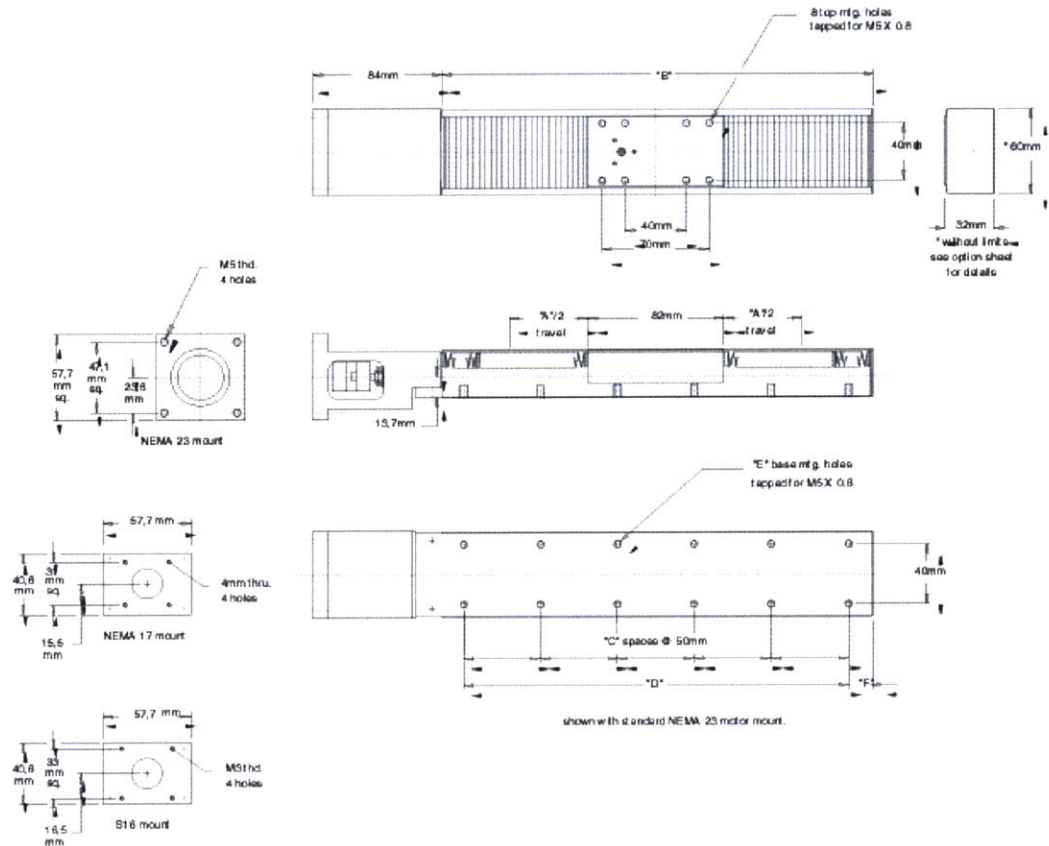
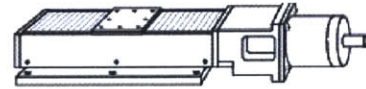


Figure 3.8, Technical Drawing of the XY Table. [4]

3.1.4 Fiber Probe, the Transilluminator and Gel Tray Holder

The fiber probe is used to collect the signal from a specific point. A picture of fiber probe is presented in Figure 3.9. It is cylindrical in shape and includes 8 fibers bundled in it. There is a cable attached at the back of the probe head, which covers the fiber bundle. The cable is inserted into the entrance slot on the spectrometer.

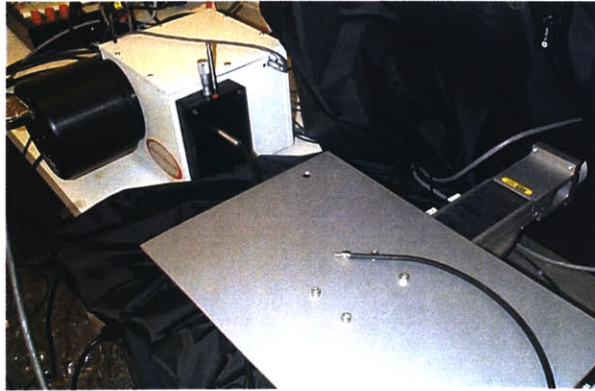


Figure 3.9, Fiber Probe Attached to the Cable.

Another part of the design is the frame holding the transilluminator. Figure 3.10 shows this part. To see the uniformity of the transilluminator power, transilluminator surface has been scanned. It was observed that there is 10-15 percent variation of transilluminator power along a horizontal line (Figure 3.11). When different horizontal lines are scanned the variation is even more. This is due to the construction of transilluminator, which contains four UV bulbs placed side by side with some distance. This introduces power level irregularity in vertical direction. This is a significant error source and must be taken care of for reliable results. One solution for this problem is to scan the background and make a background subtraction. Time wise this operation is very costly and accurate background reading and gel reading coordinate match is very tough to achieve due to the soft, weak structure of the gel. In order to circumvent this problem another more applicable approach is to fix the light power falling on the fiber probe. This is possible if probe is fixed on a single point on transilluminator surface. And this necessitates the use of a proper fixture. The fixture designed holds the transilluminator in air. This is named as transilluminator holder (Figure 3.10). Another fixture used helps to carry the gel tray on the XY table (Figure 3.12). So that when the XY table moves the gel tray moves with it. The probe is suspended and is fixed in space. The relative motion required for scanning the gel is provided by holding the probe and transilluminator fixed and translating the gel tray.



Figure 3.10, Frame Holding the Transilluminator and Gel Tray

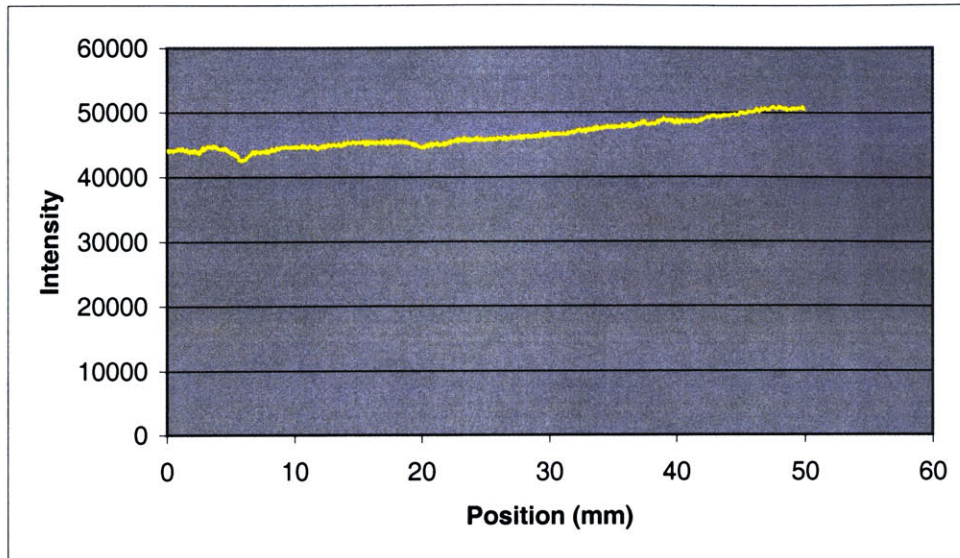


Figure 3.11, Variation of Power Level of the Transilluminator Along a Horizontal Line.

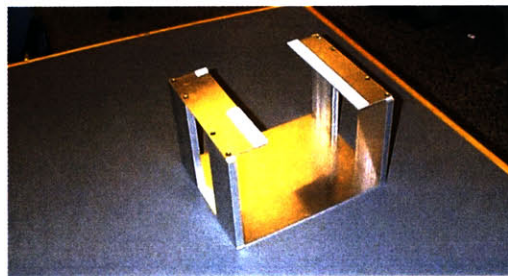


Figure 3.12, Fixture Used to Carry The Gel Tray on the XY Table.

3.2 Overview of the Software

A software is needed to control the motion of stages and to control the spectrometer to acquire the data.

3.2.1 Description of User Interface

A Windows based user interface has been programmed in order to accomplish the above tasks. C++ Builder is used for rapid graphic user interface development. The built-in class libraries of C++ Builder are utilized to build the graphical user interface. Underlying code is generated in C++. The user interface consists of two pages. Figure 3.13 shows the first page of the interface. It includes controls to move the XY table either by a number of steps or to a specified positions. Also the absolute coordinates of the platform located on XY table are displayed on this page. Figure 3.14 shows the second page of the interface. On this page there are controls to choose step size for scanning, location for files to be saved and length of the scan and also to process the acquired data. There is also a graphic window on this page to display the outcome of the processed data. Individual functionality of each button and edit box on the form may be explained as follows:

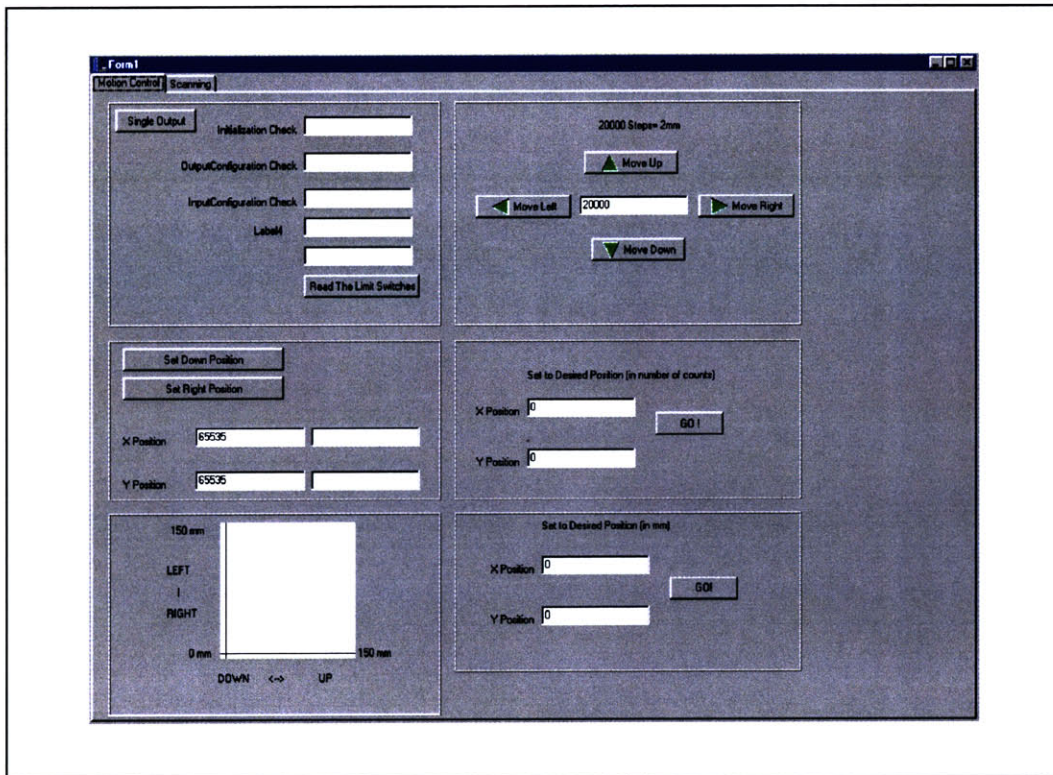


Figure 3.13, First Page of the User Interface.

Page 1 of the User Interface:

Number of Steps Edit Box: Specifies the number of steps each time the stage will move in selected direction.

X Position: Displays the absolute X coordinate.

Y Position: Displays the absolute Y coordinate.

Move Up: Moves stage upward by specified number of steps.

Move Down : Moves stage downward by specified number of steps.*Move Left*: Moves stage left by specified number of steps.

Move Right: Moves stage right by specified number of steps.

Set X Position Edit Box in Number of Steps: Specifies the absolute X position to move to in number of steps.

Set Y Position Edit Box in Number of Steps : Specifies the absolute Y position to move to in number of steps.

Set X Position Edit Box in mm: Specifies the absolute X position to move to in mm.

Set Y Position Edit Box in mm: Specifies the absolute Y position to move to in mm.

Set Right Position: Parks the stage to the rightmost position.

Set Up Position: Parks the stage to the up most position.

There are also some Edit Boxes at the upper left corner of the page; they are used as to display check information to verify the trouble free operation of the staged. Since they serve for debug purposes, they are not explained in detail. Also there is a coordinate plot at the lower left corner of the page which shows the absolute coordinates of the stage position graphically.

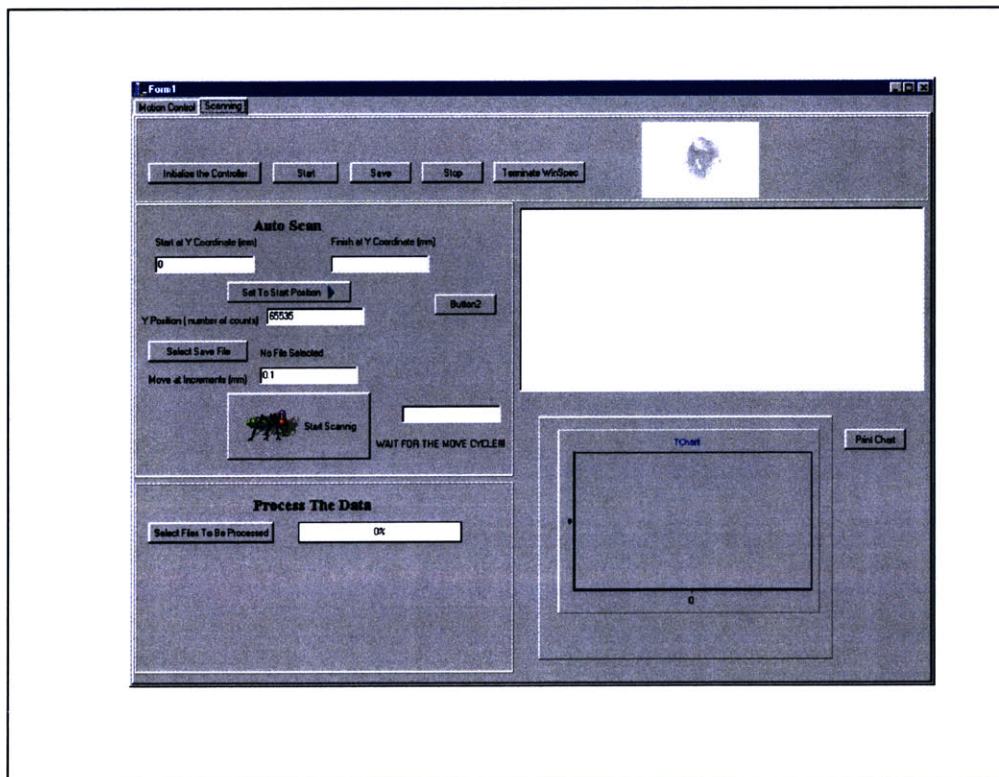


Figure 3.14, Second Page of the User Interface.

Page 2 of the User Interface:

Star at Y Coordinate (mm): Sets the starting coordinates in mm of the scan.

Finish at Y Coordinate (mm): Sets the end coordinates in mm of the scan.

Set to Start Position: Moves to start position.

Move at Increments (mm): Sets the step size for scan in mm.

Select Save file: Pops up a window to choose name and location for data files to be saved.

Start Scan: Starts the scanning operation.

Choose Files to Be Processed: Pops up a window to choose the files to be processed and processes the files. Result is plotted as a graph on the plot area at the lower right corner.

There are some buttons at the very top of the page which are used for debugging. Hence they will not be explained in detail.

3.2.1 Algorithm to control the X-Y stage Control

XY Table used in the design is driven by two stepper motors. The motors are from CompuMotor and they can be run in different modes. The mode of operation can be set by the switches on the power amplifier. Two signals are sent to the motor. The preferred mode of operation is to send the direction of motion as the first signal and number of steps as the second signal. The direction signal is either a TTL logic one or zero. Number of steps signal is a square wave signal. Each transition from logic zero to logic one represents a step. Hence it is required to send as many square waves as the number of desired steps. A PCI-6530, Digital I/O board from National Instruments is used to generate the square wave signal. The digital I/O board comes with a C++ library makes incorporation in a C program easily possible. There are set of commands to control the board. There is no command to generate a square wave, so a simple algorithm is needed. To form a square wave consecutive logic level ones and zeros are generated. The digital I/O board has no timer on it. The frequency is dependent on the speed of the computer and hardware speed of I/O board. The default frequency of square wave generation is around 100 khz. What determines the duration of a pulse (length of either a logic zero or one) is the time it takes to generate the command in the computer plus the time it takes to perform the action in the digital I/O board. The default frequency obtained is the maximum possible and due to the lack of on-board timer cannot be made faster. It is possible to make it slower by software delays. Since at this phase of the project data acquisition takes a longer time, the speed of the stage is sufficient. In the next phase of the project a faster board may be used if necessary. The stage is capable to move in four directions namely up, down, left and right. The extent of travel in these directions is controlled by four limit switches. The feedback signal from these switches is read by the digital I/O board. The algorithm of motion can be explained as follow:

- Get the direction of motion and generate the direction signal accordingly.
- Send the signal to the motor.
- Get the number of steps
- Generate the square wave signal and send it to the motor.

- After every square wave sent check whether the limit switches are reached. There is a software filter to clean the spikes that interfere with the feedback signal. This way accurate motion is achieved.
- If a limit switch is reached a warning window is displayed and motion is halted
- Home position is rightmost and up most position. Using the feedback information from the limit switches it is possible to park the stage to home position. An extra home switch is not needed.

3.2.2 Spectra acquisition from the spectrometer using COM technology

Spectral data is acquired by the spectrometer which comes with a software that makes it possible to control the operation of the spectrometer. The movement of the stages and data processing which will be mentioned in next chapter is achieved by the main software written on C++. Spectrometer software is a standalone software and from overall software point of view for smooth operation it must be incorporated into the main software. To incorporate the capability of the spectrometer software seamlessly into the written C++ code, COM (Corba Object Model) technology was used. COM technology allows the encapsulation of a standalone software into a C++ class. Such an encapsulation makes it possible to evoke menu calls of standalone software as C++ function calls. If a software supports COM technology the COM object of that software is automatically generated and registered to Windows Registry when the software is installed. When a specific COM object is included in a C++ project, its library file is generated by the compiler and function declarations become available for the programmer if they are already not in accompanying programmer's manual of the software. After that COM object is accessed same as a DLL library is accessed. It is enough to type the function names needed to be called, the compiler resolves the addresses and evokes the called function. Using COM technology, first a COM object of the WinSpec (name of the spectrometer software) software is initialized. Then at every step of scanning motion the functions in charge of data acquisition and saving the data to the hard disk are called. This way the spectral data along the scan path is recorded. The code written is presented in Appendix A.

3.3.3 Data processing

As explained in the previous chapter the method to be used for the detection of analytes in the gel is the UV absorption method. The implementation of the offered technique for visualization can be summarized as follows:

- Place the gel on the gel tray and adjust the probe with the start point of the lane to be scanned.
- Set the scanning distance and step length of data acquisition through the software.
- Initialize COM object of the spectrometer software in order to control the spectrometer.
- Move the stage as described by step length and at every step acquire the spectra of the light coming through the gel and the pass-band filter above it.

- Store the data on the hard disk.
- Continue till the last point of the scanning path.
- Process the collected data and show the results in a plot.

In this section the processing of data will be elaborated.

When data is acquired by the use of spectrometer software it is saved in a special SPE format that is recognizable by the WinSpec software. When a SPE file is opened by the WinSpec software a plot similar to the one presented in Figure 3.15 is obtained.



Figure 3.15, An SPE Format File Opened in WinSpec.

Figure 3.15 is a typical spectral data obtained during scanning. A big peak is observed around 260 nm around where the band-pass filter is centered. Under ideal conditions no other wavelengths are expected to be seen on this plot due to the existence of band-pass filter. But since there is a clearance between the probe and the upper filter surface, which it faces, visible light reflecting from the filter surface falls on the probe and contributes to the acquired spectral information. Data in the SPE format is not very useful since it is specially encoded to be opened with WinSpec software. WinSpec software has a function to convert SPE format into TXT format. This conversion gives a file containing wavelength and corresponding intensity on every row. Since the new file is in TXT

format, it is easily accessible. At every step data is acquired and saved with the location information embedded in the file name. At the end of scan there exist a file for each location stepped during scan, containing spectral information regarding that point. After the whole scan is complete, the data is processed. Each file is opened one by one and the maximum intensity value between wavelengths 200nm and 300 nm is determined. The wavelength range constraint is introduced to filter out the undesired visible range contributions as described above. The maximum value found corresponds to the peak intensity at 254 nm. This way the peak intensity at every point is determined. As the last step this data is plotted on a XY graph, where X axis is distance and Y axis is the intensity. At the locations where DNA exists an intensity drop is observed. By nature the gel is very unpredictable in the sense that any inhomogeneity in the structure during casting or any impurity formation inside the gel is very tough to eliminate and may severely effect the results to the extent of corruption, leading totally erroneous results. To solve this problem multiple passes along the lines that are off by few mm in vertical direction may be made and data may be averaged as to create a low pass filter effect. When the graph is plotted the band locations are perceived by the user. This way the gel is visualized. After this information may be used to excise the DNA from the gel, since the DNA locations are marked. Figure 3.16 shows the intensity plotted as a function of location.

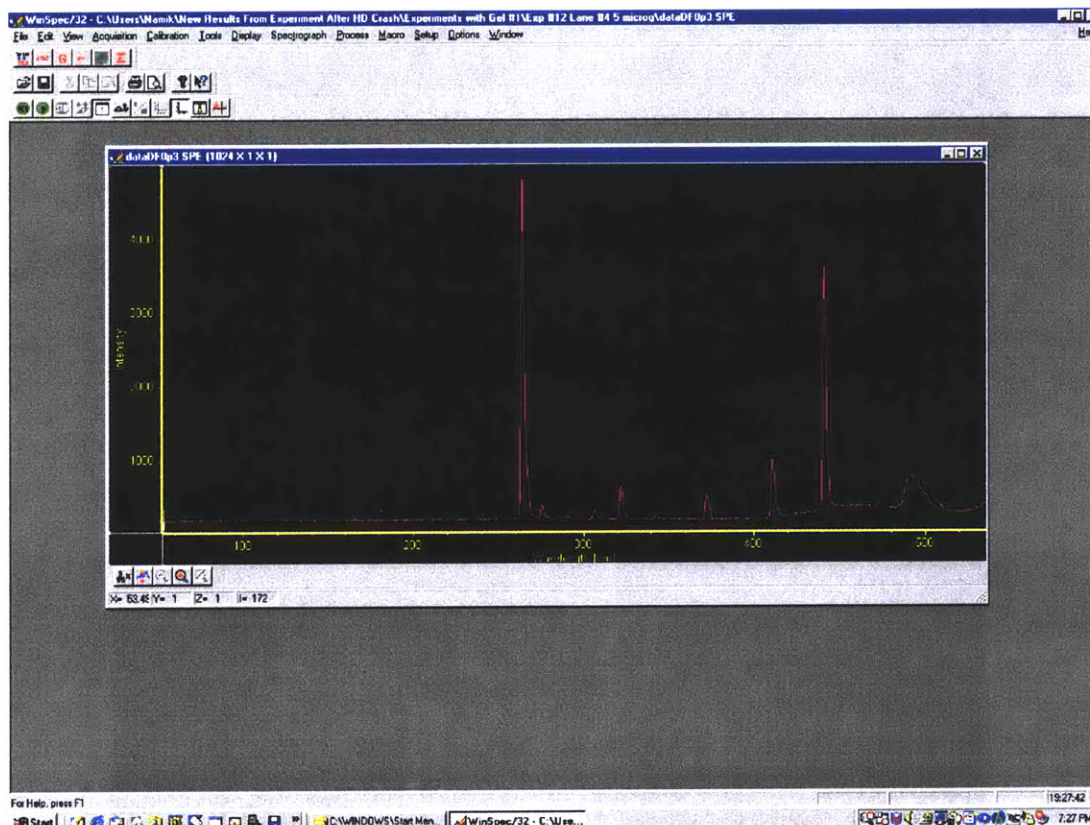


Figure 3.16, Plot Showing Intensity as a Function of Location.

3.3 References

- 1) [http:// www.ultralum.com](http://www.ultralum.com)
- 2) <http://usa.hamamatsu.com/opto-semi/ccds/default.htm>
- 3) http://www.roperscientific.com/act/prod_spectrapro150.shtml
- 4) http://www.daedalpositioning.com/Product_Information/High_Precision/400k_Series/402LN/body_402ln.html
- 5) Ealing Product Catalog

4. EXPERIMENTS

4.1 Introduction

This chapter includes experiments performed to see the feasibility of the proposed method. First general procedure of experiments is explained. Then an experiment about the transmittance of the gel tray is presented. Next, there is a preliminary experiment, which is performed on a simplified case. It is followed by three experiments performed on different agarose gels. Results of each experiment are presented and discussed.

4.2 General Procedure

The aim of the experiments is to prove the applicability and reliability of the suggested detection method and to derive the “working curve” of DNA in the gel. A working curve as shown in Figure 4.1 is the plot of analytical signal as a function of analyte concentration. These working curves are obtained by measuring the signal from a series of standards of known concentration. The working curves are then used to determine the concentration of an unknown sample or to calibrate the linearity of an analytic instrument.

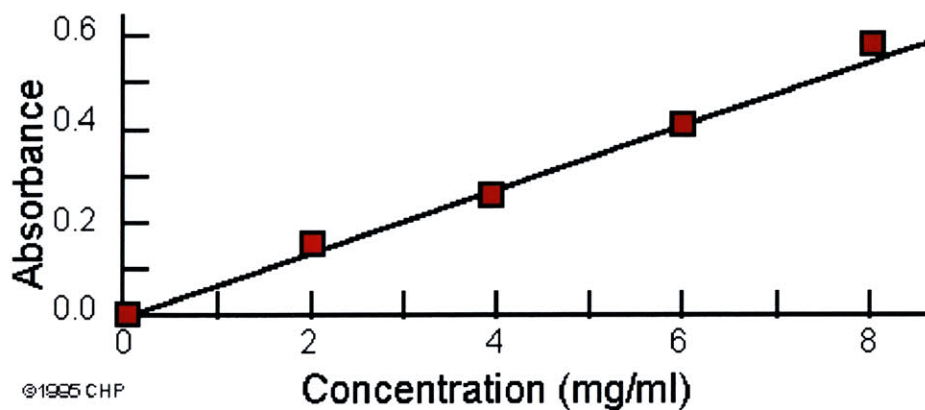


Figure 4.1, Example of a Working Curve.

If the reliability of the suggested technique is assured and the working curve of DNA in the gel can be obtained, it will be possible to quantitatively locate the DNA in the gel.

The absorption equations introduced in Chapter 2 needed for a quantitative study can be once more listed as follows;

$$(2.1) \quad A = a(\lambda) * b * c$$

where A is the measured absorbance, $a(\lambda)$ is a wavelength-dependent absorptivity coefficient, b is the path length, and c is the analyte concentration. Experimental measurements are usually made in terms of transmittance (T), which is defined as:

$$(2.3) \quad T = I / I_0$$

where I is the light intensity after it passes through the sample and I_0 is the initial light intensity. The relation between A and T is:

$$(2.4) \quad A = -\log T = -\log (I / I_0).$$

I and I_0 are measured by using the experimental setup. Therefore T and A are easily calculated. The path length b and analyte concentration c are also known quantities. So, the only unknown in equation (2.1) is $a(\lambda)$. If $a(\lambda)$ can be calculated for $\lambda=254$ nm, it would be possible to identify unknown concentrations by using this calculated value. Experiments with different concentrations are performed in order to check the reliability of the obtained $a(\lambda)$ value.

Setting up the experiment is a rather simple task. Figure 4.2 shows the setup before scanning started. The lane to be scanned is cut off the gel and any buffer solution remaining on the lane is cleaned, either by air or tissue/napkin paper. Utmost care must be given in order not to contaminate the gel during handling or cleaning.

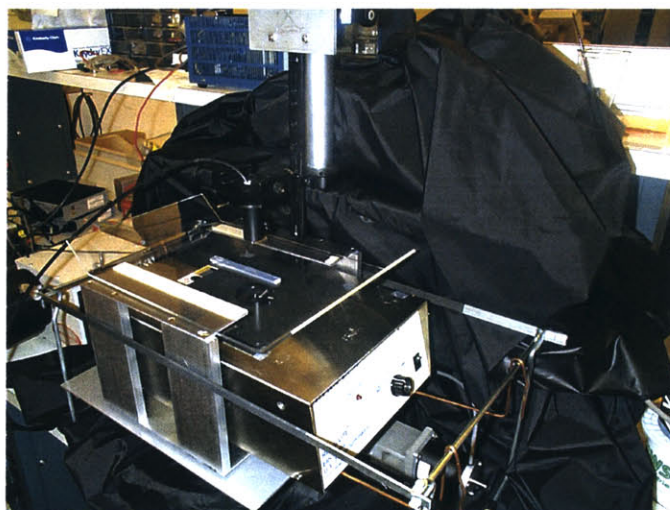


Figure 4.2, Scanning Setup.

Another important issue is the time during which the gel is exposed to the ambient air out of its protecting buffer solution and to the UV light. Out of the buffer time must be kept to a minimum, since the gel begins to shrink severely when dehydration occurs. If shrinking action occurs during the scanning, the data are corrupted due to the reshaping of the gel. The speed of the system used is enough to make two consecutive scans on a 100 mm long gel without encountering any shrinkage problem. After the scan is complete, the lanes must be laid back into the buffer solution if later use is planned. The UV light has a deteriorating effect on the DNA, if shed on the DNA for extended periods of time; it spoils the properties of DNA. The solution to this problem is embedded in the hardware design of the scanning system. Figure 4.3 shows the implementation of this solution on the system. As explained before, the relative motion for scanning is produced by holding the transilluminator and the probe fixed and moving the gel via a gel holder resting on the XY stage.

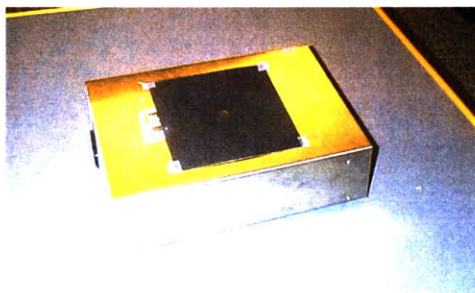


Figure 4.3, Modification on the Transilluminator to Avoid Excessive UV Light Exposure to the Gel.

The transilluminator has a light screen of 150mm*150 mm which is large enough to illuminate the entire gel area, since a gel is hardly ever larger than 150mm*150mm. If the entire gel area is subjected to exposure during the entire motion, the gel is prone to deteriorate. As a solution the whole transilluminator light screen area except the region that is aligned with the probe is covered by a black carton which blocks the light.

4.3 The Transmittance of the Gel Tray

In the design of the scanning system a UV transmitting gel tray from UVP (Ultra Violet Products) is used. To make sure that gel tray transmits in the UV range, a simple experiment has been performed. Figure 4.4 shows the spectra obtained when transilluminator was turned on with the band-pass filter introduced between the transilluminator surface and the probe.

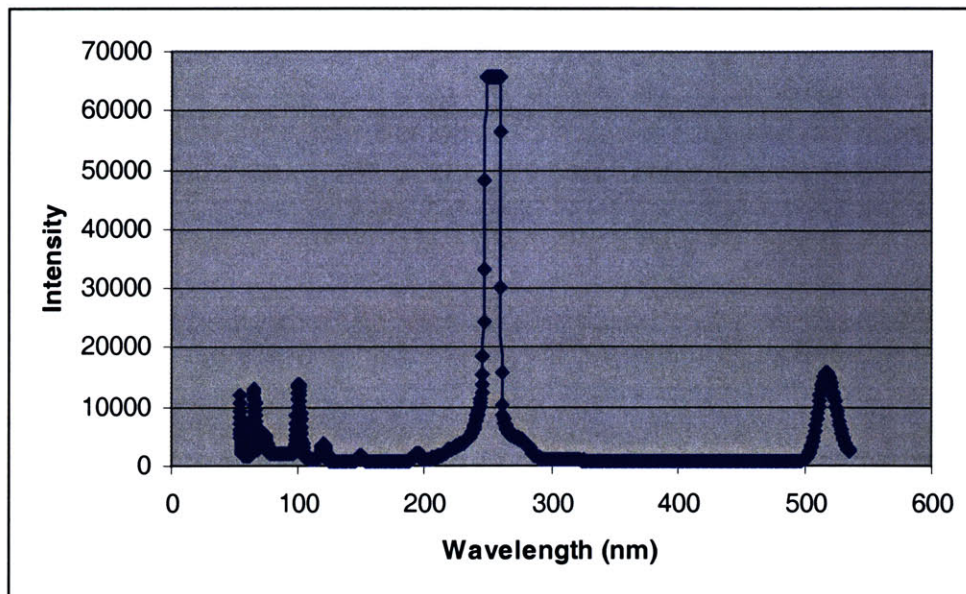


Figure 4.4, Spectra of the Transilluminator.

A 16 bit AD card is used for the experiment and maximum number of intensity levels is 65536. It is seen from Figure 4.4 that the detector saturates at around 254 nm, which is the zone of interest. This is because the transilluminator although set to lowest power setting gives out very high intensity light and causes the detector to saturate. Figure 4.5 shows the spectra obtained when the gel tray is introduced in between the transilluminator and the probe.

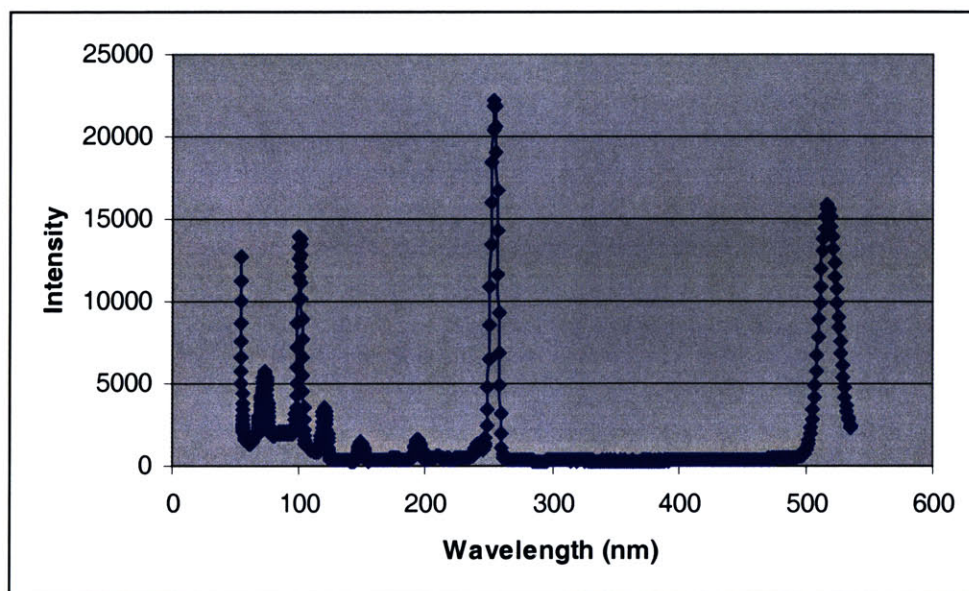


Figure 4.5, Spectra of the Gel Tray on the Transilluminator.

When the region around 254 nm is examined, it is easily observed that the intensity is around 21000 units. In the absence of gel tray this value was 65536 units which was the saturation value. 21000 units divided by 65536 units gives 32 percentage transmittance. This transmittance value is the maximum value possible, since the saturation cannot be avoided even at the lowest power setting. The exact transmittance value cannot be determined. It can be concluded that the gel tray transmittance is at most 30%. But this experiment shows that the gel tray transmits in the UV range, especially in the region of interest (around 254nm), hence it can be used in the experiments.

4.4 Preliminary Results with DNA on the Gel Tray

Before starting experiments with DNA in the agarose gel, to see the resolution of the detector some preliminary experiments with DNA sprayed on the gel tray were performed. 10 μl amount of different concentration DNA solutions have been sprayed on the gel tray forming half spheres. Then the half spheres have been scanned using the normal scanning procedure and the data has been recorded. The aim of this simple experiment is to determine the smallest concentration detectable by the CCD detector. The results are not expected to be very accurate and quantitative since there are uncertainties in the experimental setup. The biggest uncertainty is due to the shape of the DNA sample. It is in a curved shape like the upper half of a sphere. This geometry is very apt to not only scatter the light falling on it but also scatter the light going through it. This means a major source of error and very difficult to control unless a chamber confining the DNA sample completely and helping to make the solution surface straight enough, is used.

Figure 4.6 shows the transmittance graph of the bubble containing 10 μl of 1 $\text{ng}/\mu\text{l}$ solution.

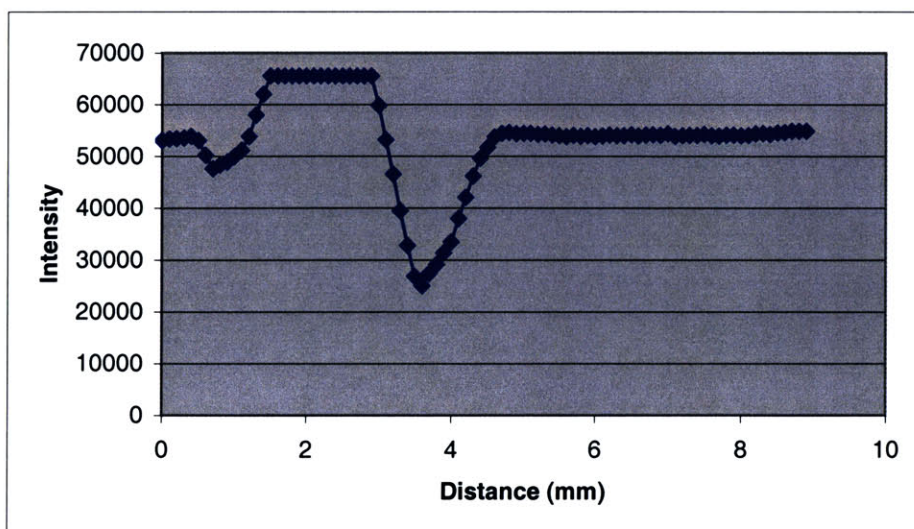


Figure 4.6, 1 $\text{ng}/\mu\text{l}$ Solution.

Figure 4.7 shows the transmittance graph of the bubble containing 10 μl of 10 $\text{ng}/\mu\text{l}$ solution.

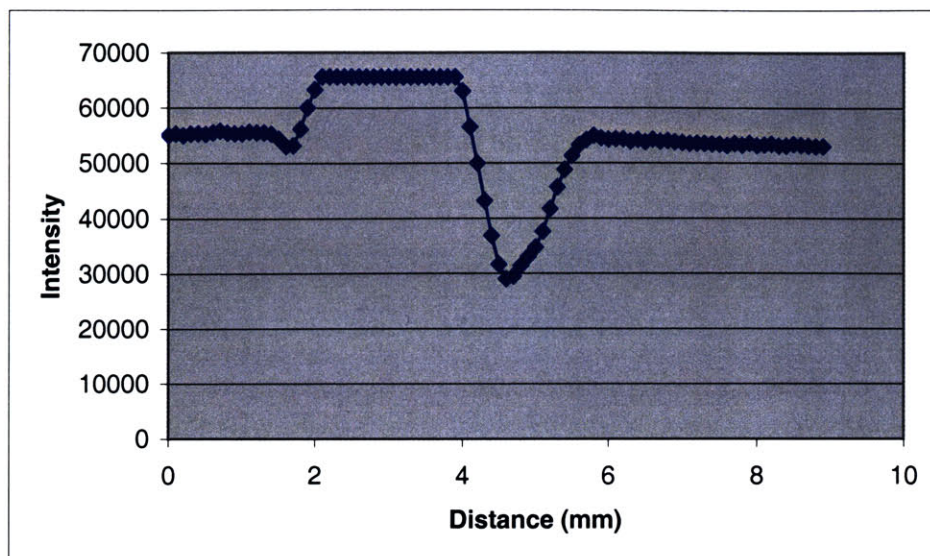


Figure 4.7 10 $\text{ng}/\mu\text{l}$ Solution.

Figure 4.8 shows the transmittance graph of the bubble containing 10 μl of 100 $\text{ng}/\mu\text{l}$ solution.

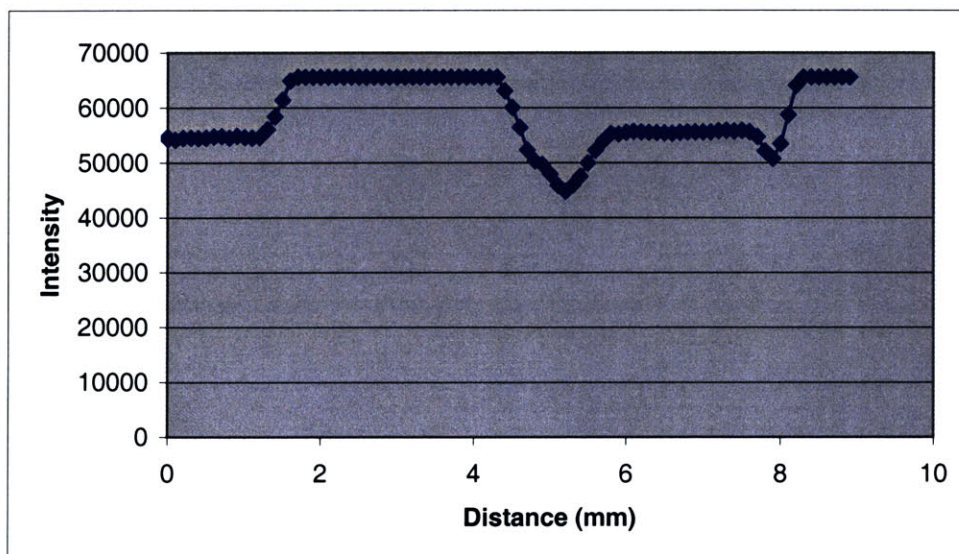


Figure 4.8, 100 $\text{ng}/\mu\text{l}$ Solution.

Figure 4.9 shows the transmittance graph of the bubble containing 10 μl of 1 $\mu\text{g}/\mu\text{l}$ solution.

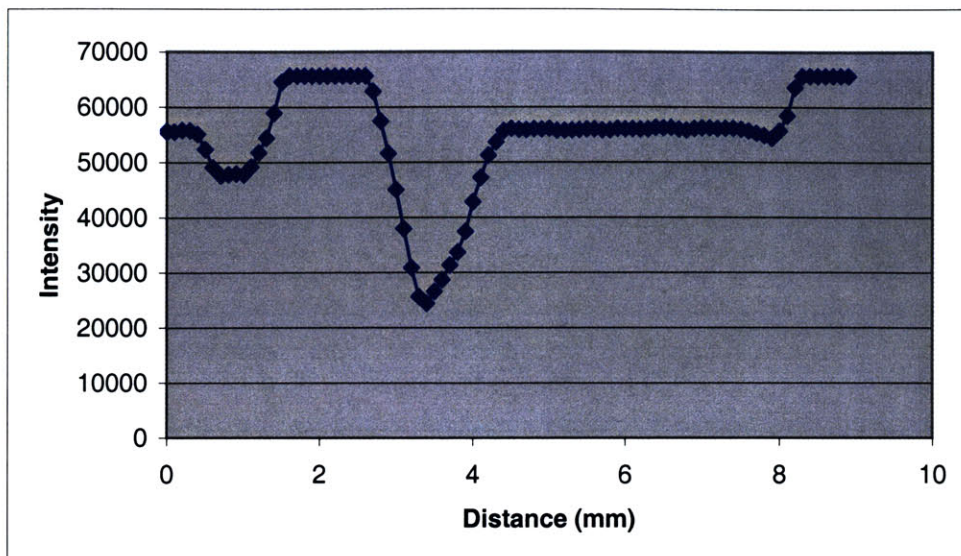


Figure 4.9, 1 $\mu\text{g}/\mu\text{l}$ Solution.

Figure 4.10 shows the transmittance graph of the bubble containing 10 μl of 10 $\mu\text{g}/\mu\text{l}$ solution.

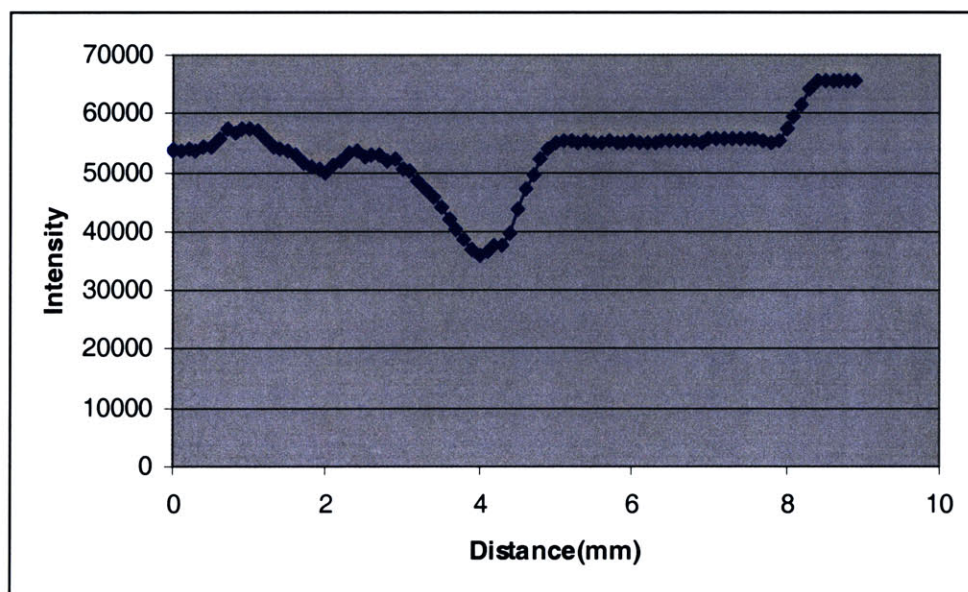


Figure 4.10, 10 $\mu\text{g}/\mu\text{l}$ Solution.

Figure 4.11 shows the transmittance graph of the bubble containing no DNA.

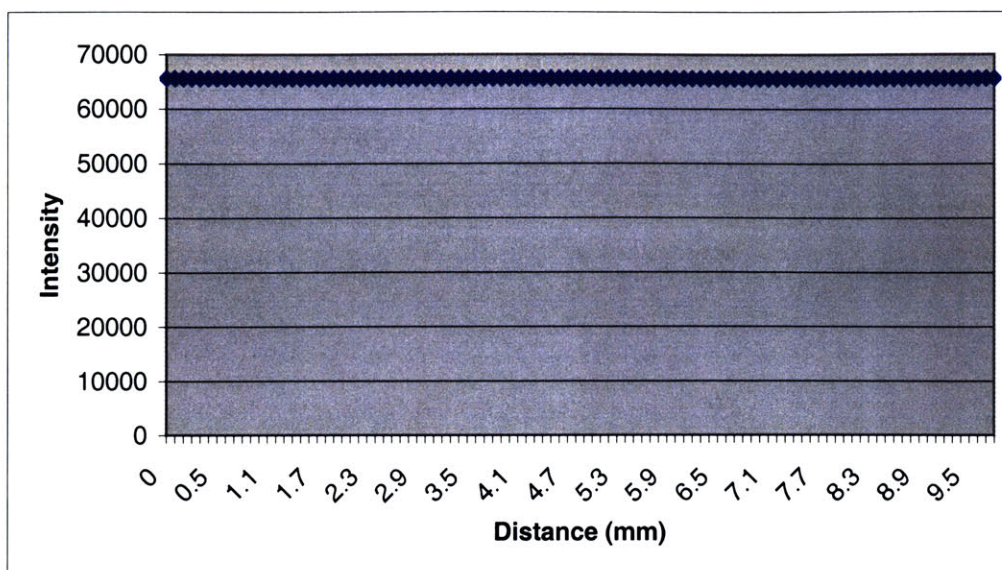
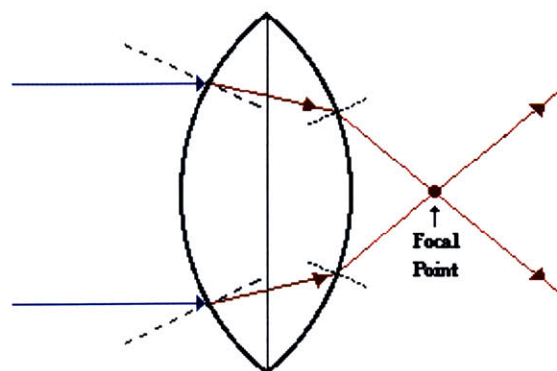


Figure 4.11, Water without DNA.

In Figures 4.6 to 4.10 spectra of DNA solution with different concentrations ranging from 1 ng/ μ l to 10 μ g/ μ l are presented. When all these plots are examined one common characteristic is noticed in all of them. Moving from origin of X axis (entitled “Distance”) to the right, in most of the graphs there exists a drop in the transmittance. After this drop region the transmittance value peaks and stays there for some distance. Following this peak a deeper drop than the first one is observed. This behavior may be explained by the fact that bubble shape introduces a great uncertainty as mentioned before. When the DNA solution is sprayed on the gel tray from the syringe, it takes a shape resembling a half-sphere. But this shape is different for each case due to the fact that liquid sits on a free surface without any walls confining it and forcing a standard shape. The liquid surface can be roughly approximated to be convex in shape, which will cause the surface to behave like a converging lens. The principle of refraction for converging lenses for parallel coming light is represented in Figure 4.12.



Incident rays which travel parallel to the principal axis will refract through the lens and converge to a point.

Figure 4.12, Principle of Refraction for Converging Lens

The light emerging from the transilluminator can be approximated as a parallel beam and falling perpendicular on the light screen of the transilluminator. At the edge regions of the bubble, the light coming from the transilluminator is refracted towards the focal point of the converging lens. In such edge regions where there is a curvature on the liquid surface, less transmitted light falls on the probe due to refraction. Therefore a drop in the transmittance graph is observed. In the regions close to the focal points an increase in the intensity is expected due to the contributions from neighboring curved regions. The common characteristic of having an intensity peak in the middle and two intensity wells at two sides of the peak may be explained in this manner. Yet this does not mean that there is no absorption due to the existence of DNA in the solution and the wells in the signal are merely due to geometrical reasons. When Figure 4.11 is examined which presents the result with pure water without any DNA in it, it is observed that there is no similar pattern as in the previous plots. The intensity stays at the constant saturation value. This shows that the existence of DNA in the solution leads to a difference in the transmittance; since in the experiments with DNA in the water, the intensity is always below the saturation value. The discussion about the converging lens effect is held to state that the results obtained are not expected to be quantitative due to the complex geometry of the liquid surface. This is also confirmable from Figures 4.6 to 4.10. Going from Figure 4.6 to Figure 4.10 the DNA concentration increases by a factor of ten at each figure. Normally it will be expected to have less and less transmittance for increasing concentration. But the transmittance pattern is quite arbitrary and the expected behavior is not observed. This can be explained by the geometrical uncertainty as stated in detail above. Also in Figures 4.8 to 4.10 there exists a step at the far right position, leveling the signal up to the saturation value. Since close to the boundary of the droplet the liquid layer gets thinner, less absorption occurs and extra amount of light falling on the detector surface causes the detector saturate in these regions.

This preliminary experiment shows the suitability of the detector although it does not give any clue for a quantitative study. But in the case of DNA in the agarose gel the problem encountered in this preliminary experiment, bubble-like liquid surface will not exist. The DNA solution will be lying homogeneously in the porous gel structure and a DNA lane will have approximately rectangular prism shape. This will eliminate the curved surface problem and allow a quantitative study.

4.5 Results with First Gel

After the preliminary experiments were completed with single DNA droplet on the gel tray, to see the applicability of the method to DNA in agarose gels, experiments with agarose gels have been performed. Each gel is comprised of 10 lanes. Each lane has a well at one end, which is used to load the lane with DNA solution. On the contrary to the usual gels used in electrophoresis, the gels used for the experiments are free of EtBr since the aim is to devise a method, which uses no stains as, explained before. The gel is 4 mm thick and 0.8% in concentration. The lane to be scanned is cut from the gel and placed on the gel tray. The start point of scan is aligned with the probe and the scan is launched. The first lane contains 100 ng of plasmid Ecoli DNA ladder that is different than the DNA used in rest of the lanes. Lane two contains again 100 ng DNA but it is mouse DNA. Lane three contains 1 μ g mouse DNA. Lane four and five contain 5 μ g and 10 μ g mouse DNA respectively. Each well is filled with some amount of DNA dissolved in 24 μ l solution. So the concentration in each lane can be determined by dividing the specific amount of DNA in that lane by 24 μ l. The signal is noticed to be very sensitive to changes in the homogeneity of the gel so to account for any noise due to inhomogeneous gel structure and water bubbles trapped between the agarose gel and the gel tray, multiple runs on the same lane are performed. Also another duplicate gel is run with EtBr and visualized to be able to get a rough idea about band locations. Although there is not a perfect match of band locations between the plain gel and the gel with EtBr - due to the effect of EtBr and other chemicals on the speed of DNA traveling through the gel- still the information from the picture under UV light can be enlightening about the band locations. A picture of this gel with EtBr taken under UV light is presented in Figure 4.13. The uppermost lane is lane number 1. DNA bands in lanes 1 and 2 are not visible in the picture although they were visible to naked eye. In lanes 3, 4 and 5 which contain 1, 5 and 10 μ g of DNA respectively, streaking is observed. This is due to the fact that there is a huge amount of DNA in these lanes and due to weak adhesion between the DNA molecules they fail to travel as a single rigid body through out the lane. Hence it is not possible to observe a single band in these lanes, instead a streaking pattern exists. The conclusion to be deduced from Figure 4.13 is, bands are located nearly 4 cm away from the edge of the gel which wells are located. So to gain time starting point is offset by 2 cm from the edge of the gel. Different lanes containing different concentrations are examined one by one and results are discussed below;

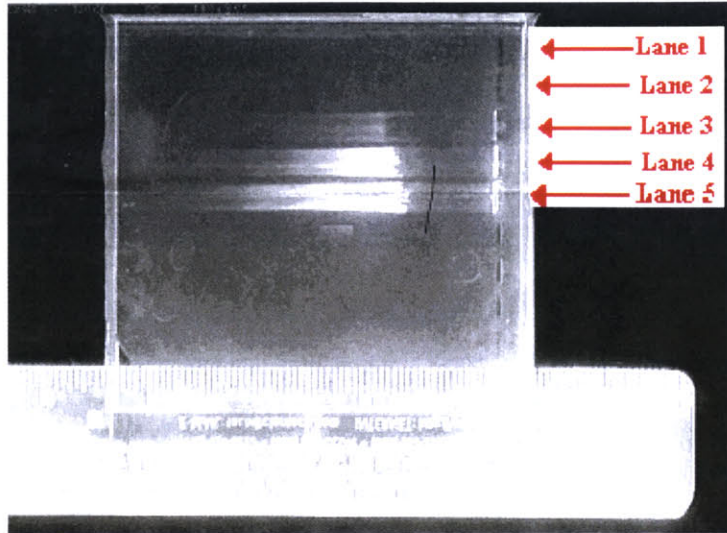


Figure 4.13, Picture of Duplicate Gel (Run with EtBr) Under UV Light.

- Lane 1:
 - Total Amount: 100 ng plasmid DNA
 - Concentration: 4.2 ng/ μ l

There are three runs done on the same lane. The results are presented in Figures 4.14-4.16.

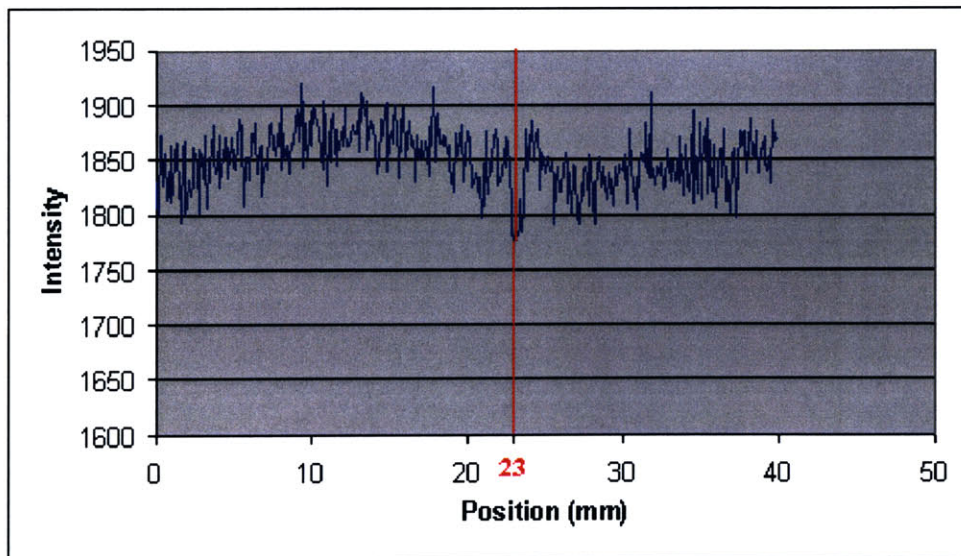


Figure 4.14, Lane 1: 100 ng Plasmid (Ladder) DNA, First Run.

When Figure 4.14 is examined it is seen that the signal is almost the same along the lane with in a 100 unit range between 1800 and 1900 unit over which the signal fluctuates. In Figure 4.14 same kind of fluctuating behavior is also present with the difference that borders have shifted down by almost 50 units. But around 23 mm there is a drop in the

signal of 100 units. This behavior is consistent in both Figures 4.14 and 4.15. This drop is identified to correspond to the 100 ng band. According to the picture presented in Figure 4.12, a band is expected to exist at around 4 cm position. Considering the 2 cm distance skipped to expedite the scan, 23 mm corresponds to 43 mm in absolute position, which is in the expected range. So the drop in the signal can be attributed to the 100 ng band. When Figure 4.16, which represents the results from the third run, is examined, no drop in the 23 mm position is observed. A 40 mm scan takes about 10 minutes. This means that before the third run, the gel have been out of the buffer which helps it to protect its properties and been subjected to ambient conditions about 20 minutes. Such duration causes changes in the gel properties leading inconsistent and unreliable results.

The absorption equations introduced in Chapter 2 needed for a quantitative study are once more listed as follows;

$$(2.1) \quad A = a(\lambda) * b * c$$

$$(2.3) \quad T = I / I_0$$

$$(2.4) \quad A = -\log T = -\log (I / I_0).$$

where A is the measured absorbance, $a(\lambda)$ is a wavelength-dependent absorptivity coefficient, b is the path length, and c is the analyte concentration, T is transmittance ,I is the light intensity after it passes through the sample and I_0 is the initial light intensity.

Using these equations $a(\lambda)$ in $\mu\text{l}/\text{mm}\cdot\text{ng}$ for first two runs are calculated. Values plugged into the equations and results are tabulated in Table 4.1.

<i>Run #</i>	<i>I (unit)</i>	<i>I_o (unit)</i>	<i>T</i>	<i>A</i>	<i>b (mm)</i>	<i>c (ng/μl)</i>	<i>a(λ)</i>
1	1724	1805	0.955	0.01993	4	4	0.00124
2	1780	1851	0.962	0.0169	4	4	0.00106

Table 4.1, Calculation of $a(\lambda)$, Wavelength-dependent Absorptivity Coefficient($\mu\text{l}/\text{mm}\cdot\text{ng}$).

Wavelength-dependent absorptivity coefficient $a(\lambda)$ is found to be 0.00124 and 0.00106 $\mu\text{l}/\text{mm}\cdot\text{ng}$ for two different runs where 0.8 % gel has been used as the transport medium. There is a lot of noise in the signal due the gel structure and there is a difference in between. Hence it may be stated that wavelength-dependent absorptivity coefficient $a(\lambda)$ is determined to lie between 0.00106 and 0.00124 $\mu\text{l}/\text{mm}\cdot\text{ng}$.

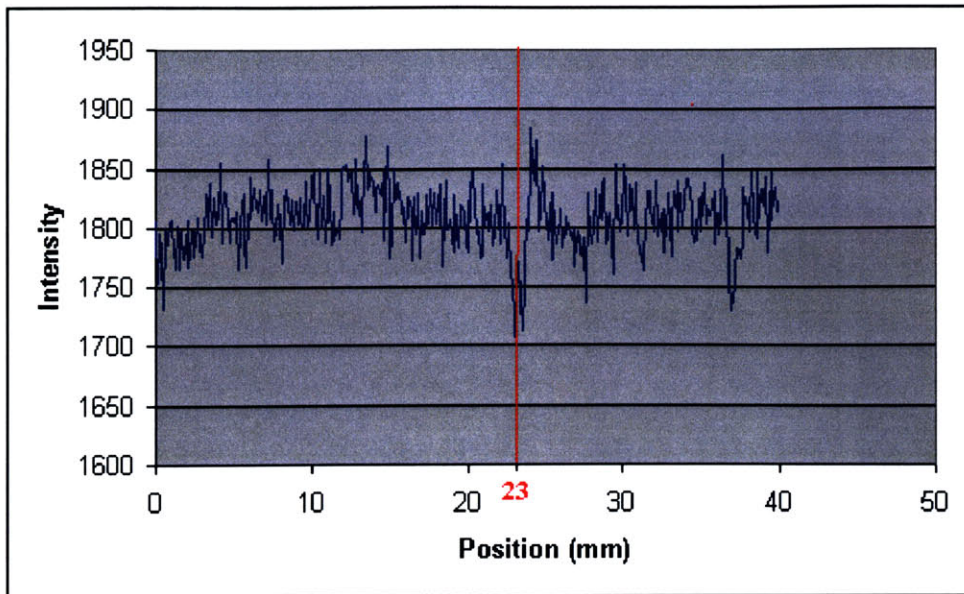


Figure 4.15, Lane 1: 100 ng Plasmid (Ladder) DNA, Second Run.

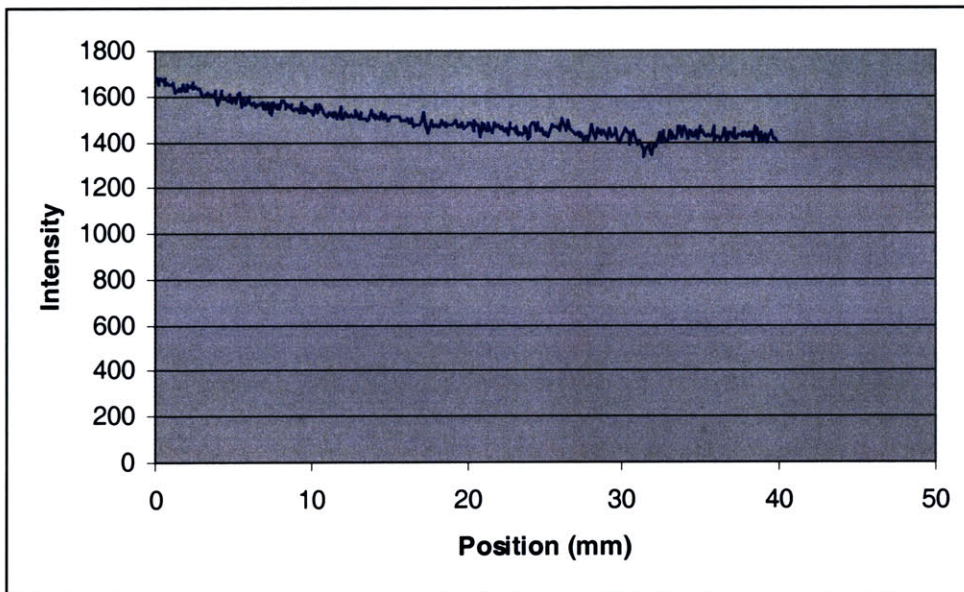


Figure 4.16, Lane 1: 100 ng Plasmid (Ladder) DNA, Third Run.

- Lane 2:
 - Total DNA Amount: 100 ng mouse DNA
 - Concentration: 4.2 ng/ μ l

There are three runs done on the same lane. The results are presented in Figures 4.17-4.19.

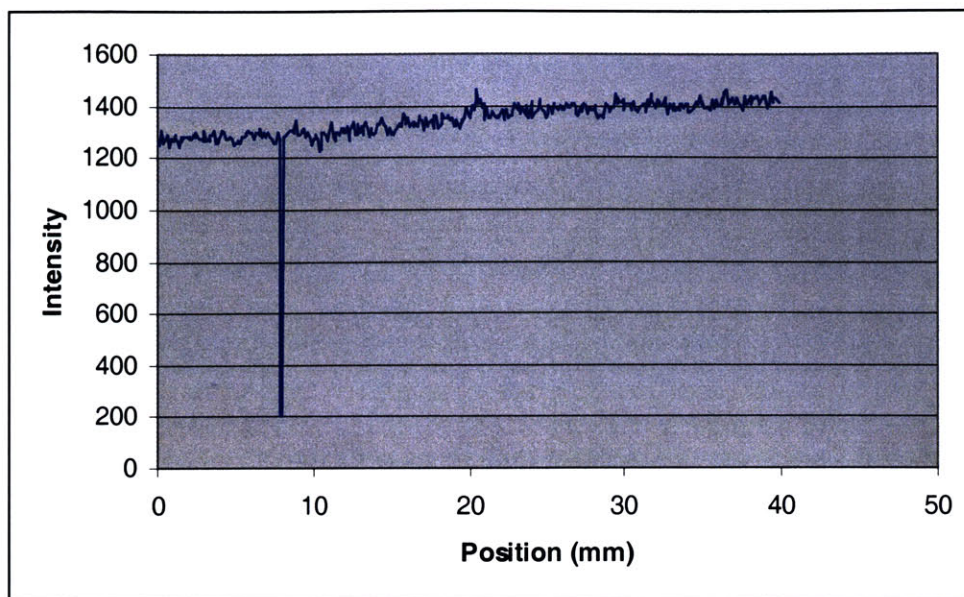


Figure 4.17, Lane 2: 100 ng Mouse DNA, First Run.

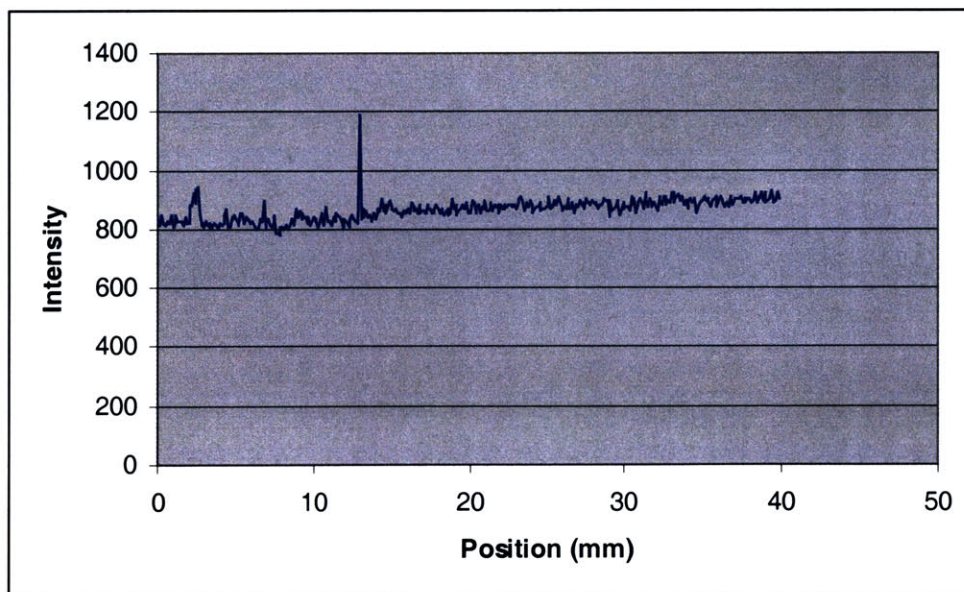


Figure 4.18, Lane 2: 100 ng Mouse DNA, Second Run.

In Figure 4.17 there is a downward spike around 8 mm and in Figure 4.18 there is an upward spike around 13 mm. Looking at the width of these spikes it can be concluded that these are nothing but noise in the signal, since 100 ng band is expected to be 2-3 mm

wide. Also spike in Figure 4.18 is bizarrely pointed upward, which makes cannot be due to the DNA absorption since absorption would cause a drop in the signal.

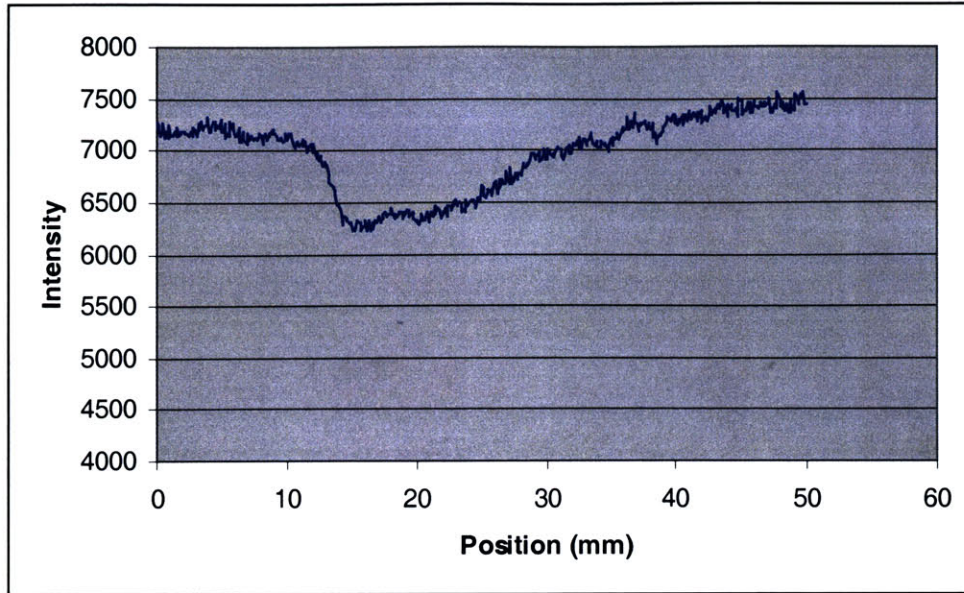


Figure 4.19, Lane 2: 100 ng Mouse DNA, Third Run.

Figure 4.19 shows the data collected in the third run. Again data is corrupted due to long waiting period. It may be argued that the drop between 11 mm and 30 mm is due to the existence of a band, but this is not realistic since the width of the band is much thicker than expected (2-3 mm). As a result it can be said that the 100 ng band could not be identified. This shows that mouse DNA is not as suitable as the plasmid ladder DNA.

- Lane 3:
 - Total DNA Amount: 1 μg mouse DNA
 - Concentration: 42 $\text{ng}/\mu\text{l}$

There are three runs done on the same lane. Results are presented in Figures 4.20-4.22. In this lane there exists streaking so no band is expected to be detected. A series of consecutive small size wells and fluctuations in the signal are expected. When Figure 4.20 is examined there exists a spike at 2 mm and similar spike also exists in Figure 4.21 at 37 mm. Due to same reasons explained for spikes in experiments performed with lane 2, these spikes are noise. In Figure 4.22 again the effects of deterioration of gel due to prolonged waiting time are dominant. There is a corruption in the signal and no meaningful results can be obtained. As a summary it can be said that lane 3 containing 1 μg DNA could not be detected as expected. Even if it were detected as expected, the result would not be sufficient for a quantitative study, since it would be impossible to know the total thickness of DNA at a specific position.

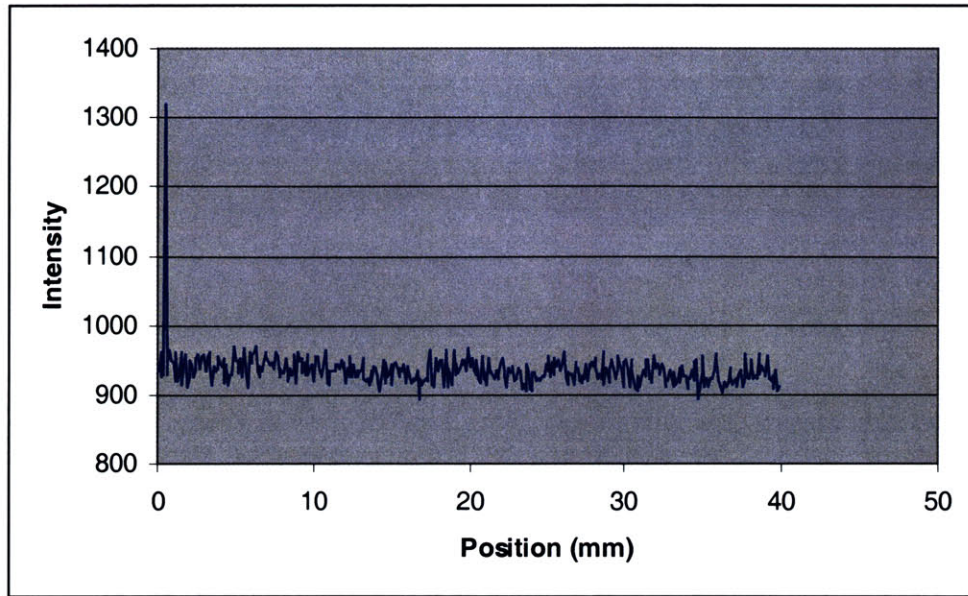


Figure 4.20, Lane 3: 1 μ g Mouse DNA, First Run.

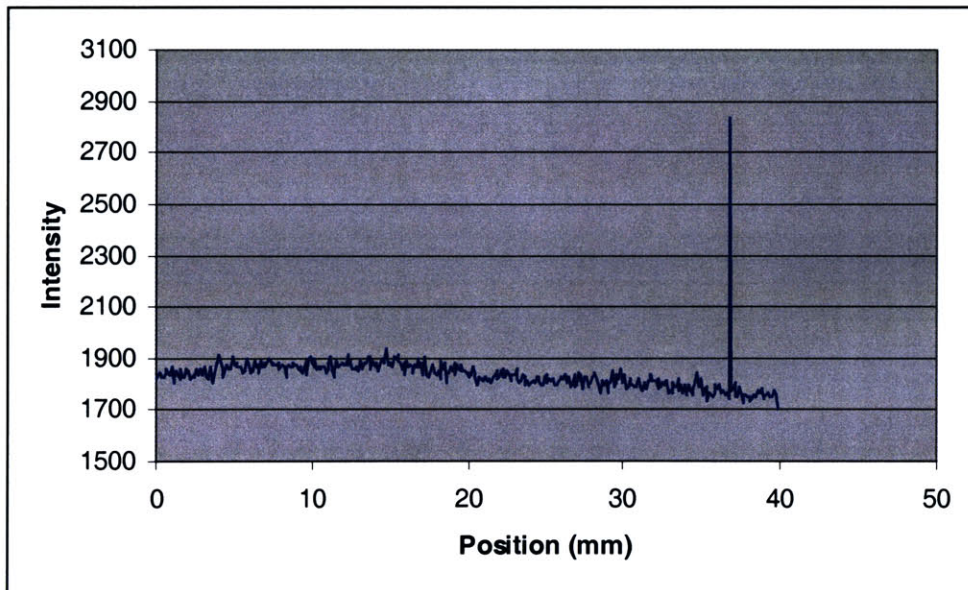


Figure 4.21, Lane 3: 1 μ g Mouse DNA, Second Run.

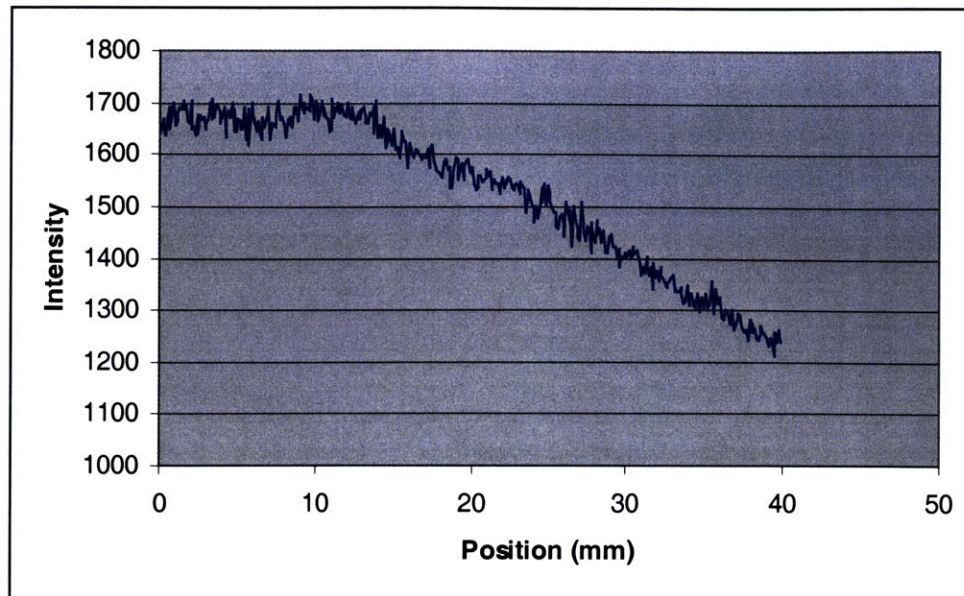


Figure 4.22, Lane 3: 1 μg Mouse DNA, Third Run.

- Lane 4:
 - Total DNA Amount: 5 μg mouseDNA
 - Concentration: 208 $\text{ng}/\mu\text{l}$

There are two runs done on this lane. Results are presented in Figures 4.23-4.24. This is one of the overloaded lanes which streaking is expected. The streaking is expected to lead to unpredictable signal drop patterns, since DNA could not preserve the band shape and spreads through the lane with a varying thickness. In Figure 4.13 leaking effect can be observed in three of the lanes. Referring to Figures 4.23 and 4.24, the continuous slight drop in the average signal level accompanied by wells of different depth can be identified as the expected signal characteristic due to leaking problem. Also there is a great consistency between two sets of data collected in different runs. Figures 4.23 and 4.24 are very similar to each other, and this similarity consolidates the above viewpoint. Compared with the previous lane, this lane contains 5 μg DNA which is five times more than the previous lane. This difference in amount makes DNA in lane 4 detectable in a repeatable way, whereas the amount of DNA in lane 3 is not sufficient to lead to similar repeatable response. Hence the result obtained from lane 4 does not contain enough clues to characterize the absorption behavior. The reason as explained for lane 3 is streaking.

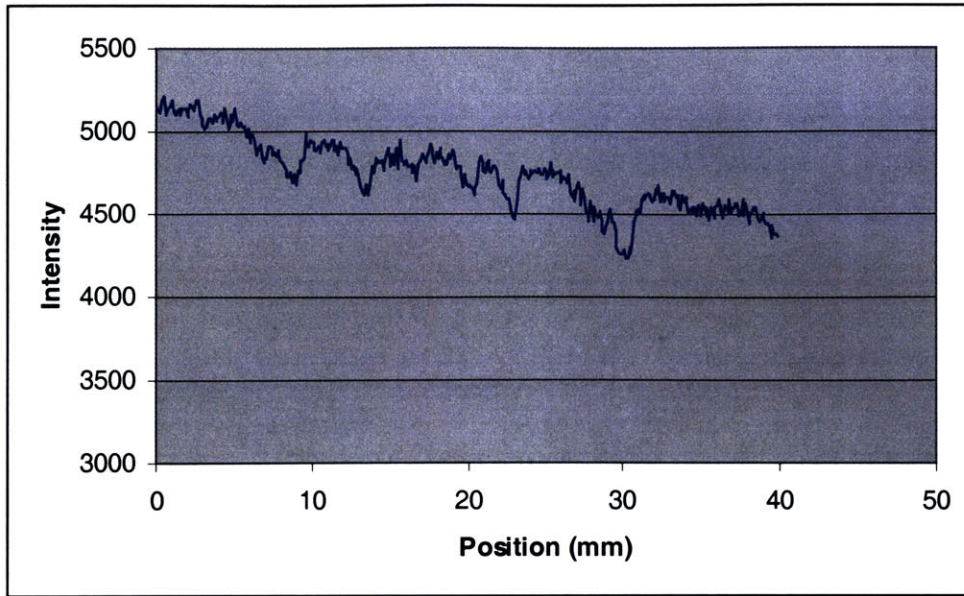


Figure 4.23, Lane 4: 5 µg Mouse DNA, First Run.

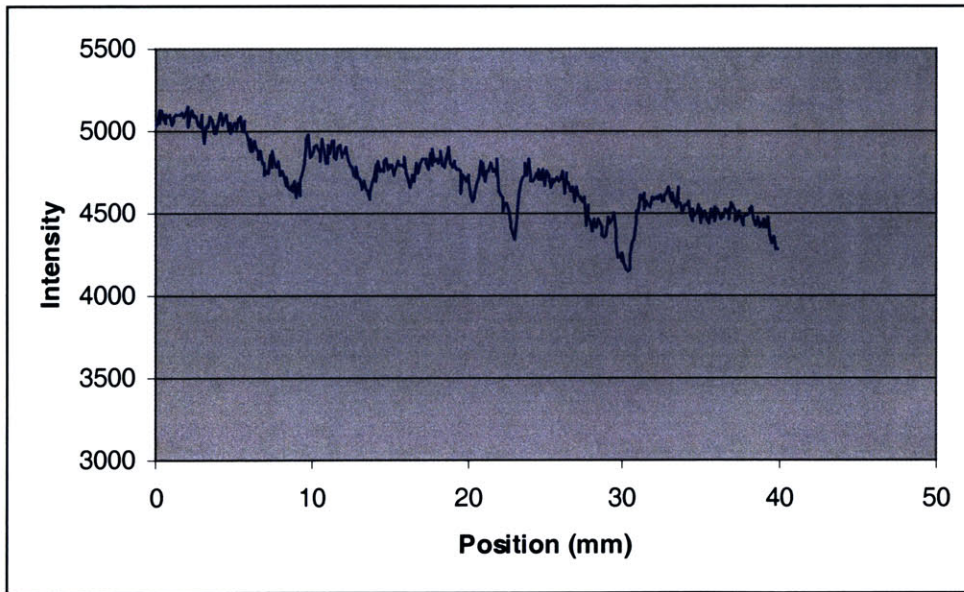


Figure 4.24, Lane 4: 5 µg Mouse DNA, Second Run.

- Lane 5:
 - Total DNA Amount: 10 µg mouse DNA.
 - Concentration: 416 ng/µl

There are three runs done on the same lane. The results are presented in Figures 4.25-4.27.

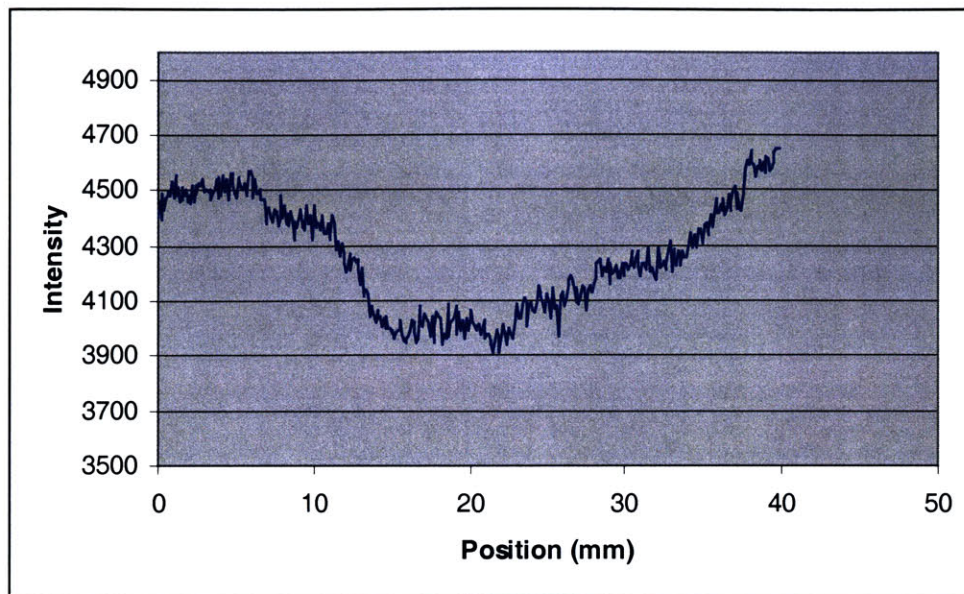


Figure 4.25, Lane 5: 10 μ g Mouse DNA, First Run.

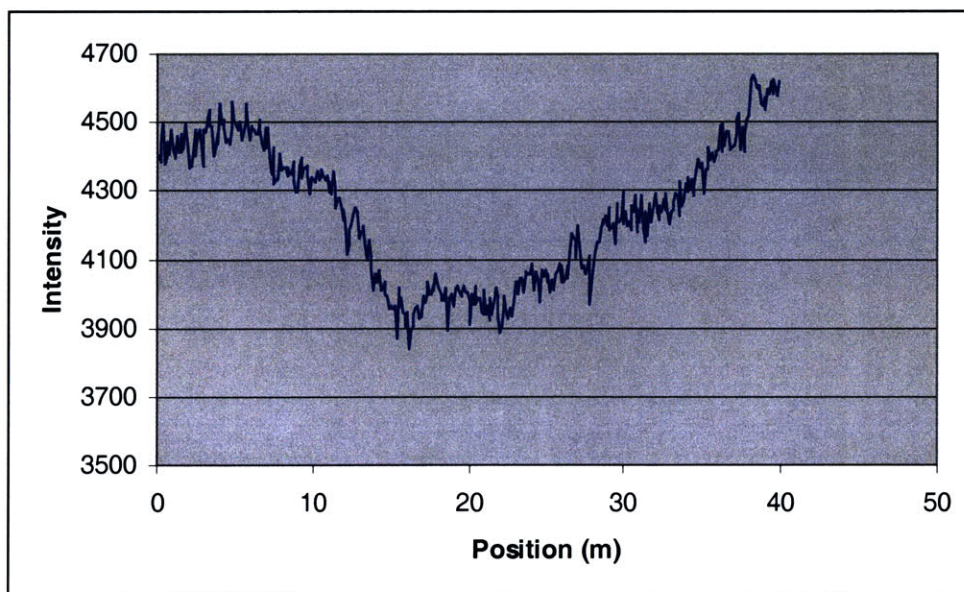


Figure 4.26, Lane 5: 10 μ g Mouse DNA, Second Run.

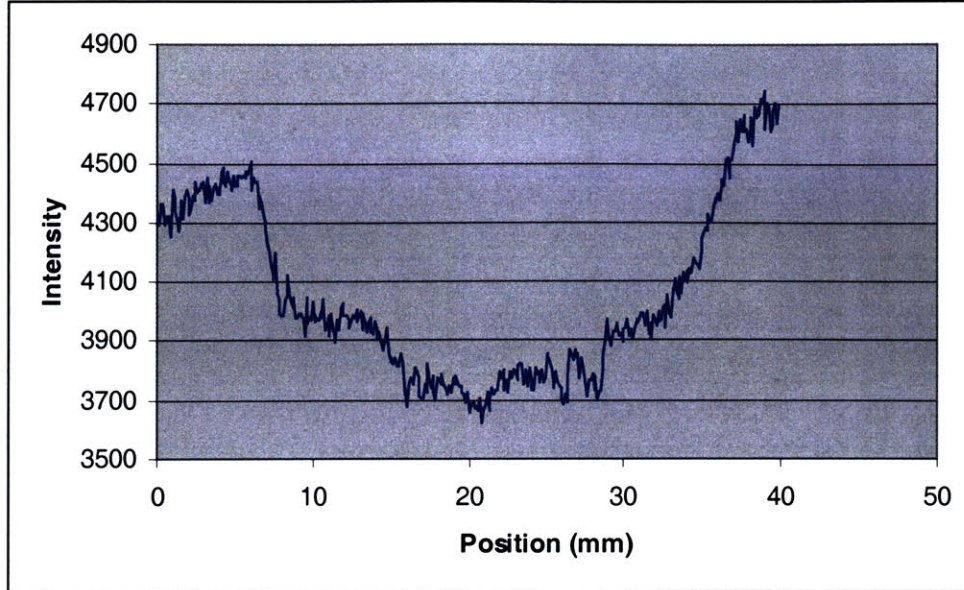


Figure 4.27, Lane 5: 10 µg Mouse DNA, Third Run.

As it was the case with lane 4, there exists a repeatable fluctuating absorption pattern due to streaking issue as usual with amounts greater than 1 µg. Although the result is repeatable and proving for the detector's ability to read this amount, it does not contribute to a quantitative study.

4.6 Results with Second Gel

Experiments have been continued on another 4 mm thick and 0.8% gel. The lane contents are given below in Table 4.2 .

<i>Lane #</i>	<i>Amount</i>
1	0
2	100 ng mouse DNA
3	1 µg mouse DNA
4	5 µg mouse DNA
5	10 µg mouse DNA
6	20 µg mouse DNA
7	0
8	400 ng plasmid DNA
9	250 ng DNA ladder

Table 4.2, Contents of Gel 2.

A duplicate of this gel with EtBr has also been run, and a picture of that gel under UV light is presented in Figure 4.28.

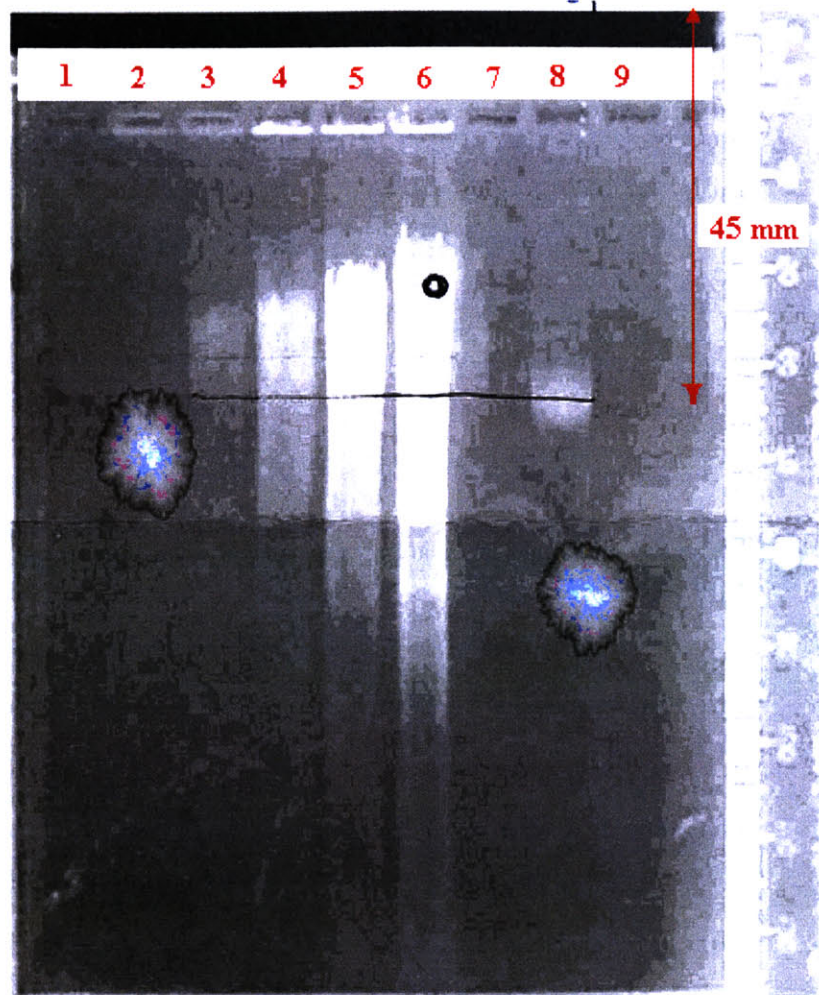


Figure 4.28, Picture of Duplicate Gel Run With EtBr Under UV Light. Lane 1 is the Leftmost Lane.

As it can be seen in Figure 4.28 in lanes 3,4,5 and 6, which contain 1,5,10 and 20, μg mouse DNA respectively streaking is observed. 100 ng band, although visible to naked eye, is not visible in the picture. The only visible band in the picture is the 400 ng plasmid DNA band in lane 8. Since a well formed band is needed for a quantitative study only lane 8, which contains 100 ng plasmid DNA is investigated. The scan has been started 2 cm off the edge of the gel to skip the empty gel region.

- Lane 8:
 - Total DNA Amount: 400 ng plasmid DNA
 - Concentration: 16 ng/ μl

There are three runs done on the same lane. Results are presented in Figures 4.29-4.31. At around 26 mm there is a well of same depth and shape in all three plots. The data is very repeatable and there is also great consistency in the well shape, which pertains information about the band shape. Referring to Figure 4.28, it is seen that the band in lane 8 is located at a position close to 45 mm (measured with respect to the upper edge of the gel) and its width is about 4-5 mm with faint ends. Although the exact location and shape of the band in the plain gel may differ from its duplicate with EtBr, this information about location and band width may construct a rough basis to compare to and in this case they perfectly agree. Figures 4.29-4.31 show that the band location agrees with the band location in duplicate gel with EtBr. In Figures 4.29-4.31 the wells are located between 25-30 mm. But the 2 cm distance skipped to expedite the scan must be taken into account. Adding 20 mm to the 25 mm gives an absolute position with respect to the upper edge of 45 mm, hence leading to reasonable agreement with the band location in duplicate gel. As long as the width is concerned the wells in Figures 4.29-4.31 have a width of about 4-5 mm, which also overlaps with the results from duplicate gel. The depth of the well is not constant all through the well, as it was expected that a band with faint ends (as observed in Figure 4.28) would have less absorption close to the boundaries and this would lead to shorter well depth at the edges of the well. This characteristic is also supporting in evidence of the correctness of the scan. In Figures 4.29 to 4.31 there is also a continuous slight increase in the signal level as moved from left to right. This can be explained by the inhomogeneity in the gel structure. Something to note in this experiment is that lane 8 contains plasmid DNA, not mouse DNA. As it was also the case in experiments with first gel (first lane with 100 ng plasmid DNA) plasmid DNA gives repeatable, robust results whereas mouse DNA does not. The difference may stem from the fact that there may be a quality difference between two different kinds of DNA leading poor results with mouse DNA.

The absorption equations introduced in Chapter 2 needed for a quantitative study are once more listed as follows;

$$(2.1) \quad A = a(\lambda) * b * c$$

$$(2.3) \quad T = I / I_0$$

$$(2.4) \quad A = -\log T = -\log (I / I_0).$$

where A is the measured absorbance, $a(\lambda)$ is a wavelength-dependent absorptivity coefficient, b is the path length, and c is the analyte concentration, T is transmittance, I is the light intensity after it passes through the sample and I_0 is the initial light intensity.

Using these equations $a(\lambda)$ in $\mu\text{l}/\text{mm}\cdot\text{ng}$ for three runs are calculated. Values plugged into the equations and results are tabulated in Table 4.3.

<i>Run #</i>	<i>I (unit)</i>	<i>I_o (unit)</i>	<i>T</i>	<i>A</i>	<i>b (mm)</i>	<i>c (ng/μl)</i>	<i>a(λ)</i>
1	5494	6200	0.8861	0.0525	4	16	0.00082
2	5472	6175	0.08861	0.0525	4	16	0.00082
3	5521	6213	0.08886	0.0513	4	16	0.00080

Table 4.3, Calculation of $a(\lambda)$, Wavelength dependent Absorptivity Coefficient ($\mu\text{l}/\text{mm}\cdot\text{ng}$).

Wavelength-dependent absorptivity coefficient $a(\lambda)$ is found to be $0.00082 \mu\text{l}/\text{mm}\cdot\text{ng}$ for this specific experiment where 0.8 % gel has been used as the transport medium. When compared to the results in Table 4.1 (where $a(\lambda)$ was found to lie between 0.00106 and $0.00124 \mu\text{l}/\text{mm}\cdot\text{ng}$), a 30-50% difference is observed between two sets of results.

There is also another method being investigated for stain free detection, which is planned to be incorporated with scanning method. The method involves taking a snapshot image of the gel using the same CCD camera and a lens system. It aims to supply initial information about the band locations, which may not be as precise as to perform an accurate quantitative study. The precise information is to be collected by using the scanning system. Figure 4.32 shows the snapshot image of lane 8. The band is visible in Figure 4.32 and it is located at an absolute position of 45 mm as expected. This verifies that the well in Figures 4.29-4.31 is due to the existence of a DNA band at an absolute position of 45 mm. The wavelength-dependent absorptivity coefficient is also calculated with intensity values taken from Figure 4.32. Results are presented in Table 4.4:

<i>Run #</i>	<i>I (unit)</i>	<i>I_o (unit)</i>	<i>T</i>	<i>A</i>	<i>b (mm)</i>	<i>c (ng/μl)</i>	<i>a(λ)</i>
1	2490	2720	0.9154	0.0383	4	16	0.00059

Table 4.4, Calculation of $a(\lambda)$, Wavelength-dependent Absorptivity Coefficient ($\mu\text{l}/\text{mm}\cdot\text{ng}$) from the Snapshot Image.

The wavelength-dependent absorptivity coefficient is found to be $0.00059 \mu\text{l}/\text{mm}\cdot\text{ng}$, which is almost 25% less than the value obtained from the scanning experiment. The snapshot method is not expected to be as accurate as the scanning method, but the wavelength-dependent absorptivity value obtained from snapshot method is in reasonable agreement with the result from scanning experiment. This is a supporting clue for the correctness of the quantitative result obtained from scanning experiment.

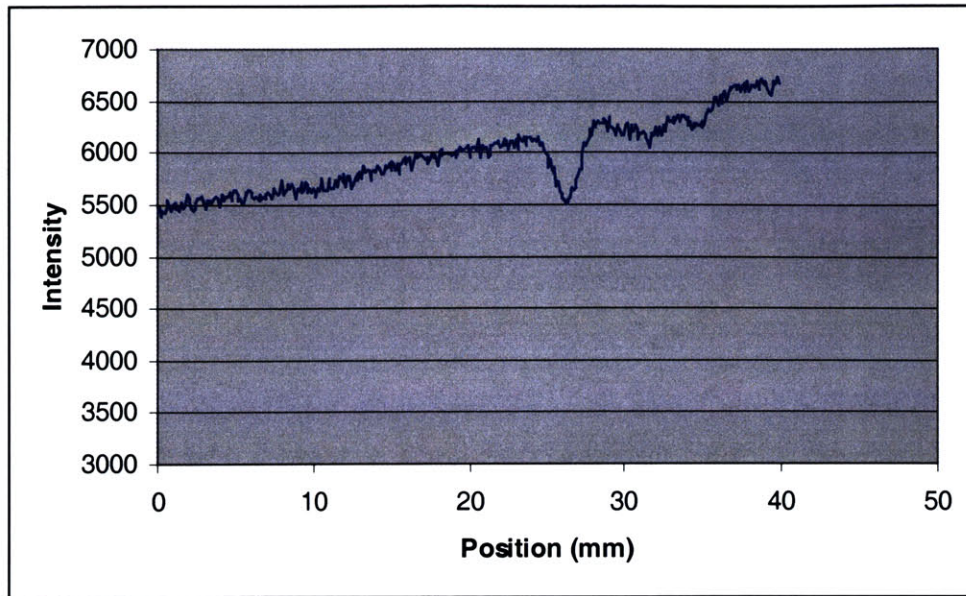


Figure 4.29, Lane 8: 400 ng plasmid DNA, First Run.

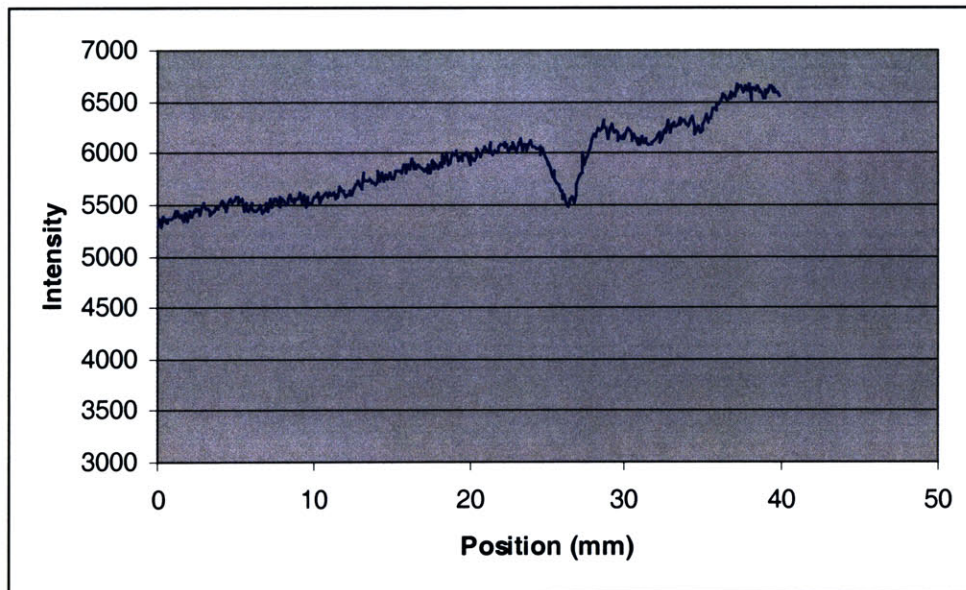


Figure 4.30, Lane 8: 400 ng plasmid DNA, Second Run.

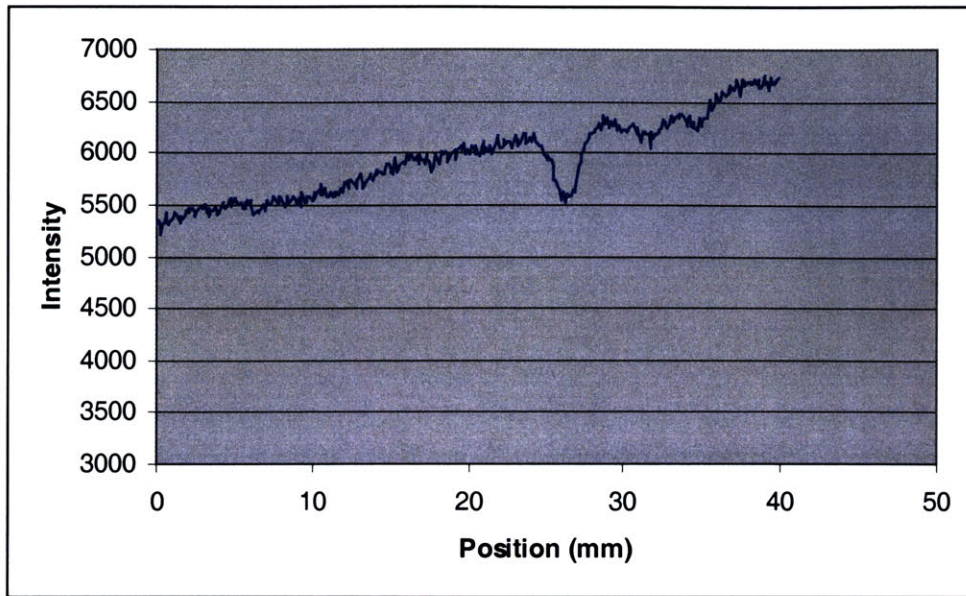


Figure 4.31, Lane 8: 400 ng plasmid DNA, Third Run.

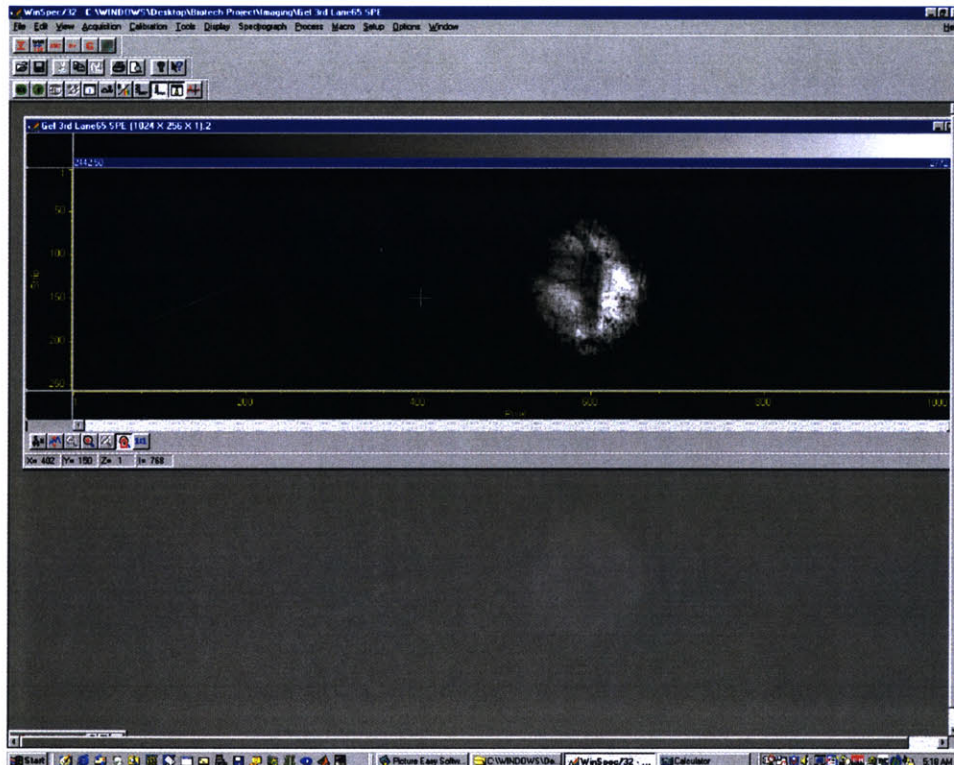


Figure 4.32, Snapshot Image of Lane 8. The Band is at Located at an Absolute Position of 45 mm.

4.7 Results with Third Gel

Experiments have been continued on another 4 mm thick and 0.8% gel. In the previous experiments it has been observed that plasmid DNA led to better results than mouse DNA. In this gel, plasmid DNA has been used in all lanes. The concentrations are chosen to be below 1 μg to prevent streaking. The lane contents are given below in Table 4.5 .

<i>Lane #</i>	<i>Amount</i>
1	100 ng plasmid DNA
2	250 ng plasmid DNA
3	400 ng plasmid DNA
4	550 ng plasmid DNA
5	700 ng plasmid DNA
6	850 ng plasmid DNA
7	1 μg plasmid DNA
8	0
9	0

Table 4.5, Contents of Gel 3.

A duplicate of this gel with EtBr has also been run, and a picture of that gel under UV light is presented in Figure 4.31.

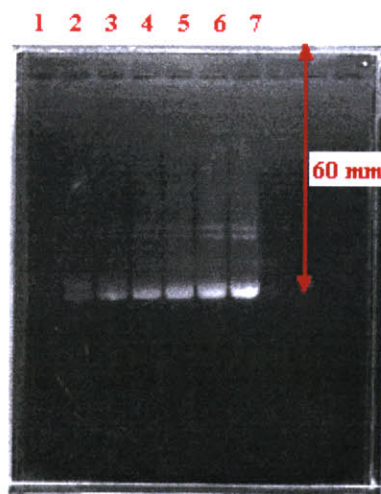


Figure 4.33, Picture of Duplicate Gel Run With EtBr Under UV Light. Lane 1 is the Leftmost Lane.

As it can be seen in Figure 4.33 no streaking is observed. 100 ng band, although visible to naked eye, is not visible in the picture. The bands are located at an absolute position of 60

mm. The scan has been started 2 cm off the edge of the gel to skip the empty gel region. The results are presented below:

- Lane 1:
 - Total DNA Amount: 100 ng plasmid DNA
 - Concentration: 4 ng/ μ l

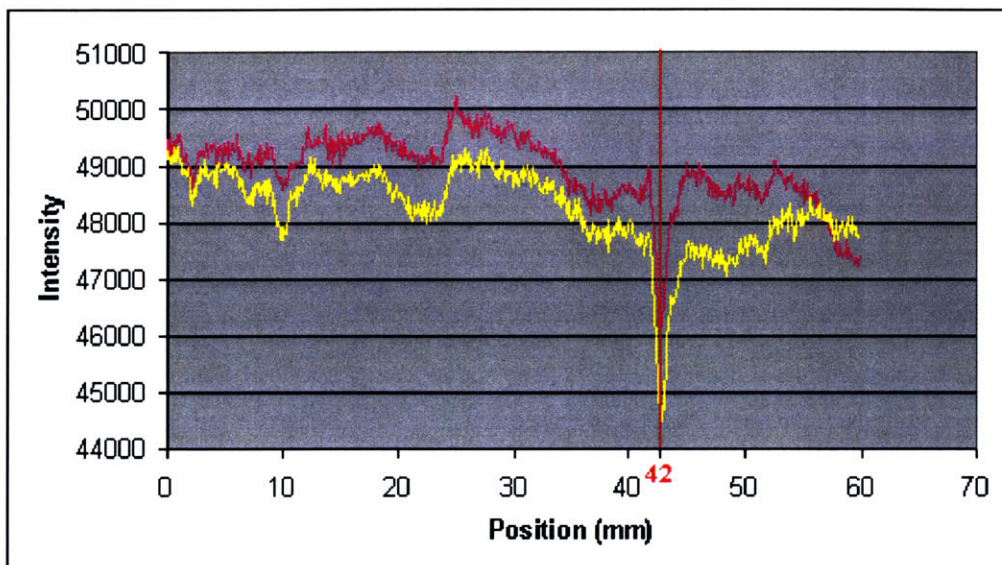


Figure 4.34, Lane 1: 100 ng Plasmid DNA. Two Different Runs With 1 mm Offsets.

When Figure 4.34 is examined, it is seen that there is a well at a relative position of 42 mm in both runs that have been performed along different lines. Adding 20 mm offset value on 42 mm gives an absolute position of 62 mm. This absolute position value obtained agrees with the value read from Figure 4.34. As explained before, due to the absence of some chemicals in the plain gel DNA is expected to move at a different speed in plain gel than in gel with EtBr. The signal level at other locations fluctuates over a small range, which is due to noise in experiment. Compared with Figures 4.29-4.31, the width of the absorption band is thinner. This is expected since this lane contains 100 ng plasmid DNA whereas the lane investigated in Figures 4.29-4.31 contains 400 ng plasmid DNA. The result of the quantitative study is tabulated in Table 4.6:

<i>Run #</i>	<i>I (unit)</i>	<i>I_o (unit)</i>	<i>T</i>	<i>A</i>	<i>b (mm)</i>	<i>c (ng/μl)</i>	<i>a(λ)</i>
1	46159	48750	0.945	0.2371	4	4	0.001482
2	44484	47493	0.936	0.2842	4	4	0.001776

Table 4.6, Calculation of $a(\lambda)$, Wavelength-dependent Absorptivity Coefficient($\mu\text{l}/\text{mm}\cdot\text{ng}$).

Wavelength-dependent absorptivity coefficient $a(\lambda)$ is found to be 0.001481 $\mu\text{l}/\text{mm}\cdot\text{ng}$ and 0.001776 $\mu\text{l}/\text{mm}\cdot\text{ng}$ for two different runs. When compared to the results in Table 4.1 (where $a(\lambda)$ was found to be 0.00106 and 0.00124 $\mu\text{l}/\text{mm}\cdot\text{ng}$), a 20-70% difference is observed between two sets of results. When compared to the results in Table 4.3 (where $a(\lambda)$ was found to be 0.00082 $\mu\text{l}/\text{mm}\cdot\text{ng}$), a 80-115% difference is observed between two sets of results.

Results for lane 2-7 are presented below in Figure 4.35-4.40. When these figures are examined, it is seen that the results are all corrupted. Hence it is not possible to perform the quantitative study on any other lane and retrieve useful information. The reason for corrupted data could be a problem in the preparation of the gel. Due to inhomogeneous gel formation the transmittance of the gel may differ leading to erroneous results. Another possibility is the erroneous run of the DNA. In the traditional electrophoresis method, DNA is run with EtBr which is an intercalating agent. It means that EtBr it wedges itself into the grooves of DNA and stays there physically. Its intercalating characteristics help to keep the DNA molecules together. So during the travel through the gel, DNA solution moves without streaking and spreading. Since in the method offered no EtBr is used, streaking risk always exists and there is no way of verifying whether a gel is run properly or not. Unexpected data is the only clue, which may help to identify an improperly run gel. The Figures 4.35-4.40 will not be discussed in detail; they are presented only to show the problem existing with the gel.

Considering these facts about the gel, data collected from lane 1 is also very likely to contain noise. This is actually apparent in Figure 4.34. There is a fluctuation in the intensity signal, which is about 1000 units. Keeping the I_0 level same as in Table 4.5 and decreasing the I value by 1000 (since there is less data points for this value, it is more vulnerable to noise) a new quantitative study is performed and results are presented in Table 4.7:

<i>Run #</i>	<i>I (unit)</i>	<i>I_o (unit)</i>	<i>T</i>	<i>A</i>	<i>b (mm)</i>	<i>c (ng/μl)</i>	<i>a(λ)</i>
1	47159	48750	0.967	0.0144	4	4	0.000962
2	45484	47493	0.957	0.0187	4	4	0.001173

Table 4.7, Calculation of $a(\lambda)$, Wavelength-dependent Absorptivity Coefficient ($\mu\text{l}/\text{mm}\cdot\text{ng}$).

Wavelength-dependent absorptivity coefficient $a(\lambda)$ is found to be 0.000962 $\mu\text{l}/\text{mm}\cdot\text{ng}$ and 0.001173 $\mu\text{l}/\text{mm}\cdot\text{ng}$ for two different runs. These results agrees much better with the

results in Table 4.1 (where $a(\lambda)$ was found to be 0.00106 and 0.00124 $\mu\text{l}/\text{mm}\cdot\text{ng}$) and Table 4.3 (where $a(\lambda)$ was found to be 0.00082 $\mu\text{l}/\text{mm}\cdot\text{ng}$). It can be concluded that if the noise in the signal is considered, the results from all three experiments agree with a reasonable error. (8% to 50%) Also one point to note is that the equation for absorption includes a logarithmic expression. Hence, even a small contribution due to noise may lead to a great error in the $a(\lambda)$ value.

Even without taking noise into account, the results from three experiments show that the wavelength-dependent absorptivity coefficient $a(\lambda)$ is in the interval of 0.00082 $\mu\text{l}/\text{mm}\cdot\text{ng}$ to 0.001776 $\mu\text{l}/\text{mm}\cdot\text{ng}$.

- Lane 2:
 - Total DNA Amount: 250 ng plasmid DNA
 - Concentration: 10 $\text{ng}/\mu\text{l}$

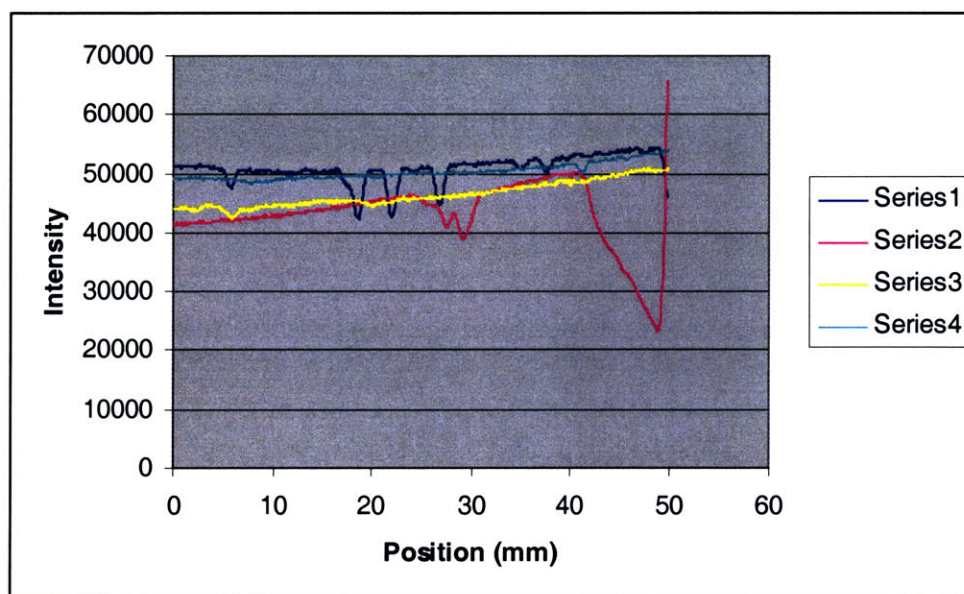


Figure 4.35, Lane 2: 250 ng Plasmid DNA. Four Different Runs With 1 mm Offsets.

- Lane 3:
 - Total DNA Amount: 400 ng plasmid DNA
 - Concentration: 17 $\text{ng}/\mu\text{l}$

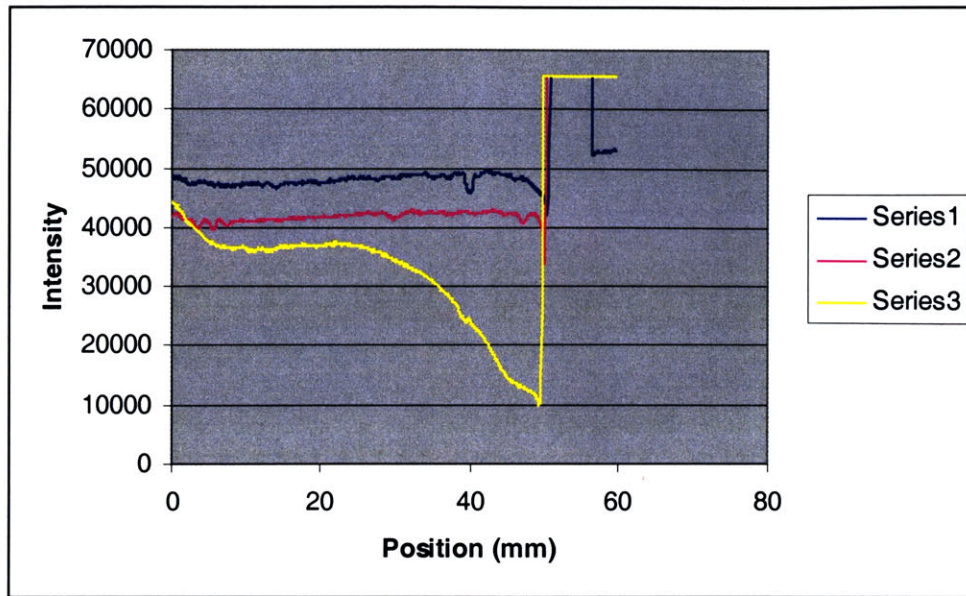


Figure 4.36, Lane 3: 400 ng Plasmid DNA. Three Different Runs With 1 mm Offsets.

- Lane 4:
 - Total DNA Amount: 550 ng plasmid DNA
 - Concentration: 23 ng/ μ l

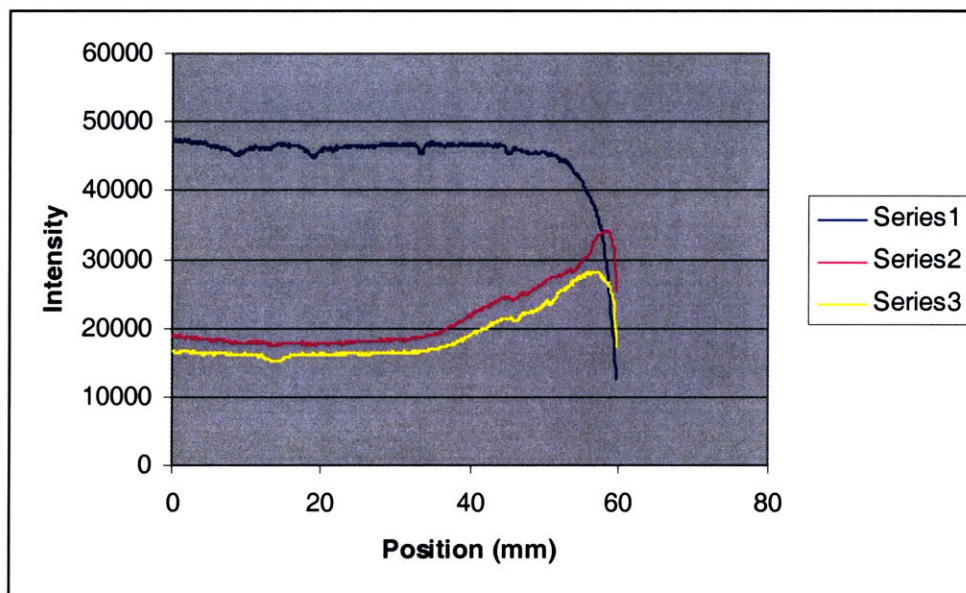


Figure 4.37, Lane 4: 550 ng Plasmid DNA. Three Different Runs With 1 mm Offsets.

- Lane 5:
 - Total DNA Amount: 700 ng plasmid DNA
 - Concentration: 29 ng/μl

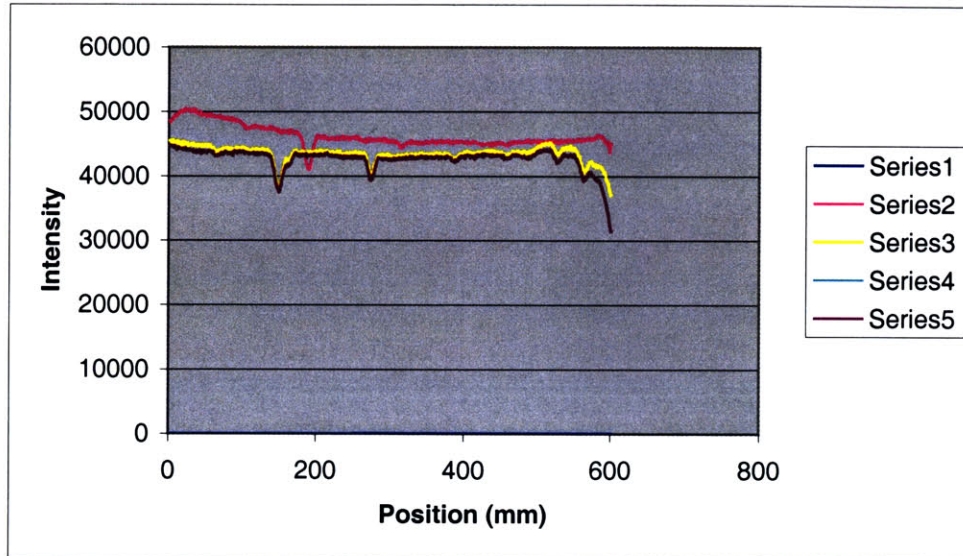


Figure 4.38, Lane 5: 700 ng Plasmid DNA. Three Different Runs With 1 mm Offsets.

- Lane 6:
 - Total DNA Amount: 850 ng plasmid DNA
 - Concentration: 35 ng/μl

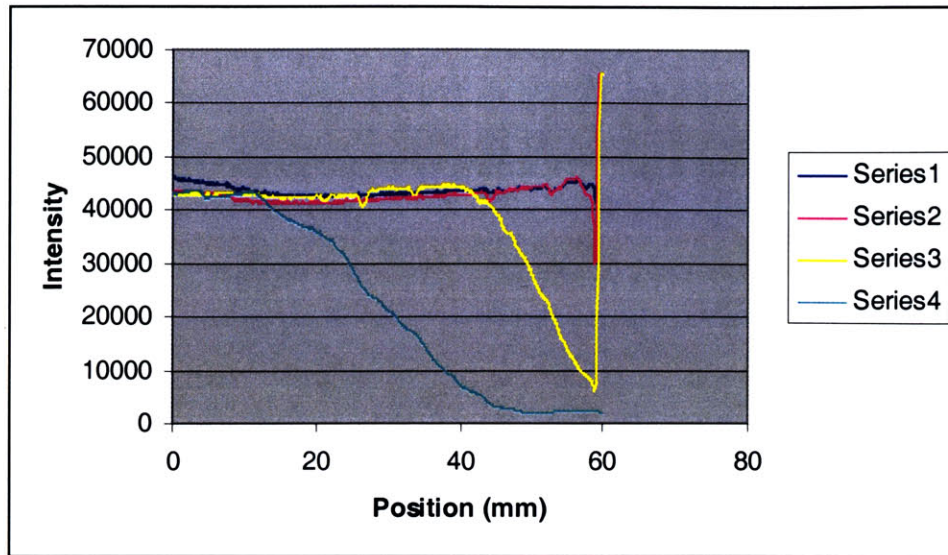


Figure 4.39, Lane 6: 850 ng Plasmid DNA. Four Different Runs With 1 mm Offsets.

- Lane 7:
 - Total DNA Amount: 1 μg plasmid DNA
 - Concentration: 35 $\text{ng}/\mu\text{l}$

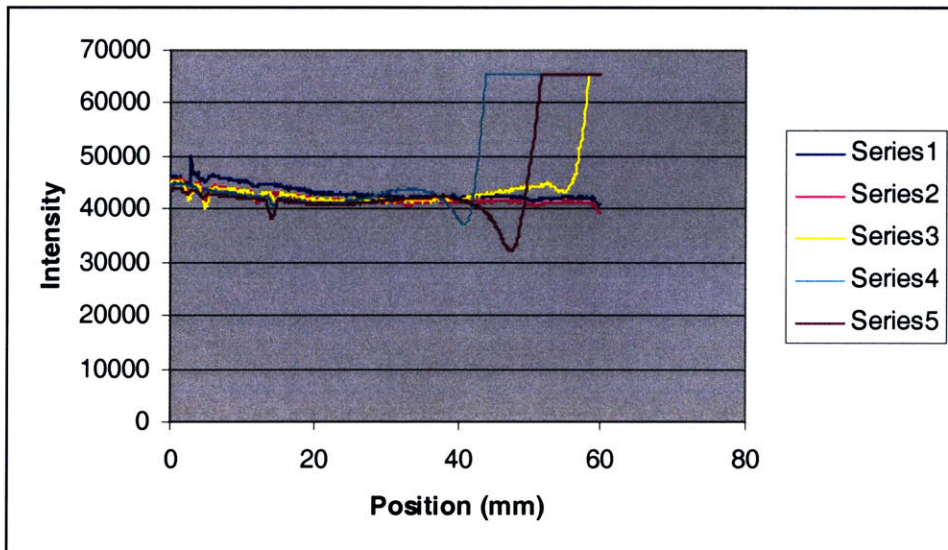


Figure 4.40, Lane 6: 1 μg Plasmid DNA. Five Different Runs With 1 mm Offsets.

4.8 Comparison of Results

The quantitative results obtained from different experiments may be tabulated as follows:

Gel # 1:

<i>Run #</i>	<i>Type of the DNA</i>	<i>a(λ) ($\mu\text{l/mm-ng}$)</i>
1	Plasmid DNA	0.00124
2	Plasmid DNA	0.00106

Table 4.8, Results of Experiments with First Gel.

Gel # 2:

<i>Run #</i>	<i>Type of the DNA</i>	<i>a(λ) ($\mu\text{l/mm-ng}$)</i>
1	Plasmid DNA	0.00082
2	Plasmid DNA	0.00082
3	Plasmid DNA	0.00080

Table 4.9, Results of Experiments with Second Gel.

Gel # 3:

<i>Run #</i>	<i>Type of the DNA</i>	<i>a(λ) ($\mu\text{l/mm-ng}$)</i>
1	Plasmid DNA	0.001481
2	Plasmid DNA	0.001776

Table 4.10, Results of Experiments with Third Gel.

When results presented in Tables 4.8-4.10 are examined it is observed that the $a(\lambda)$, wavelength-dependent absorptivity coefficient ($\mu\text{l/mm-ng}$) is determined to lie in the interval of 0.00082 to 0.001776 $\mu\text{l/mm-ng}$. The results from gel 1 and gel 3 are from the lane, which contained 100 ng plasmid DNA. Whereas the result from gel 2 is from the lane which contained 400 ng plasmid DNA. Since result from gel 2 is from a lane with higher amount of DNA, it can be thought to be less prone to noise due to gel structure.

Considering also the supporting results from the snapshot experiment which are presented in Table 4.4, it is possible to state that the exact value of wavelength-dependent absorptivity coefficient($\mu\text{l/mm-ng}$) is more likely to be at the lower limit of the aforementioned interval .

5. CONCLUSION

In this thesis, a novel stain free detection system for slab gel electrophoresis is examined. Currently, stained techniques are used to identify electrophoretic bands in gels. The stains utilized in these methods involve health risks since they are mutagenic. Also stains like EtBr are intercalating agents meaning they wedge themselves into the grooves of DNA and stay there. Since this includes a physical contact the stains remain in the DNA at the end of the experiment. This makes further use DNA very difficult. The stains need to be removed by chemical techniques which are time wise very costly. Also these operations are very inefficient, retrieve rates are very low which leads to waste of most of the analyte.

The specific method we addressed aims to eliminate the use of any kind of stains and therefore inherently increase the end product efficiency. The method introduces the absorption method as the means of detection. The physical law governing the absorption technique is the Beer-Lambert Law. The Beer-Lambert Law defines the linear relation, which correlates absorption value to the analyte concentration, path length of the light and wavelength-dependent absorptivity coefficient. Although the proposed method is intended to apply to all kind of different analytes, to achieve primary goals and prove the feasibility of the method, as the first step detection of DNA molecules are targeted. Hence absorption pattern at a wavelength of 254 nm (which is characteristic absorption peak for DNA) is examined. After the method is proven to work robustly, it will be extended to all kind of different analytes. The unique approach used in the proposed detection system is the use of a scanning technique incorporated with absorption technique utilizing a high QE (Quantum efficiency) CCD camera as the detector. Experiments have been performed to determine the only unknown parameter - wavelength-dependent absorptivity coefficient $a(\lambda)$ - in the Beer-Lambert Law. The value of $a(\lambda)$ is dependent on the wavelength and also on the transmission media. In our case wavelength of interest is 254 nm and the specific transmission media is agarose gel with 0.8% concentration. Each lane in the agarose gel is scanned under UV light and transmittance values at 254 nm are recorded as a function of position. The recorded data are processed to see the absorption pattern along the lane. The drop in the signal indicates the existence of a DNA band.

Experiments have been performed on three different agarose gels, which are 4 mm thick, and with 0.8% concentration. The value of wavelength-dependent absorptivity coefficient $a(\lambda)$ was determined to lie in the interval of 0.00082 $\mu\text{l}/\text{mm}\cdot\text{ng}$ to 0.001776 $\mu\text{l}/\text{mm}\cdot\text{ng}$. More experiments are needed to be performed in order to accurately fix the value of $a(\lambda)$. The resolution of the method was found to be 4 ng/ μl .

The work in this thesis can be extended in several directions:

- 1) There are numerous uncertainties with the gel, which must be fixed. The homogeneity (structural and chemical uniformity) of the gel is very crucial to ensure uniform gel absorption. Otherwise there is no way of reliably determining what percentage of the signal is actually absorbed by the DNA sample and what percentage of it absorbed by the gel. This was the case in the third gel examined and only one of the lane gave useful results, the results from the remaining were all corrupted. The homogeneity of the gel may not be that important in the traditional way where the visualization is performed by human eye and no quantitative information is required to be deduced from the appearance of the bands. In traditional electrophoretic detection methods, fluorescence methods are used to locate the bands and bands are quantified by the use of standard lanes. Since one of the aims of our method is the quantification of the analyte forming the bands, the proposed method is extremely sensitive to the gel uniformity. Therefore the gel homogeneity must be satisfied. The gel preparation method must be standardized as not to leave any chance for any inhomogeneous formations in the gel. This is a must to get reliable result and to determine the value of $a(\lambda)$ with a greater accuracy.
- 2) The streaking problem must be solved. In the traditional electrophoresis method, DNA is run with EtBr, which is an intercalating agent. It means that EtBr it wedges itself into the grooves of DNA and stays there physically. Its intercalating characteristics help to keep the DNA molecules together. So during the travel through the gel, DNA solution moves without streaking and spreading. More the amount of analyte, more likely is streaking to occur. Since in the our method no EtBr is used, streaking risk always exists and there is no way of verifying whether a gel is run properly or not since there exists no other methods to read unstained gels. Unexpected data is the only clue, which may help to identify an improperly run gel. To solve this problem, a new procedure for reliably running the DNA in the absence of intercalating agents must be defined. This may include the use of new chemicals, which will not damage the goals of the method.
- 3) The gel transmittance characteristics were observed to be dependent on the duration of exposure to ambient air. Therefore out of the buffer gel time must be minimized for robust method reliability. One suggestion is the use of a faster digital I/O board, which will enable to move the stages faster and complete the scan in shorter time.
- 4) The results are dependent on the gel concentration. Experiments must be performed with gels of different concentrations in order to cover all gel concentration range. This means determination of wavelength-dependent

absorptivity coefficient for different gel concentrations and also gels cast of different gel materials, like acrylamide gels.

- 5) A more stable gel holder must be utilized. The gel tray used to carry the gel is made of plastic. And it was figured out that the transmittance value of plastic changes with time, which may lead to inconsistent results. To circumvent this problem glass gel tray made of calcium fluoride could be used.

6. APPENDIX A: C++ CODE

```
// *HEADER FILE OF THE PROGRAM*//  
// *INCLUDES THE NECESSARY HEADER FILES AND CLASS ECLARATIONS*//
```

```
//-----  
#ifndef was_it_savedH  
#define was_it_savedH  
//-----  
#include <Classes.hpp>  
#include <Controls.hpp>  
#include <StdCtrls.hpp>  
#include <Forms.hpp>  
#include <Buttons.hpp>  
#include <ComCtrls.hpp>  
#include <ExtCtrls.hpp>  
#include <nidaq.h>  
#include "fstream.h"  
#include <stdlib.h>  
#include <OLEAuto.hpp>  
#include "WINX32Lib_TLB.h"  
#include "comobj.hpp"  
#include <Dialogs.hpp>  
#include <Graphics.hpp>  
#include "CGAUGES.h"  
#include <Chart.hpp>  
#include <Series.hpp>  
#include <TeEngine.hpp>  
#include <TeeProcs.hpp>  
#include <time.h>
```

```
//-----  
class TForm1 : public TForm  
{  
    __published: // IDE-managed Components  
        TPageControl *PageControl1;  
        TTabSheet *TabSheet1;  
        TPanel *Panel1;  
        TLabel *Label1;  
        TLabel *Label2;  
        TLabel *Label3;  
        TLabel *Label4;  
        TBitBtn *BitBtn1;  
        TEdit *Edit1;  
        TEdit *Edit2;  
        TEdit *Edit3;  
        TEdit *Edit4;  
        TEdit *Edit5;  
        TBitBtn *BitBtn6;  
        TPanel *Panel2;  
        TLabel *Label5;
```


TBitBtn *BitBtn3;
TEdit *Edit8;
TBitBtn *BitBtn2;
TBitBtn *BitBtn4;
TBitBtn *BitBtn5;
TPanel *Panel3;
TLabel *Label6;
TLabel *Label7;
TBitBtn *BitBtn9;
TBitBtn *BitBtn11;
TEdit *Edit6;
TEdit *Edit7;
TEdit *Edit11;
TEdit *Edit12;
TPanel *Panel4;
TLabel *Label8;
TLabel *Label9;
TLabel *Label10;
TEdit *Edit9;
TEdit *Edit10;
TBitBtn *BitBtn10;
TPanel *Panel5;
TImage *Image1;
TLabel *Label11;
TLabel *Label12;
TLabel *Label13;
TPanel *Panel6;
TLabel *Label14;
TLabel *Label15;
TLabel *Label16;
TEdit *Edit13;
TEdit *Edit14;
TButton *Button1;
TTabSheet *TabSheet2;
TPanel *Panel7;
TBitBtn *BitBtn15;
TBitBtn *BitBtn16;
TBitBtn *BitBtn17;
TBitBtn *BitBtn18;
TBitBtn *BitBtn19;
TPanel *Panel8;
TEdit *Edit15;
TEdit *Edit16;
TLabel *Label17;
TLabel *LEFT;
TLabel *Label19;
TLabel *RIGHT;
TLabel *Label21;
TLabel *Label22;
TLabel *Label23;
TLabel *Label18;
TLabel *Label20;
TEdit *Edit17;
TLabel *Label24;
TBitBtn *BitBtn7;
TEdit *Edit18;

```

TLabel *Label25;
TBitBtn *BitBtn8;
TBitBtn *BitBtn12;
TOpenDialog *OpenDialog1;
TLabel *Label26;
TEdit *Edit19;
TListBox *ListBox1;
TImage *Image2;
TPanel *Panel9;
TLabel *Label27;
TBitBtn *BitBtn13;
TOpenDialog *OpenDialog2;
TCGauge *CGauge1;
TPanel *Panel10;
TChart *Chart1;
TAreaSeries *Series1;
TLabel *Label28;
TButton *Button2;
TBitBtn *BitBtn14;
void __fastcall BitBtn1Click(TObject *Sender);
void __fastcall BitBtn9Click(TObject *Sender);
void __fastcall BitBtn11Click(TObject *Sender);
void __fastcall BitBtn4Click(TObject *Sender);
void __fastcall BitBtn3Click(TObject *Sender);
void __fastcall BitBtn2Click(TObject *Sender);
void __fastcall BitBtn5Click(TObject *Sender);
void __fastcall BitBtn10Click(TObject *Sender);
void __fastcall Button1Click(TObject *Sender);
void __fastcall BitBtn7Click(TObject *Sender);

void __fastcall BitBtn8Click(TObject *Sender);
void __fastcall BitBtn12Click(TObject *Sender);
void __fastcall BitBtn13Click(TObject *Sender);
void __fastcall BitBtn14Click(TObject *Sender);
void __fastcall FormCreate(TObject *Sender);
void __fastcall FormClose(TObject *Sender, TCloseAction &Action);
void __fastcall BitBtn15Click(TObject *Sender);
void __fastcall BitBtn16Click(TObject *Sender);
void __fastcall BitBtn19Click(TObject *Sender);
void __fastcall BitBtn17Click(TObject *Sender);
void __fastcall BitBtn18Click(TObject *Sender);
void __fastcall Button2Click(TObject *Sender);

private: // User declarations
Variant WApp;
Variant ex;
Variant dx;
Variant theFrame;
Variant calib;
int bres;
AnsiString SaveFile;
AnsiString SaveFileModified;

public: // User declarations
void StartAcquisition(void);

```

```

void SaveSpectrum( void);
void SaveSpectrum( AnsiString File);
void InitializeController(void);

__fastcall TForm1(TComponent* Owner);
};

void sleep( clock_t wait );
void MoveUP(long stepno);
void MoveDOWN(long stepno);
void MoveRIGHT(long stepno);
void MoveLEFT(long stepno);

//-----
extern PACKAGE TForm1 *Form1;
//-----
#endif

/** MAIN C++ OF THE PROGRAM**/

//-----
#include <vcl.h>
#pragma hdrstop
#include <utilcls.h>
#include "was_it_saved.h"
//-----
#pragma package(smart_init)
#pragma link "CGAUGES"
#pragma resource "*.dfm"
TForm1 *Form1;

bool upswitchhit=0;
bool downswitchhit=0;
bool leftswitchhit=0;
bool rightswitchhit=0;
long xlast,ylast;

//PROCEDURE TO SET THE CURSOR POSITION ON THE FIRST PAGE OF THE //USER
INTERFACE

void SetCursorPosition(void)
{

Form1->Canvas->Pen->Color = clBlue;
Form1->Canvas->Pen->Style = psSolid;
Form1->Canvas->Pen->Width =3;

TRect NewRect = Rect(0,0,Form1->Image1->Width,Form1->Image1->Height);

```

```
Form1->Image1->Canvas->Brush->Color = clRed;
Form1->Image1->Canvas->FillRect(NewRect);
```

```
Form1->Image1->Canvas->MoveTo(0,Form1->Image1->Height-StrToInt(Form1->Edit7->Text)/10000);
Form1->Image1->Canvas->LineTo(Form1->Image1->Width,Form1->Image1->Height-StrToInt(Form1->Edit7->Text)/10000);
```

```
Form1->Image1->Canvas->MoveTo(StrToInt(Form1->Edit6->Text)/10000,0);
Form1->Image1->Canvas->LineTo(StrToInt(Form1->Edit6->Text)/10000,Form1->Image1->Height);
Form1->Image1->Canvas->Refresh();
```

```
}
```

```
//-----
// DELAY PROCEDURE WAITS FOR wait MILISECONDS
```

```
void sleep( clock_t wait )
{
    clock_t goal;
    goal = wait + clock();
    while( goal > clock() )
        ;
}
```

```
//*****
```

```
//MOVES THE STAGE UP AS "stepno" NUMBER OF COUNTS
```

```
void MoveUP(long stepno)
{
    i16 iStatus = 0;
    i16 iRetVal = 0;
    i16 iDevice = 1;
    i16 iOutputChan = 1;
    i16 iInputChan = 2;
    i16 iGain = 1;
    f64 dVoltage = 0.0;
    i16 iIgnoreWarning = 0;
    short devicecode=256;
    i32 data=0;
    i32 InputData=0;
    i32 CheckData=0;
```

```
iStatus=Init_DA_Brds(iDevice,&devicecode);
Form1->Edit1->Text=iStatus;
```

```
iStatus=DIG_Prt_Config(iDevice,iOutputChan,0,1);
Form1->Edit2->Text=iStatus;
```

```
iStatus=DIG_Prt_Config(iDevice,iInputChan,0,0);
Form1->Edit3->Text=iStatus;
```

```

for(long i=0;i<stepno;i++)
{
DIG_In_Prt(iDevice, iInputChan,&InputData );
InputData=InputData&4;
InputData=InputData>>2;

if (InputData==1 && CheckData==1)
{
Application->MessageBox("Upper Limit Switch Reached!!! Please Move Down!!!","Limit Switch
Warning",MB_OK);
upswitchhit=1;
Form1->Edit5->Text="Please Move Down!!!";
break;

}

CheckData=InputData;
iStatus = DIG_Out_Prt(iDevice, iOutputChan,data );

//Form1->Edit4->Text=iStatus;

data=!data;

Form1->Edit6->Text=StrToInt(Form1->Edit6->Text)+1;
if (i%100==0) Form1->Edit6->Refresh();
}
SetCursorPosition();

}
//*****//
//MOVES THE STAGE DOWN AS "stepno" NUMBER OF COUNTS

void MoveDOWN(long stepno)
{
i16 iStatus = 0;
i16 iRetVal = 0;
i16 iDevice = 1;
i16 iOutputChan = 1;
i16 iInputChan = 2;
i16 iGain = 1;
f64 dVoltage = 0.0;
i16 iIgnoreWarning = 0;
short devicecode=256;
i32 data=0;
i32 InputData=2;
i32 CheckData=0;

iStatus=Init_DA_Brds(iDevice,&devicecode);
Form1->Edit1->Text=iStatus;

iStatus=DIG_Prt_Config(iDevice,iOutputChan,0,1);
Form1->Edit2->Text=iStatus;

```

```

iStatus=DIG_Prt_Config(iDevice,iInputChan,0,0);
Form1->Edit3->Text=iStatus;

for(long i=0;i<stepno;i++)
{
DIG_In_Prt(iDevice, iInputChan,&InputData );
InputData=InputData&8;
InputData=InputData>>3;

if (InputData==1 && CheckData==1)
{
Application->MessageBox("Down Limit Switch Reached!!! Please Move Up!!!","Limit Switch
Warning",MB_OK);
downswitchhit=1;

Form1->Edit5->Text="Please Move Up!!!";
break;
}

CheckData=InputData;
iStatus = DIG_Out_Prt(iDevice, iOutputChan,data );
//Form1->Edit4->Text=iStatus;
if(data==2) data=0;
else data=2;
Form1->Edit6->Text=StrToInt(Form1->Edit6->Text)-1;
if (i%100==0) Form1->Edit6->Refresh();
}
SetCursorPosition();
}
//*****//

//MOVES THE STAGE RIGHT AS "stepno" NUMBER OF COUNTS

void MoveRIGHT(long stepno)
{
i16 iStatus = 0;
i16 iRetVal = 0;
i16 iDevice = 1;
i16 iOutputChan = 0;
i16 iInputChan = 2;
i16 iGain = 1;
f64 dVoltage = 0.0;
i16 iIgnoreWarning = 0;
short devicecode=256;
i32 data=0;
i32 InputData=0;
i32 CheckData=0;

iStatus=Init_DA_Brds(iDevice,&devicecode);
Form1->Edit1->Text=iStatus;

iStatus=DIG_Prt_Config(iDevice,iOutputChan,0,1);
Form1->Edit2->Text=iStatus;

```

```

iStatus=DIG_Prt_Config(iDevice,iInputChan,0,0);
Form1->Edit3->Text=iStatus;

for(long i=0;i<stepno;i++)
{
DIG_In_Prt(iDevice, iInputChan,&InputData );
InputData=InputData&1;

if (InputData==1 && CheckData==1)
{
Application->MessageBox("Right Limit Switch Reached!!!Please Move Left","Limit Switch
Warning",MB_OK);
rightswitchhit=1;
Form1->Edit5->Text="Please Move Left!!!";
break;
}
CheckData=InputData;
iStatus = DIG_Out_Prt(iDevice, iOutputChan,data );
//Form1->Edit4->Text=iStatus;
data=!data;
Form1->Edit7->Text=StrToInt(Form1->Edit7->Text)-1;
Form1->Edit18->Text=Form1->Edit7->Text;
if (i%100==0)
{
Form1->Edit7->Refresh();
Form1->Edit18->Refresh();
}
}
SetCursorPosition();

}
//*****//

//MOVES THE STAGE LEFT AS "stepno" NUMBER OF COUNTS

void MoveLEFT(long stepno)
{
i16 iStatus = 0;
i16 iRetVal = 0;
i16 iDevice = 1;
i16 iOutputChan = 0;
i16 iInputChan = 2;
i16 iGain = 1;
f64 dVoltage = 0.0;
i16 iIgnoreWarning = 0;
short devicecode=256;
i32 data=0;
i32 InputData=2;
i32 CheckData=0;

iStatus=Init_DA_Brds(iDevice,&devicecode);
Form1->Edit1->Text=iStatus;

```

```

iStatus=DIG_Prt_Config(iDevice,iOutputChan,0,1);
Form1->Edit2->Text=iStatus;

iStatus=DIG_Prt_Config(iDevice,iInputChan,0,0);
Form1->Edit3->Text=iStatus;

for(long i=0;i<stepno;i++)
{
DIG_In_Prt(iDevice, iInputChan,&InputData );
InputData=InputData&2;
InputData=InputData>>1;
if (InputData==1 && CheckData==1)
{
Application->MessageBox("Left Limit Switch Reached!!!Please Move Right","Limit Switch
Warning",MB_OK);
leftswitchhit=1;

Form1->Edit5->Text="Please Move Right!!!";
break;
}
CheckData=InputData;
iStatus = DIG_Out_Prt(iDevice, iOutputChan,data );
//Form1->Edit4->Text=iStatus;
if(data==2) data=0;
else data=2;
Form1->Edit7->Text=StrToInt(Form1->Edit7->Text)+1;
Form1->Edit18->Text=Form1->Edit7->Text;
if (i%100==0)
{
Form1->Edit7->Refresh();
Form1->Edit18->Refresh();
}

}
SetCursorPosition();

}
//-----

// STARTS DATA ACQUISITION

void TForm1::StartAcquisition(void)
{
bool wait=true;
if(ex.OleFunction("Start",(TVariant) dx) )
{
}

if(wait) wait=ex.OleFunction("WaitForExperiment");
dx.OleProcedure("GetFrame",1,(TVariant) theFrame);
//dx.OleProcedure("PutFrame",1,(TVariant) theFrame);
dx.OleProcedure("Update");
}

```



```

}
//-----

//INITIALIZES THE CONTROLLER
void TForm1::InitializeController(void)
{
WApp=WApp.CreateObject("WinX32.Winx32App");
WApp.OleProcedure("Hide", false);
ex=ex.CreateObject("WinX32.ExpSetup");
dx=dx.CreateObject("WinX32.DocFile");
calib=calib.CreateObject("WinX32.CalibObj");
}

//*****

//SAVES THE SPECTRUM AS NAMIK

void TForm1::SaveSpectrum( void)
{
ex.OleFunction("Stop");
dx.OleFunction("Saveas", "namik", 1);
}

//*****

//SAVES THE SPECTRUM WITH A GIVEN NAME

void TForm1::SaveSpectrum( AnsiString File)
{
ex.OleFunction("Stop");
dx.OleFunction("Saveas", File.c_str(), 1);
}

//-----
__fastcall TForm1::TForm1(TComponent* Owner)
: TForm(Owner)
{
}
//-----

//PERFORMS SOME TASK FOR DEBUGGING PURPOSES

void __fastcall TForm1::BitBtn1Click(TObject *Sender)
{
i16 iStatus = 0;
i16 iRetVal = 0;
i16 iDevice = 1;
i16 iChan = 0;
i16 iGain = 1;
f64 dVoltage = 0.0;
i16 iIgnoreWarning = 0;
short devicecode=256;

iStatus=Init_DA_Brds(iDevice,&devicecode);

```

```

Edit1->Text=iStatus;
iStatus=DIG_Prt_Config(iDevice,iChan,0,1);
Edit2->Text=iStatus;
iStatus = DIG_Out_Prt(iDevice, iChan,15 );
Edit3->Text=iStatus;

}
//-----

//SETS DOWN POSITION

void __fastcall TForm1::BitBtn9Click(TObject *Sender)
{
i16 iStatus = 0;
i16 iRetVal = 0;
i16 iDevice = 1;
i16 iOutputChan = 1;
i16 iInputChan = 2;
i16 iGain = 1;
f64 dVoltage = 0.0;
i16 iIgnoreWarning = 0;
short devicecode=256;
long wavecount;
i32 updata=0;
i32 downdata=0;
i32 InputData;
wavecount=1600000; // 800000 corresponds to 80 mm
int errorcount=0;

upswitchhit=0;
downswitchhit=0;
rightswitchhit=0;
leftswitchhit=0;

iStatus=Init_DA_Brds(iDevice,&devicecode);
Edit1->Text=iStatus;

iStatus=DIG_Prt_Config(iDevice,iOutputChan,0,1);
Edit2->Text=iStatus;

iStatus=DIG_Prt_Config(iDevice,iInputChan,0,0);
Edit3->Text=iStatus;

DIG_In_Prt(iDevice, iInputChan,&InputData);
DIG_In_Prt(iDevice,iInputChan,&InputData);

Form1->Refresh();

while(!downswitchhit)
{
MoveDOWN(5000);
}
}

```

```
Application->MessageBox("Bottom Position Set", "Bottom Position Message", MB_OK);
Edit6->Enabled=true;
Edit6->Text=0;
```

```
}
//-----
```

```
//SETS RIGHT POSITION
```

```
void __fastcall TForm1::BitBtn11Click(TObject *Sender)
{
i16 iStatus = 0;
  i16 iRetVal = 0;
  i16 iDevice = 1;
  i16 iOutputChan = 1;
  i16 iInputChan = 2;
  i16 iGain = 1;
  f64 dVoltage = 0.0;
  i16 iIgnoreWarning = 0;
  short devicecode=256;
  long wavecount;
  i32 updata=0;
  i32 downdata=0;
  i32 InputData;
  wavecount=1600000; // 800000 corresponds to 80 mm
  int errorcount=0;

  upswitchhit=0;
  downswitchhit=0;
  rightswitchhit=0;
  leftswitchhit=0;

  iStatus=Init_DA_Brds(iDevice,&devicecode);
  Edit1->Text=iStatus;

  iStatus=DIG_Prt_Config(iDevice,iOutputChan,0,1);
  Edit2->Text=iStatus;

  iStatus=DIG_Prt_Config(iDevice,iInputChan,0,0);
  Edit3->Text=iStatus;

  DIG_In_Prt(iDevice, iInputChan,&InputData);
  DIG_In_Prt(iDevice,iInputChan,&InputData);

  Form1->Refresh();

  while(!rightswitchhit)
  {
    MoveRIGHT(5000);
  }
}
```

```
Application->MessageBox("Right Position Set", "Right Position Message", MB_OK);
Edit7->Enabled=true;
Edit7->Text=0;
Edit18->Text=0;
```

```
}
//-----
//MOVES UP
```

```
void __fastcall TForm1::BitBtn4Click(TObject *Sender)
{
    long wavecount;
    wavecount=StrToInt(Edit8->Text);
    MoveUP(wavecount);
}
//-----
```

```
//MOVES RIGHT
```

```
void __fastcall TForm1::BitBtn3Click(TObject *Sender)
{
    long wavecount;
    wavecount=StrToInt(Edit8->Text);
    MoveRIGHT(wavecount);
}
//-----
```

```
// MOVES LEFT
```

```
void __fastcall TForm1::BitBtn2Click(TObject *Sender)
{
    long wavecount;
    wavecount=StrToInt(Edit8->Text);
    MoveLEFT(wavecount);
}
//-----
```

```
// MOVES DOWN
```

```
void __fastcall TForm1::BitBtn5Click(TObject *Sender)
{
    long wavecount;
    wavecount=StrToInt(Edit8->Text);
    MoveDOWN(wavecount);
}
//-----
```

```
// SETS TO DESIRED X-Y POSITION GIVEN IN NUMBER OF COUNTS
```

```
void __fastcall TForm1::BitBtn10Click(TObject *Sender)
{
    if ( StrToInt(Edit9->Text) > StrToInt(Edit6->Text))
    {
```

```

        MoveUP(StrToInt(Edit9->Text)-StrToInt(Edit6->Text));
    }

    if ( StrToInt(Edit9->Text) < StrToInt(Edit6->Text) )
    {
        MoveDOWN(StrToInt(Edit6->Text)-StrToInt(Edit9->Text));
    }

    if ( StrToInt(Edit10->Text) > StrToInt(Edit7->Text) )
    {
        MoveLEFT(StrToInt(Edit10->Text)-StrToInt(Edit7->Text));
    }
    if ( StrToInt(Edit10->Text) < StrToInt(Edit7->Text) )
    {
        MoveRIGHT(StrToInt(Edit7->Text)-StrToInt(Edit10->Text));
    }

}
//-----

// SETS TO DESIRED X-Y POSITION GIVEN IN MILIMETERS

void __fastcall TForm1::Button1Click(TObject *Sender)
{
    if ( StrToFloat(Edit13->Text)*10000 > StrToInt(Edit6->Text) )
    {
        MoveUP( (StrToFloat(Edit13->Text)*10000)-StrToInt(Edit6->Text) );
    }

    if ( StrToFloat(Edit13->Text)*10000 < StrToInt(Edit6->Text) )
    {
        MoveDOWN( StrToInt(Edit6->Text)-StrToFloat(Edit13->Text) *10000);
    }

    if ( StrToFloat(Edit14->Text)*10000 > StrToInt(Edit7->Text) )
    {
        MoveLEFT( (StrToFloat(Edit14->Text)*10000)-StrToInt(Edit7->Text) );
    }
    if ( StrToFloat(Edit14->Text)*10000 < StrToInt(Edit7->Text) )
    {
        MoveRIGHT(StrToInt(Edit7->Text)-StrToFloat(Edit14->Text)*10000);
    }

}
//-----

//SETS THE STAGES TO START POSITION FOR SCAN

void __fastcall TForm1::BitBtn7Click(TObject *Sender)
{
    if ( StrToFloat(Edit15->Text)*10000 > StrToInt(Edit7->Text) )
    {
        MoveLEFT( (StrToFloat(Edit15->Text)*10000)-StrToInt(Edit7->Text) );
    }
}

```

```

if ( StrToFloat(Edit15->Text)*10000 < StrToInt(Edit7->Text))
    {
        MoveRIGHT(StrToInt(Edit7->Text)-StrToFloat(Edit15->Text)*10000);
    }
Edit16->Text=StrToInt(Edit15->Text)+10;
}
//-----

//STARTS SCANNING ACTION

void __fastcall TForm1::BitBtn8Click(TObject *Sender)
{
    InitializeController();

    float startpoint;
    startpoint=StrToFloat(Edit15->Text);
    SaveFile=SaveFile+"DF";
    SaveFileModified=SaveFile;

    for (float index=StrToFloat(Edit15->Text);index<=StrToFloat(Edit16->Text);index=index+StrToFloat(Edit17->Text) )
    {
        StartAcquisition();
        SaveSpectrum(SaveFileModified);

        if ( StrToFloat(Edit15->Text)<StrToFloat(Edit16->Text)) MoveLEFT(StrToFloat(Edit17->Text)*10000);
        else MoveRIGHT(StrToFloat(Edit17->Text)*10000);

        /* Delay for 350 msec*/
        sleep( (clock_t)0.350 * CLOCKS_PER_SEC );

        SaveFileModified=SaveFile+FloatToStrF(index, ffGeneral,4,4);
        int dotpos;

        if(dotpos=SaveFileModified.Pos(".") )
        {
            SaveFileModified.Delete(dotpos,1);
            SaveFileModified.Insert("p",dotpos);
        }
        ListBox1->Items->Add(SaveFileModified);

    }

}
//-----

//SELECTS FILENAME FOR THE FILES THAT WILL BE SAVED

void __fastcall TForm1::BitBtn12Click(TObject *Sender)
{
    if(OpenDialog1->Execute() )
    {

```

```

SaveFile=OpenDialog1->FileName;
Label26->Caption=SaveFile;

}
}
//-----

//SELECTS FILES TO BE PROCESSED

void __fastcall TForm1::BitBtn13Click(TObject *Sender)
{
ifstream in;
ofstream datafile;
AnsiString NewString;
double wavelength,intensity,maxwavelength,maxintensity;
int lineno,DFposition;

//Series1->ParentChart=Chart1;
Series1->Clear();
CGauge1->Progress=0;
datafile.open("GraphFile",ios::trunc);

if (OpenDialog2->Execute() )
{
Form1->Refresh();
for (int i=0; i< OpenDialog2->Files->Count ;i++)
{
in.open(OpenDialog2->Files->Strings[i].c_str());
lineno=1;
maxintensity=0;
maxwavelength=0;
while( !in.eof() && lineno==1 )
{
in>>wavelength>>lineno>>intensity;
if (intensity>maxintensity &&wavelength>200 &&wavelength <300)
{
maxintensity=intensity;
maxwavelength=wavelength;
}
}

}

NewString=OpenDialog2->Files->Strings[i];
DFposition=NewString.Pos("DF"); //Find the position of string DF
NewString.Delete(1,DFposition+1); //Delete everythin before DF
DFposition=NewString.Pos(".");
NewString.Delete(DFposition-2,6);
DFposition=NewString.Pos("p");
if(DFposition!=0)
{
NewString.Delete(DFposition,1);
NewString.Insert(".",DFposition);
}
else NewString=NewString+ ".";
}
}

```

```

//ListBox1->Items->Add(NewString);

Series1->AddXY(StrToFloat(NewString),maxintensity,NewString,clBlue);
float dummy=StrToFloat(NewString);
datafile<<dummy<<" "<< maxintensity<<endl;

//ListBox1->Items->Add(maxintensity);
//ListBox1->Items->Add(OpenDialog2->Files->Strings[i].c_str());
in.close();
CGauge1->Progress= (i+1)*1.0/(OpenDialog2->Files->Count)*100;
}

}
Series1->ParentChart=Chart1;
Series1->Repaint();
datafile.close();
}
//-----

//PRINTS THE GRAPH IN CHART OBJECT WINDOW

void __fastcall TForm1::BitBtn14Click(TObject *Sender)
{
Chart1->Print();
}

//-----

//FORM-CREATE EVENT

void __fastcall TForm1::FormCreate(TObject *Sender)
{
ifstream readfile("datafile.txt");

if(readfile)
{
readfile>>xlast;
readfile>>ylast;
readfile.close();
}
else
{
xlast=0;
ylast=0;
}

Form1->Edit6->Text=xlast;
Form1->Edit7->Text=ylast;
Form1->Edit18->Text=ylast;

Form1->Canvas->Pen->Color = clBlue;
Form1->Canvas->Pen->Style = psSolid;
Canvas->Pen->Width =3;

```



```
Form1->Image1->Canvas->MoveTo(0,Form1->Image1->Height-ylast/10000);
Form1->Image1->Canvas->LineTo(Form1->Image1->Width,Form1->Image1->Height-ylast/10000);
```

```
Form1->Image1->Canvas->MoveTo(xlast/10000,0);
Form1->Image1->Canvas->LineTo(xlast/10000,Form1->Image1->Height);
```

```
}
//-----
```

```
//FORM-CLOSE EVENT
```

```
void __fastcall TForm1::FormClose(TObject *Sender, TCloseAction &Action)
{
ofstream writefile("datafile.txt",ios::trunc);
writefile<<StrToInt(Form1->Edit6->Text)<<endl;
writefile<<StrToInt(Form1->Edit7->Text)<<endl;
writefile.close();
}
//-----
```

```
//REMAINIG FUNCTIONS ARE FOR DEBUG PURPOSES
```

```
void __fastcall TForm1::BitBtn15Click(TObject *Sender)
{
InitializeController();
}
//-----
```

```
void __fastcall TForm1::BitBtn16Click(TObject *Sender)
{
StartAcquisition();
}
//-----
```

```
void __fastcall TForm1::BitBtn19Click(TObject *Sender)
{
SaveSpectrum();
}
//-----
```

```
void __fastcall TForm1::BitBtn17Click(TObject *Sender)
{
ex.OleFunction("Stop");
}
//-----
```

```
void __fastcall TForm1::BitBtn18Click(TObject *Sender)
{
WApp.OleFunction("Quit");
}
//-----
```

```
//-----  
  
void __fastcall TForm1::Button2Click(TObject *Sender)  
{  
  
    long i = 600000L;  
    clock_t start, finish;  
    double duration;  
  
    /* Delay for a specified time. */  
    ListBox1->Items->Add("Delay for three seconds" );  
    sleep( (clock_t)0.250 * CLOCKS_PER_SEC );  
    ListBox1->Items->Add( "Done!");  
  
}
```